OPTIMISATION OF AN INDUSTRIAL SCALE BALL MILL USING AN ONLINE PULP AND BALL LOAD SENSOR

Thesis submitted in fulfilment of the degree of Master of Science

Pratish Keshav

KSHPRA001

May 2013

ABSTRACT

The secondary milling circuit at Waterval UG2 Concentrator had undergone a circuit change with the commissioning of the IsaMill, a horizontally stirred mill, in parallel with the secondary ball mill. The operation treats the PGM bearing UG2 ore type and produces a final concentrate enriched with PGM's. The concept was to treat the finer silicate rich fraction in the IsaMill and the coarser chromite rich fraction through the ball mill. This circuit is typical of a UG2 plant in which maximum silicate with minimal chromite breakage is targeted. As a result of the circuit change an opportunity for optimisation around the industrial scale ball mill was considered for this study.

Of concern in this study were new operating conditions for the mill in the changed circuit at which improved performance could be obtained. Another objective was to investigate if a difference in breakage response for the silicate and chromite fractions could be identified for different operating conditions in the ball mill.

The secondary mill at Waterval UG2 Concentrator was already fitted with an online ball and pulp load sensor, the Sensomag. The information obtained from the sensor is in the form of shoulder and toe positions for the ball and pulp filling in the rotating ball mill. The mill was surveyed at various ball filling and mill % solids conditions and information from the online sensor was used to understand the mill performance, particularly with regards to mill load behaviour. Hence a final objective was to demonstrate that the information obtained from the online sensor could be related to mill operating conditions. The sensor output was envisioned to eventually form part of the mill control philosophy. Samples were taken of the mill feed and discharge streams at the different operating conditions and analysed for grind as well as PGM and Cr_2O_3 content. The majority of the PGM's in the UG2 ore are in the silicates and thus the PGM distribution results would indicate the amount of breakage in the silicate fraction. Cr_2O_3 is used as an indicator of the chromite content in UG2 ore.

In order to identify optimum mill performance the results were analysed using different measures which include general grind, particle and species distributions, reduction ratios, sieve efficiencies and specific energy. By comparing the results the differences and limitations of certain techniques were identified.

It was found that the mill performance varied at different operating conditions. The optimum ball filling was found to be around 30%, which is similar to site operational target. The optimal % solids for this mill however seems to be higher than what the mill is typically operated at. No peak in % solids for mill performance was obtained. Scope exists to determine how far from the investigated maximum of 75% solids (by mass) does the optimum in-mill density lie for this mill. Thus new optimum conditions in terms of % solids do exist for the mill in the modified circuit.

Results also showed that the size reduction of the silicates increased with an increase in mill % solids and ball filling degree. For chromite, the mill % solids did not appear to have any effect at low ball fillings, but a slight shift was observed at the higher ball fillings tested. The trend suggests that the size reduction of both silicates and chromite increased with an increase in ball filling, albeit at different rates.

Finally, the test work has demonstrated that the online sensor outputs can be related to mill performance. Differences in shoulder and toe positions for the ball and pulp loads were distinct between operating conditions. Improved grind performance was observed at conditions that resulted in lower free pulp angles. Thus the sensor could be used as a control tool to identify and maintain optimum mill operational conditions. The Sensomag should be incorporated into a mill controller that looks at more than just mill ball filling. Conditions that result in optimum mill efficiency can be identified and the mill may be controlled using the sensor data.

It is recommended that the mill continue to be run at 30% ball filling and at higher mill % solids than the maximum reached in this work.

DISCLAIMER

I know the meaning of plagiarism and declare that all the work in the document, save for that which is properly acknowledged, is my own.

Date:_____08/05/2013_____

Signature:_____

ACKNOWLEDGEMENTS

Special thanks have to be given to the many individuals and organisations that made this study possible. Firstly to my supervisor for your continued support and guidance over the great distance that typically makes a part time study like this that much more difficult. Thanks to Anglo American Platinum for supporting and allowing me to do this study and to publish this information. A great thank you needs to go out to all the operational staff and management at Waterval UG2 Concentrator for facilitating and assisting with the test work required in this study. To all the various stakeholders involved in the test work - thank you for your contributions and support. These include, but are not limited to, Magotteaux, UCT, the University of the Witwatersrand and Anglo American Research.

Finally, a most significant word of thanks must go out to my dear wife. None of the words in this thesis would have materialised without her motivation, support and love. Thank you for always believing in me and pushing me to understand that nothing is impossible or beyond our reach.

Table of Contents

List of Figures

List of Tables

Glossary of Terms

AG	–	Autogenous Grinding
BIC	–	Bushveld Igneous Complex
BWI	–	Bond Work Index
BMS	–	Base Metal Sulphides
Cr_2O_3	–	Chromium (III) oxide (*used as a measure of chromite content for this study*)
DEM	–	Discrete Element Modelling
EGL	–	Effective Grinding Length
MF2	–	Mill-Float-Mill-Float
MIG	–	Mainstream Inert Grinding
OWI	–	Operating Work Index
PGE	–	Platinum Group Element
PGM	–	Platinum Group Metal
PLC	–	Programmable Logic Controller
PSD	–	Particle Size Distribution
RPM	–	Rustenburg Platinum Mines
RTD	–	Residence Time Distribution
SAG	–	Semi-Autogenous Grinding
SCADA	–	Supervisory Control and Data Acquisition
UG2 Reef	–	Upper Ground 2 Reef
VSD	–	Variable Speed Drive
% solids	–	Percentage solids in a slurry by mass or volume (*referred to by mass for the rest of this study*)

Nomenclature

μm – micrometers (microns)

gpt – grams per ton

ktpm – kilo-tons per month

kW – kilowatt

kWh/t – kilowatt hour per ton

m – meters

m^3/hr – cubic meters per hour

mm – millimetres

mV - millivolts

MW – megawatt

ppm – parts per million

t/h – tons per hour

t/m^3 – tons per cubic meter

1 INTRODUCTION

1.1 BACKGROUND

Comminution plays a critical part in most mineral processing operations. A typical concentrator plant uses crushing and milling for the size reduction of the material being treated as preparation for downstream separation processes such as flotation. The efficiency of the separation process is usually dependent on the degree of grinding that occurs and the effectiveness thereof. The aim is to liberate desired particles before the separation stage. However this preparation for the separation process typically consumes a lot of energy and comes at a huge cost. Reports by Charles and Gallagher (1982), La Nauze and Temos (2002) and Musa and Morrison (2009) mention that as much as 75% of a concentrator plant's total consumed electrical energy is due to the comminution process. Added to this is the cost of process materials required such as grinding media. By not ensuring optimum comminution performance significant financial loss is expected from energy and materials consumed in the grinding process. Also the potential mineral recovery or yield loss from the downstream separation process as a result of poor feed preparation is undesirable for the operation.

The concentrator at which the test work for this study was carried out is a fully operational production plant designed to treat the UG2 ore type containing platinum group metals (PGM's). This operation had at the time of the study undergone a circuit change in its secondary milling circuit. The addition of the IsaMill, a horizontally stirred mill developed by Xstrata Technology, in parallel to the secondary mill meant that the old ball mill was operating under conditions different to original design. A study was performed at various operational conditions to try and find the best operating practise for the ball mill in the new circuit configuration to prevent losses as mentioned above.

The presence of chromite in the UG2 ore type presents a challenge in the processing of this reef, as described by Rule (2011). The circuit change to the secondary circuit hopes to take advantage of finer grinding of the PGM-rich silicate fraction in the IsaMill. The coarser grinding of the tougher chromite-rich fraction takes place in the old ball mill. The split of silicates and chromite is however not exact. The chromite is an unwanted product in a UG2 operation. The excessive grinding of this fraction in the ball mill has been described to be a waste of energy and promotes downstream recovery of this unwanted product by Valenta and Mapheto (2010) and Minnaar, Smit and Terblanche (2005). Thus the effect of the various operating conditions on the respective breakage of

the silicate and chromite fractions across the ball mill are of interest here, especially after circuit change.

The ball mill was also fitted with a Sensomag unit - an online ball and slurry load detector developed by Magotteaux. This unit gave valuable data about the changing mill load behaviour throughout the test work and was used to understand the results obtained from the various operating conditions. By using the data obtained from this unit to understand mill dynamics, the unit may be used as an online controller to ensure optimum milling conditions are always met.

1.2 OBJECTIVES

As a result of the circuit change to the secondary milling circuit the amount of material treated in the ball mill had substantially decreased from the original design. This provided an opportunity for some optimisation to be done around the ball mill, and the Sensomag unit was used as an investigative tool in this study.

As described above the ball mill was not operating under conditions as per original design. It is thus postulated that the operation of the ball mill subsequent to the circuit change was not at an optimum in terms of milling efficiency and performance. New operating parameters were to be investigated to find the best operating regime for this ball mill in its new circuit configuration. The variable conditions allowed in this study were ball filling and slurry density and their effect on general size reduction of particles across the ball mill was investigated. Different measures for analysing mill performance in terms of particle size reduction across the mill were also investigated. These include target grind, reduction ratios, sieve efficiencies and specific energies at various operating conditions and for different size classes.

The PGM's in UG2 ore predominantly occur in the silicate matrix as described by Rule (2011). Thus the PGM distribution results around the mill would indicate the amount of breakage in the silicate fraction. Cr_2O_3 is used as an indicator of the chromite content in UG2 ore. The difference in the distribution of PGM and Cr_2O_3 per size class was investigated in an attempt to understand the effect of different operating conditions on silicate and chromite breakage in the ball mill. The processing of the UG2 ore type at this operation has the challenge of inherent chromite recovery in the final concentrate, which negatively affects downstream operations. Conditions which limit the over-grinding of this chromite fraction, whilst promoting the breakage of the silicate fraction, were

to be investigated across the ball mill. This would mean that the energy consumed in the milling operation would be more efficiently used towards a desired outcome. The expected result of this would be improved silicate breakage and PGM liberation and recovery with minimal effect on unwanted chromite size reduction and downstream recovery, or maintained PGM liberation and reduced chromite breakage.

Finally, the mill is fitted with an online ball and pulp position sensor, the Sensomag, which can be used to monitor the charge dynamic behaviour within this mill. The results of this unit can be used to understand the mill behaviour and performance. It is postulated that this tool may be used to operate the ball mill at conditions that will result in optimal milling efficiency, in respect of the above objectives. If the data obtained can be associated with certain milling behaviour and performance, then the unit can be used to always operate the mill at optimal milling conditions.

1.3 HYPOTHESES

Hypothesis 1

There exists an optimum ball filling and % solids which gives the highest reduction in particle size.

The mill is not operating under optimal conditions. Following the circuit change there exists a set of operating conditions at which the mill performs optimally.

Hypothesis 2

A combination of operating variables exists where the breakage behaviour of the silicates is different to that of the chromite fraction.

The greatest challenge in treating UG2 ore is the high chromite content of the reef. There is a need to minimise the grinding of the chromite fraction and maximise the grinding of the silicate fraction, wherein the majority of the targeted PGM's lie.

Hypothesis 3

The charge kinematic information of shoulder and toe position for both pulp and balls can be related to grind performance of the secondary ball mill.

The Sensomag unit gives online information about the dynamic behaviour of the mill load. If this information can be used to explain mill performance at various conditions, then the parameters obtained from the unit can be used to control the mill at an optimum performance level.

1.4 LAYOUT

An introduction to this study has already been made in the above sections. In terms of addressing the stated hypotheses, a literature review concerning the topics of interest will first be covered. This review is broken into sections of mill load behaviour, mill load measurement methods, techniques for analysing mill performance and finally a description of the UG2 ore type and treatment process. This will be followed by the methodology chapter in which the plant circuit, experimental parameters, survey setup and the sampler used for obtaining a mill discharge sample are described. The next two chapters describe the results obtained from the test work performed and the discussion around these results. The sections in these chapters are broken down in terms of analysing general milling performance, evaluating the effect of varying mill operating conditions on mill performance, looking at the difference in breakage between the silicate and chromite fractions (through PGM and Cr_2O_3 distributions) and finally the mill load behaviour in terms of data obtained from the Sensomag unit for the different operating conditions. This study is then concluded with a summary of findings and recommendations chapter in which the way forward and limitations of this study are also described.

The general layout of each chapter in this study will begin with a brief introduction to the particular chapter, followed by the sections as described above and finally a brief summary for the chapter. The appendices referred to in the body are available at the end of this study after the titles of the literature referenced are laid out.

2 LITERATURE REVIEW

2.1 PREFACE

This chapter serves to recognise the knowledge and findings that is shared in the mineral processing industry and is relevant to the subject under consideration for this study. A review of published work relevant to the hypotheses being tested will be covered in this chapter. These include general milling performance, specifically looking at the effect of charge behaviour on the performance of the mill. It also includes methods or techniques used to infer mill load and other operating conditions. Since the ore type plays a key role in optimising the circuit, different types of PGM bearing ores and in particular the challenges of processing the UG2 ore type are reviewed. An introduction to fine grinding technology and the effect this has on the conventional milling circuit is given. The particular interest in terms of mill load behaviour was the positioning of the toe and shoulder, as these were measurable outcomes obtained from the Sensomag in this study. Equipment used in this study to understand the influence of the mill load provided an on-line measurement of the shoulder and toe positions. The effect of these on actual mill performance or grinding efficiency is of interest. The measurements provided by this sensor may be used as a tool to operate the mill to the specific requirements needed to address the challenges of processing the UG2 ore type.

2.2 MILL LOAD BEHAVIOUR

2.2.1 Charge shape with shoulder and toe position

This section describes the current understanding of the shoulder and toe positions for a rotating charge within a mill. It is commonly known that the charge within a tumbling mill represents a kidney-shape during motion, as illustrated by Napier-Munn, Morrell, Morrison and Kojovic (1996). For this kidney-shape, the position along the mill shell to which the charge is lifted in the upward direction of the rotating mill is referred to as the shoulder of the charge, as illustrated in figure 2.1. Similarly, the bottom position that is the first part of the charge to come into contact with the downward moving shell on the other side is termed the toe of the charge.

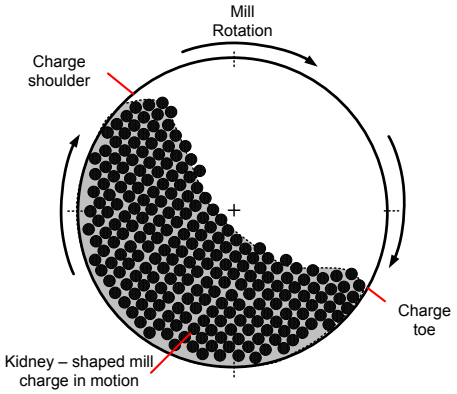

Figure 2.1 Illustration of tumbling mill charge in motion with shoulder and toe positions

2.2.2 Mill speed

In this section the effect of mill speed on the behaviour of the load in a tumbling mill is discussed. It should be noted that the test work in this investigation was carried out in an industrial mill that was operated at a fixed speed. However, the behaviour of the mill load under various conditions needs to be understood to optimise the process.

Cleary (2001) conducted a study wherein the behaviour of a ball mill charge at different operating conditions was simulated through discrete element methods (DEM) modelling in a 5 m long ball mill. The variables in his work included charge level and properties (ball filling, ball shape, rock shape, ball type, rock size distribution etc.), lifter shape and pattern and finally mill speed. The measured parameters from the DEM modelling were charge shape and behaviour as well as predicted mill power draw. It was found that at low speeds larger particles were concentrated around the outside of the charge, and at high speeds these would tend to accumulate in the centre of the charge. Also at low speeds, the charge behaved as though it was fluidised and had a cascading type flow, which in turn means that it was flowing smoothly with particles gliding over each other. As the mill speed increased, the observed shoulder position moved slightly higher and the toe moved slightly lower. There was an increase in the cataracting behaviour, which can be described as the charge carry and projection towards the toe region by lifters. This behaviour steadily increased with increasing mill speed until at speeds close to mill critical speed, centrifuging of the charge occurred. This means that part of the charge is carried at the speed of the rotating shell all the way around the circumference of the mill. The predicted power draw peaked at 100% of critical speed. However actual test work done by Liddell and Moys (1988) which was performed in a lab scale tumbling mill predicted peak power draw at 82% critical speed. This difference in the two results was explained by test conditions being different in that the liner types for the two tests were not similar, and that the DEM modelling had to make some simplifying assumptions. The factors

given that could affect these assumptions were rock or particle shape and pulp density amongst a few others. Further literature indicates that particle size distribution, ball size and distribution as well as slurry rheology also affect the charge behaviour. These will be referenced and discussed later in this literature review (see sections 2.2.4, 2.2.5 and 2.2.6).

Liddell and Moys (1988) performed their test work on a tumbling mill at various mill speeds and fillings. They investigated the effect on the shoulder and toe positions of the charge. In the paper the authors mention that the charge behaviour results obtained from the ball mill studies would also be applicable to autogenous milling. However, it is a very broad statement, as the charge dynamics in an autogenous mill could be different to that of a ball mill. The effect of different particle sizes and shapes would certainly affect the charge dynamic through slurry rheology and will be elaborated on further in this literature review (see section 2.2.6). Another concern from the investigation performed was that 13mm woven-wire mesh liners were used instead of lifter bars or wave liners. The authors stated that the main reason for this was to avoid charge slip and to ensure that the liner would not influence charge motion. On the other hand this is not representative of true mill dynamics as the effect of liners on the charge dynamic is significant (see section 2.2.7). Voidage was assumed to be constant for the basis of the calculations in their investigation, which is a frequent assumption for an otherwise complex problem. It should be noted that this is not entirely accurate and considering that the charge is dynamic (especially at the various conditions tested), the voidage should consequently be a function of this dynamic charge behaviour. The results from Liddell and Moys (1988) show that there is a more significant change in shoulder position than in toe position for a given filling as the speed increases, which is also described by Napier-Munn *et al*. (1996). As observed by Cleary (2001), the shoulder tends to rise up the mill in the direction of motion more with increasing mill speed, and is higher at a given mill speed for a higher mill filling. The toe position also moves in the direction of the mill motion (lower) as the mill speed is increased. At very high speeds, the toe position goes against the trend and moves sharply against the direction of the mill rotation (higher), possibly indicating centrifuging conditions, but this observation was not discussed by Cleary (2001). Napier-Munn et al (1996) explained that when centrifuging begins, the shoulder and toe angles tend to move towards the horizontal axis of the mill. They also mention that the entire charge does not centrifuge at the same speed – rather the outer layers centrifuge first and more layers start centrifuging as the mill speed increases further.

A pilot plant scale study was performed by Lux and Clermont (2004) on the influence of mill speed and pulp density on a ball mill, which was in a circuit configuration typical of a regrind mill on a

UG2 plant (see section 2.5). Once again, the volume of voids was estimated by assuming that the voidage is constant. The volume of the charge will change with changing mill speed and pulp density, as described by Cleary (2001), Tangsathitkulchai and Austin (1989), as well as Songfack and Rajamani (1999). It is not clear why no attempt was made to justify the assumption of constant voidage which contradicts the observations of many authors. Test results for increased mill speed show an increasing absorbed power and a decreasing solids hold-up, as illustrated in figure 2.2. These trends are similar to the observations of Songfack and Rajamani (1999) and can be explained by more cataracting behaviour as the mill speed increases, thus less effective charge volume is available as more balls are in free flight. This decrease in effective mill volume available for grinding results in a decrease in slurry hold-up. It will also increase power draw as more balls are pushed into projection. The best grind results for these particular scenarios were obtained at the lowest mill speed, indicating that there could have been ball charge expansion and poor media – particle interaction with increased mill speeds.

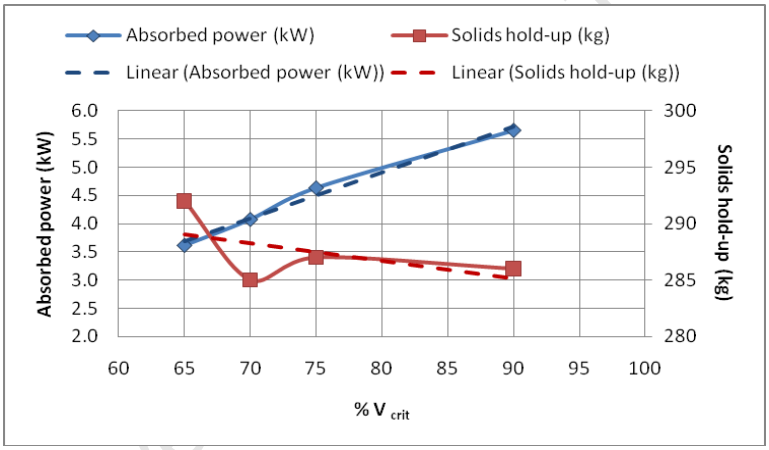

Figure 2.2 Effect of changing mill speed on absorbed power and solids hold-up, by Lux and Clermont (2004)

Behera, Mishra and Murty (2007) analysed the vibration signatures of a tumbling mill to understand the mode of charge motion under varying mill speed, volumetric filling, powder loading and grinding time conditions. They showed that the amplitude of vibration increased from low mill speeds up towards mill critical speed, then dropped suddenly at speeds beyond critical speed. This is consistent with cascading charge motion at low speeds, leading up to a more cataracting charge closer to critical speed, then a centrifuging charge at really high mill speeds around the mill critical speed. They also noticed significant insensitivity of vibration to changing mill speeds at very high solids loading – meaning that under overload conditions it is very difficult to get the charge dynamic again.

2.2.3 Ball filling

This section attempts to summarise the literature on the effect of mill filling on the mill performance and load behaviour. The mill filling is a collective of ball and particle filling and the difference between these two is especially pronounced for SAG mills where large rock particles make up a significant amount of the mill charge. For a regrind ball mill, such as the one in this study, the majority of the charge is made up of the ball charge in the mill. The effect of the ball charge is discussed in this section and the effect of the slurry load will be dealt with through slurry density and hold-up in the mill later in this chapter.

Napier-Munn *et al* (1996) stated that higher mill fillings resulted in higher shoulder positions and lower toe positions. As a result, the speed at which a charge centrifuges is a function of the mill filling. Higher mill fillings will start centrifuging at much lower speeds. Therefore it can be explicitly seen that there is no single centrifuging speed for a given mill – rather it is dependant on the mill operating conditions, which determine the effects of interactive forces within the charge, as well as the balance of gravitational and centrifugal forces. The results of Napier-Munn *et al* (1996) mentioned here is similar to that reported by Liddell and Moys (1988). An explanation given by these two sets of authors for the climbing shoulder position with increased mill filling is that more crowding in the charge occurs as the filling increases and also that greater bed pressure is exerted onto the liners from a larger filling and this assists in lifting the load higher. These can be considered as interaction effects within the charge and are a function the dynamic behaviour of the mill load.

Included in the paper by Cleary (2001) on the DEM modelling of a tumbling ball mill was the effect of ball filling on the charge dynamic and power draw. He also confirmed that as the filling degree decreased the shoulder and toe positions retreated slightly (both move down) so that the charge is spread out more thinly over a smaller section of the mill shell. This is consistent with the observations of Liddell and Moys (1988) and the explanations of Napier-Munn *et al* (1996). The free surface profile changed from being bi-linear to being increasingly curved as the toe and shoulder positions moved slowly towards each other (decreasing mill filling). An observation made by Cleary (2001) was that as the filling degree decreased, the change in the area covered by the charge was far less pronounced than the change in charge volume, thus a small change in shoulder or toe position could mean a radical change in charge volume. This observation suggests that the shoulder and toe positions need to be monitored, as a slight change in either one would be drastic in terms of the change in the dynamic behaviour of the charge.

Cleary (2001) states that with decreasing charge level, there is still a relatively constant velocity difference across the charge. Because the charge depth is also decreasing significantly with lower filling degrees, this should lead to increasing shear rates within the charge and more efficient grinding. However, compression in the charge decreases as the filling level decreases. Also with decreasing mill filling, the amount of material not being ground due to cataracting balls (and a loss of particle-media contact) appears to be relatively constant in comparison to the significantly decreasing volume of material in the actual cascading charge.

Within a regrind ball mill the majority of the grinding takes place within the charge (more abrasion or attrition rather than impact breakage). It can be deduced that the fraction of the total charge which is not undergoing grinding (due to cataracting) is significantly greater at a lower filling. This in turn means that the total grinding efficiency would be worse off at lower filling degrees. This is followed with the observation of a decrease in power draw with decreasing mill filling levels for the range modelled. This observation by Cleary (2001) is congruent with the torque arm rule from centre of mass (or gravity) and the centre of the mill, and where the power is a product of the torque and rotation rate (Napier-Munn *et al*. 1996). It is shown by Cleary (2001) that within this data range, power draw increases with mill filling degree and hence mill load. There is an initial sharp increase, but the power tends to increase less rapidly as the filling increases. As explained above, this is due to the centre of mass of the charge moving closer to the centre of the mill (lower torque arm required to keep charge in motion, even though it weighs more). The effect of mill speed is that the rate of increase in power draw with increasing load is greater for higher speeds than for lower speeds, i.e. power draw becomes more sensitive to the load as the mill speed increases.

2.2.4 Ball size

The effect of ball size on milling performance has been studied by many workers (Austin, Shoji and Buckie 1976; Concha, Magne and Austin, 1992 etc.). This section reviews a few of these studies and tries to summarise the known effects that ball size has on the milling performance, particularly for a regrind ball mill as in the application used in this study.

Katubilwa and Moys (2009) performed various lab scale tests to relate ball size diameter to the particle size with the maximum breakage rate, as well as the grinding rate constants. The tests were also aimed at providing information relating ball size distribution to the milling rate of the mill and to model these relationships. They compared conditions where the charge was made up of an equal number of balls per size class to a charge made up of an equal mass of balls per size class in terms

of mill grinding efficiency. The former scenario had more mass in the top size of balls and was therefore better for impact breakage; the latter had more balls (and hence surface area) in the small size and was therefore better for abrasion type breakage. The outcomes confirmed that the finer ball size would give better grinding rates up to a certain particle size. For particle sizes larger than that, more energy from larger balls would be required for better breakage rates. These results were confirmed by Erdem and Ergűn (2009) who found that one could achieve higher breakage rates in coarser fractions with the use of bigger balls. They performed batch dry grinding tests at different ball sizes. A critical size was again found around which larger or smaller balls gave better breakage rates. They explained this well in terms of a given relationship between ball size and the particle size at which maximum breakage occurs.

Focusing more on finer particle size grinding due to the conditions and configuration of the milling circuit surveyed in this thesis, a study from Partyka and Yan (2007) is of interest. They report that ball mills are not utilised for very fine grinding due to perceived poor energy efficiencies experienced when grinding to finer sizes, where the traditional ball mill cut-off size is around 45 µm. Fine grinding here was defined to be size reduction to 80% passing between 45 and 25 µm, and ultra-fine grinding below 25 µm. They tested the effect of ball size on product size distribution in fine grinding application, and also investigated the effect of varying feed top size. The results of Partyka and Yan (2007) confirm that smaller media is the most efficient in generating fine particles (45 – 25 µm), but is unable to cause breakage in coarser particles (>45 µm). They also state that there are current limitations as to just how small grinding ball diameters can go to in a tumbling ball mill, and just how energy efficient a tumbling mill is in fine grinding applications. The limitations include that tumbling ball mill speeds have to be low due to the onset of centrifuging conditions with high mill speeds, large parts of the mill volume have to be kept empty to allow for a tumbling charge and also that the sizes of the inactive zones in the charge increase with decreasing ball size. These all lead to poor grinding and energy efficiencies in tumbling mills at finer sizes. Partyka and Yan (2007) refer to vertical (e.g. Svedala Vertimill) and horizontal (e.g. IsaMill) stirred mills which are used in industry for more efficient fine and ultra-fine grinding. These will be discussed in more detail later in this chapter as the need for the finer grinding of on UG2 ore types is emphasised.

2.2.5 Slurry percentage solids

This section considers the effect that slurry density has on the mill load behaviour and charge dynamics, and the resultant effect on milling efficiency. Slurry density is determined by the ratio of solids to water (or whatever the transport medium is) and is generally referred as by % solids by

either mass or volume. The relationship between slurry (or pulp) density and % solids can be seen in Appendix A. The relationship that is also well developed in literature is the correlation between slurry (or pulp) density and viscosity; the viscosity tends to increase as the slurry density increases (Napier-Munn et al. 1996).

As an introduction to this section, the study by Yekeler, Ozkan and Austin (2001) should be mentioned in which dry versus wet grinding was compared in terms of milling rates achieved in a lab scale mill. They compared milling only powder to milling the same amount of powder in a slurry (mixed with water). Results showed that higher milling rates were achieved with wet grinding than dry grinding for quartz. This was explained by best conditions being achieved in ball mills where the slurry density makes grinding more efficient than dry grinding. The slurry helps to ensure better ball and particle contact for breakage to occur, and aids in the transport of the solids through the mill.

Tangsathitkulchai and Austin (1989) investigated the effects of slurry density on the milling of quartz in a lab scale ball mill. They mention that viscosity modifying agents are used in industry to control slurry rheology during the milling process. Through their results, they showed how slurry density affected the power draw for the mill. The focus of their work was on ball and particle (or ball and slurry) interaction. They specifically mention that the spatial distribution of solids particles within a ball mill was affected by the slurry density within that mill. Through the use of mill end wall pictures depicting the dynamic behaviour of the ball charge and slurry, they explain that at a low % solids or low slurry density, the slurry pool is large and very turbulent and the balls are cascading. As the % solids increase, the pool size decreases and particle packing in between balls increases. At an optimum % solids, the slurry appears to reside completely in the ball charge and the highest average power draw is observed. This was justified by explaining that as the slurry density and hence viscosity increases, the friction of sliding between the balls increases and the balls are then able to be carried higher up the mill wall as a result (less charge slippage or cascading). This would imply an increase in shoulder position with increasing density. Also, as the viscosity increases, more particles hold to the ball surfaces and are less likely to drain away from the collision zones between balls which in turn means better breakage rates would be expected.

At % solids levels higher than this optimal, a layer of particles starts to form around the inner shell of the mill, essentially creating packing. This reduces effective volume available for milling, restricts lift and shifts the centre of gravity of the total mill and charge closer to the mill axis, thus

resulting in a lower power draw. Eventually the % solids get so high that the ball charge centrifuges with the viscous pulp and results in a very low power draw. Also observed was that there was a similar pattern or trend for both power draw and breakage rate at different % solids conditions. However, at % solids conditions higher than the optimal, the fractional decrease in breakage rate is much higher than the corresponding decrease in power. As the particles start packing around the mill shell, the kinetic energy from the moving balls is not being utilised for breakage, as there are poor particle - ball interactions – leading to highly inefficient milling conditions. At high % solids, it is expected that more attrition type grinding occurs as the viscous pulp will tend to absorb the impact of falling balls. At low % solids, the ball and particle interaction is not at an optimum as there are a lot of ball-on-ball impacts due to the low concentration of solids in the pulp. This leads to inefficient milling conditions as a lot of energy is wasted in ball-on-ball contact. Thus the effect of slurry density is most significant in terms of the ball and particle interaction within the mill, the transport effect of the material through the mill and the overall behaviour of the mill charge.

In addition to mill speed, Lux and Clermont (2004) also investigated the effect of slurry density on the efficiency of a pilot scale secondary stage grinding mill. The results also indicated that there was an initial increase in absorbed power followed by a decrease with increasing slurry density, as illustrated in figure 2.3. There was also an exponential increase in solids hold-up (the mass of solids in the slurry load of the mill) with increasing slurry density, which was similar to that reported by Songfack and Rajamani (1999) and will be reviewed further in the next section of this chapter. These results were explained by the slurry density and viscosity within the mill being affected by the high feed % solids and the increasing difficulty with which the material is transported through the mill. The absorbed power initially increased with the % solids, then dropped significantly as the solids hold-up increased exponentially (indications of the mill heading towards overload conditions). This is also in accordance to the observations of Tangsathitkulchai and Austin (1989), and their explanation for these events is given above. However, the test at this pilot plant mill were done on a mill with capabilities of measuring pulp and ball angles in the rotating mill (although how they measured it is not described in the paper). These measurements indicate that there was a significant ball load expansion and continued linear pulp expansion after 73% solids (the % solids condition after which the power dropped away and solids hold-up increased significantly). This goes against the explanation given by Songfack and Rajamani (1999) to describe the exponentially increasing slurry hold-up at very high % solids. This indicates that the response of the load shoulder and toe angles to changing conditions is not as yet fully understood and a review of the latter mentioned paper will now follow. Behera et al (2007) noticed significant insensitivity of measured

vibration to changing mill speeds at very high solids loading – meaning that at overload conditions it is very difficult to get the charge dynamic again and should typically be avoided in operation.

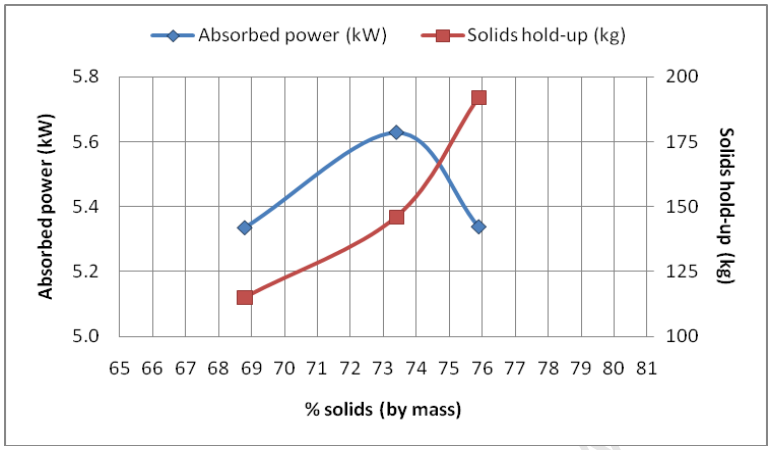

Figure 2.3 Effect of changing slurry % solids on absorbed power and solids hold-up, by Lux and Clermont (2004)

2.2.6 Slurry hold-up and residence time in a mill

The hold-up of slurry in a mill is the amount of slurry that is held within the charge of the mill. It determines how quickly material passes through the mill, or the throughput attained from that mill. The time taken for the material to pass through the mill can be referred to as the residence time of that material in the mill, and is usually given as a mean or a distribution as the slurry is not truly homogeneous. The slurry can be considered in terms of its solids content and water content. The solids hold-up is also a term used to ascertain milling performance or load behaviour, as described in Lux and Clermont (2004). An assumption that is usually made about the slurry mean residence time is that both solid and liquid components have the same mean residence time, as explained in Napier-Munn *et al*. (1996), which might not necessarily always hold true. This section looks at how hold-up is affected by various mill operating parameters and tries to relate it to load behaviour.

Songfack and Rajamani (1999) performed pilot plant scale test work to test the effect of hold-up or residence time in an overflow ball mill. They stated that for given operating conditions, the slurry flow pattern in a mill determines the slurry hold-up and the residence time distribution (RTD) of solids exiting the mill. Low charge filling levels lead to high steel on steel collisions and excessive filling levels lead to cushioning of grinding media impacts or collisions, both leading to poor grinding efficiency as discussed earlier in this chapter. Songfack and Rajamani (1999) explain that when the % solids in the slurry hold-up is greater than that of the feed or discharge, the mean residence time of the solids is higher than the mean residence time of the liquid, as described by

Rogers and Austin (1984). This also implies that fines have more of a chance of being carried with the liquid, thus a greater hold-up of more coarse solid particles would be expected.

Songfack and Rajamani (1999) also showed that the effect of feed % solids on slurry hold-up increases gradually with increasing feed % solids at low values for % solids. This increase suddenly becomes drastic and increases exponentially as the slurry density and viscosity within the mill is affected by the high feed % solids, as noted also by Lux and Clermont (2004). At a slight increase in mill feed % solids the slurry hold up weight increases in part due to a slurry volume increase (from a result of the increased resistance to flow due to increased viscosity). Thus it would be expected that the pulp shoulder and toe would move out a bit (away from each other) as a result of this volume expansion. The slurry weight also increases due to increased slurry density. A further increase in the % solids of the feed causes more drastic effects on slurry density and viscosity in the mill and affects the motion of grinding media charge. Songfack and Rajamani (1999) describe a reduced shoulder and toe angle which actually results in a decreased pool level and slurry volume in the mill. This counteracts the effects of slurry hold-up increase from the earlier mentioned increase in density and viscosity. At very high % solids, grinding media and slurry move as a continuum. Shoulder and toe angles move even closer to the mill centre (volume decreases) but because of the high viscosity, the discharge of slurry from the mill becomes difficult and grinding media might even be seen exiting the mill with the slurry – until overload conditions are met. This last description of events by Songfack and Rajamani (1999) contradicts the observations made by Lux and Clermont (2004), who saw an expansion in ball volume with increasing % solids beyond the optimal % solids. These differences in charge behaviour must be questioned. Lux and Clermont (2004) had an online sensor (which was assumed to be calibrated and accurate as no limitations were mentioned) that could give shoulder and toe positions as the mill ran at different conditions. In the test work performed by Songfack and Rajamani (1999) there was no sensor to determine these positions, nor was there any visual means of determining the shoulder and toe positions. Rather, they were given in terms of the opinions of Songfack and Rajamani (1999) as to the sequence of events within the dynamic charge to suit the observed outcomes of slurry hold-up and power draw.

Songfack and Rajamani (1999) also observed that as mill speed increased, the slurry hold-up increased due to the charge being lifted higher (higher shoulder) and charge expansion which results in increased voidage and hence increased available slurry volume in the pool. This explains why assuming a constant voidage in the charge over a range of dynamic conditions is not accurate. As mill speed increases and more cataracting is observed, less effective charge volume is available

as more balls are in free flight and this decrease in effective mill volume results in a decrease in slurry hold-up. Increasing mill speed eventually leads to centrifuging and this will significantly reduce the slurry hold-up. Slurry hold-up increases as ball filling % increases (more volume available for the slurry from increased ball load and pool level) at a given condition. Finally, the authors observed that an increase in slurry feed rate had a lesser effect on increasing slurry hold-up than an increase in the degree of ball filling.

2.2.7 Liner wear and design

All tumbling mills have some form of liners that serve to protect the mill shell from wear against the dynamic motion and action of the tumbling charge, as well as to help convey the rotational energy of the mill into the charge such that a tumbling and dynamic charge is promoted wherein particle breakage can occur. Therefore the actual design of the liner or operating with a worn liner has a significant effect on the behaviour of the load in a tumbling mill and this section aims to understand this relationship between liner life or design, mill behaviour and performance.

As discussed above, Cleary (2001) performed DEM modelling of a ball mill at various operating conditions, including lifter bar shape, wear and pattern. The output parameters as charge shape and power draw were modelled and simulated. Different face angles and lifter heights were modelled as a representative indication of new liners and ready to be replaced (or worn) liners. As increasing liner wear was observed, the toe position lifted slightly (moved away from shoulder). The main change is that cataracting material was thrown on lower trajectories due to shallower face angles from increasing liner wear. This implies that whereas a new liner set might throw material against the shell, worn liners cause cataracting material to fall closer to the toe due to a decrease in lifter height and face angle. The charge surface is still mainly bi-linear in its dynamics. As more liner wear is seen, the shoulder angle is a little lower and the toe angle is a bit higher – this implies less charge lift due to wearing lifters. The amount of cataracting material is thus reduced and the material lands on the charge surface between charge toe and mill centre. When the liners are almost completely worn there is almost no cataracting material. The toe location is higher and is also higher than the lowest point on the top surface of the charge due to the purely cascading charge. At low mill speeds the highest power draw is observed with new lifters and at high speeds the lowest power draw is observed with new lifters. The explanation given for this is that the new lifters are more likely to trap material to centrifuge at higher speeds. There is an expectation of more charge slippage and less power draw as liners get older and when the charge is not centrifuging. This indicates that it might be useful to be able to vary mill speed with liner lifetime to ensure maximum

power draw (less material centrifuging) and more effective grinding. Makokha and Moys (2006) also reported higher power draws (mill running below at 75% critical speed) with new lifter bars installed.

2.3 MILL LOAD MEASUREMENT METHODS USING SENSORS AND SIGNALS

The previous sections of this chapter dealt with the effects of various operating parameters on mill load behaviour and mill performance. They provided a fundamental understanding as to how a mill load is affected at different conditions experienced during the operation of the mill, and an attempt was made to identify how one would expect this variation in mill load behaviour to affect the operation of the mill in terms of mill power and achieved grind. This section now attempts to find different reported methods of how the mill load can actually be measured and how the behaviour of this mill load can be monitored.

A number of different methods of obtaining the mill load and its conditions have been cited in literature, from vibration measurement on the mill shell to acoustic measurements in the proximity of the mill structure itself. The most fundamental method would be to stop the mill and measure the charge volume after a crash stop, or to perform a grind out and measure the ball charge, as described by Napier-Munn *et al.* (1996). This tends to restrict one to measure only during plant stoppages and has a production impact. It is now common practise to have an online indication of mill load, either via load cells placed below the mill trunnion support or inferred from the trunnion oil pressure. Both methods give an indication of the load as it increases or decreases and can be effectively used in advanced control logic to optimise the mill performance. The advantages and disadvantages of these as well as other techniques will be tabulated later in this section. The following is an account of some of the information shared in literature regarding the techniques of measuring mill load and monitoring its behaviour.

Kolacz (1997) made use of a *piezoelectric strain transducer* which detects strain changes in the mill shell to infer mill load measurement. This unit was installed at the midpoint on the shell where the highest deformation takes place. When mill rotation takes it to the top of the mill, the position there indicates compression on the mill shell and when at the bottom position it indicates tension on the mill shell. The difference between these readings gives the total strain variation, which is reported to be directly proportional to the mill load. Kolacz (1997) refers to many other techniques of mill

load measurement:

- *From analysis of mill power consumption*. This requires proper investigation and understanding of the relationship between power and load. Under this scenario plants tend to operate far from the optimal point due to safety concerns around control and operation, as described for autogenous mills by Olsen (1976).
- *In dry milling applications, from the differential pressure between the inlet and outlet of the mill*. If the mill load increases, there will be more material exposed to the flowing air and as a result of increased drag from the material, the differential pressure will increase. The inverse applies for conditions when the mill load decreases. However, there are many other factors which affect differential pressure such that it is not a direct measure or indicator of mill load. These factors include mill speed, lifter type and wear, particle size distribution, ambient conditions etc.
- *From mechanical vibration and the variation in acoustic pressure near the mill*. Described by Zeng and Forssberg (1993), this is a rather complex and complicated method.
- *From oil pressure measurement on trunnion bearings* during operation, also described by Olsen (1976). This is also an indirect measurement and subject to bearing and oil condition.
- *From load cells placed under the trunnion* of an operating mill. This is typically the most accurate method to get a direct load reading for the mill. This is however an expensive measure and very difficult to retrofit into an existing mill.

The benefits, according to Kolacz (1997), of the strain transducer are given as low threshold (strains being measured are quite small), simple overload protection so that the transducer can not be damaged, and that it simple to install. The limitations of the strain transducer include sophistication in terms of correlating strains to mill load, low threshold due to small magnitudes of strains that needs to be measured means that there is low resolution in terms of signal received, and finally the inability to distinguish between ball load and pulp load (it measures overall strain only and has been developed for dry grinding cement industry). The signal is radio transmitted from the mill shell to the receiver and then to a processor for display and control. It was found that there was a need to filter or condition the signal to smooth out the residual noise. However, it does not seem that there was any validation information or test done to confirm the outcomes of the results from the unit.

Almond and Valderrama (2004) discussed the Impactmeter (*an acoustic sensor*) for determining mill load, more specifically the trajectories inside an operational SAG mill (load movement and

impact areas). This method is based on using microphones near the mill together with specialised hardware and software to distinguish between high and low impact operating conditions in terms of mill load behaviour. The control philosophy behind this system would be to minimise high impact operating conditions, through either an operator or automatic control system, which could minimise liner and ball breakage, as well as inefficient use of milling energy. Almond and Valderrama (2004) mentioned that the SAG analyser uses an acoustic sensor (microphone) on the mill shell to identify the toe and shoulder positions. The paper claims that the integrated controller and system gives the following outputs:

- Total volumetric filling %.
- Ball volumetric filling %.
- Ore volumetric filling %.
- Charge apparent density.
- Angular position of total charge shoulder and toe (but there is no distinction between ball and rock or slurry position).

Also, the ball level is estimated from the load volume and the mill control system – thus it is not a direct measure but rather model based and is an estimation.

This method of *analysing noise and vibration signals* to obtain load measurements was done by Si, Cao, Zhang and Jia (2008) in an industrial scale mill at a thermal power plant. They also mention different types of load measuring techniques – like *diagnostic X-ray method* (Powell and Nurick, 1996), which according to Si, Cao, Zhang and Jia (2008) is accurate to monitor load behaviour but the investment cost is substantial at an industrial level. In their paper Si, Cao, Zhang and Jia (2008) refer to a softsensing technique – the primary parameter (mill load in this case) may be inferred by combining secondary parameters which are low-cost and easy to measure. Noise and vibration signals were analysed through a novel information extraction method by complex noise filtering and modelling. The advantages that were claimed are lower model complexity, high estimated accuracy and good generalisation ability. However, proper validation against operational measured parameters was again not provided.

Campbell, Holmes, Spenser, Phillips Barker and Davey (2006) used an on-line *surface vibration monitor employing accelerometers fixed to mill liner bolts* to study load behaviour. They achieved on-line shoulder and toe measurements in an industrial scale SAG mill. Su, Wang, Yu and Lu (2008) analysed *vibration from two accelerometers installed on the mill shaft bearing house* to

infer the level of coal powder filling and operating conditions in an industrial ball mill. The test work discussed earlier by Behera *et al.* (2007) also used accelerometers directly on the mill shaft in a lab mill. Signals were used to categorise the charge motion and grinding state of the mill; these results were discussed in the mill speed section of this chapter. The use of a *microphone on the mill shell* to determine the location of the charge toe was investigated by Martins, Zepeda, Picard, Radziszewski and Roy (2006). They ran pilot and industrial test work and reported their findings in terms of identifying the impact region that comprised the charge toe in this paper. As described in the mill speed and filling sections earlier in this chapter, Liddell and Moys (1988) performed a lab scale investigation of a ball mill to investigate charge shoulder and toe positions at various mill speeds and fillings using a *conductivity probe mounted in the mill shell*. The presence of the charge completed the circuit between the probe and the liner. However, it is not quite clear if it is the ball charge or the pulp level that was being measured. Finally, Cleary (2001) showed that *DEM modelling* may be used to determine shoulder and toe positions for a charge across various mill operating conditions.

In terms of commercially available tools, the *Outokumpu MillSense* analyser is a non-contact method to determine charge volume based on a ripple in the power draw of the mill motor. The ripple is the peak in power draw caused by the impact of the lifters with the toe of the charge as the mill is rotating, and is a smooth continuous ripple because the milling is rotating. The theory is that if the toe of the charge moves, the ripple will be affected such that a single peak comes either earlier or later. Järvinen, Laurila, Karesvuori and Blanz (2006) presented a paper in which they describe just how the MillSense may be used to determine the charge volume. It is based on high frequency sampling of mill power and a proximity switch to synchronise measurements to mill rotation and is thus easy to setup and the maintenance requirements are very low. The frequency of the ripple is analysed and noise filtered out, although it is not explicitly explained as to how they derive the charge volume from this. They also mention that through various models and estimations, ball charge can be obtained. They show how it was used to predict ball filling in an industrial application, but no data validation was presented. The authors mentioned that at the time of the paper, geometrical models were being developed to estimate liner wear as well. They proposed to develop ball trajectory models based on liner wear estimation models and measured mill speed.

Another commercially available tool to determine charge behaviour is the *Magotteaux Sensomag*. This is an online sensor that sits within the mill liner set and determines the ball and pulp shoulder and toe positions through a conductive and inductive sensor. This is discussed in more detail by

Keshav, de Haas, Clermont, Mainza and Moys (2011). This unit was used in conjunction with the surveys in this study to test the hypotheses presented in this study. More detail about this unit will be presented in chapter 3 below.

Table 2.1 is presented for easier comparison of the different types of mill load and charge behaviour measuring techniques.

Table 2.1 A summary of the advantages and disadvantages of various different techniques to determine mill load and charge behaviour

Method / Type	Pros	Cons
Routine stoppage and measurement inside mill from crash stops and grind-outs	• Actual measurement • Inspect physical conditions inside mill	• Significant production impact. • Limited to planned maintenance stoppages only – too far apart in succession.
Mill power measurement	• Quick to implement. • Most mills have indication of mill absorbed power.	• Relationship between mill load and power needs to be extensively investigated and understood. • In the absence of the above, tendency to operate far from optimum operating conditions as a safety buffer. • Risk of easily overloading mill.
Mill power ripple analysis (e.g. MillSense)	• Quick to implement. • Non-intrusive and non-contact. • Low maintenance requirements. • Claim to be able to estimate charge volume, ball charge, liner wear and ball trajectory from single measurement.	• Not clear how charge volume calculations are obtained from measurements. • Verification of evolved models and estimations for predicting charge volume, ball charge, liner wear and ball trajectory not presented.
DEM modelling	• Non-intrusive and non-contact. • Fairly well researched area and plenty of development. • Can be done for any mill given known operating	• Dependent on modelling. • Difficult to verify unless compared to surveyed results. • Need extensive amount of information about the

	specifications and geometry.	mill to get accurate results. • Still mainly in the research application.
Air differential pressure in dry milling	• Simple and easy to implement.	• Only applicable to dry milling. • Not a direct measure. • Many other factors affect differential pressure.
Mechanical vibration and variation in acoustic pressure	• Non-intrusive. • Easy to retrofit existing mills.	• Complex and complicated. • Affected by noise, other vibrations and pressures in the vicinity of the equipment. This might be substantial for industrial mills in complex plants.
From trunnion bearing oil pressure	• Non-intrusive. • Does not require additional hardware or software if the mill is supported by oil flow through trunnion bearings – fairly economical option.	• An indirect measurement of load and the pressure is subject to influences other than just mill load. • Dependent on oil and bearing condition.
Load cells below supported mill trunnion	• Direct measurement of entire mass of mill.	• Expensive option. • Very difficult to retrofit existing operational mills.
Piezoelectric strain transducer on mill shell	• Simple to install. • Low threshold (small strains measured).	• Indirect measure of load from mill shell strain – complex correlation. • Low resolution due to small strain values measured.
Acoustic and vibration sensor (e.g. Impactmeter and SAG analyser)	• Can be either near mill or on mill shell itself. • Easy to retrofit existing mills.	• Only picks up impact points on the shell – no direct differentiation between rocks, balls or slurry. • Can require complex modelling and signal processing etc. to obtain primary parameters.
Intrusive conductive sensor	• Can be used online to	• Does not give both ball

	obtain shoulder and toe positions.	and pulp levels. • Needs to be validated industrially.
Intrusive conductive and inductive sensor (e.g. Sensomag)	• Online measurement of load through shoulder and toe angles. • Differentiates between ball and pulp levels. • Well validated against actual measurements.	• Can be expensive to setup and maintain. • Needs to be fitted into existing liner design on the inside of the mill (intrusive sensor). • Can require complex modelling and signal processing etc. to obtain primary parameters.

2.4 TECHNIQUES FOR ANALYSING MILL EFFICIENCY AND PERFORMANCE

Some of the methods and techniques presented in literature to describe mill efficiency and performance are described in this section. These are explored in this review as the hypotheses presented in the introduction of this study require the analysis of different milling parameters to determine the most efficient operational conditions.

Napier-Munn *et al* (1996) define the grinding efficiency measurement of a mill in terms of the ratio between the operating work index and the Bond work index (BWI). The latter index is obtained from well established ball mill grindability laboratory tests on an ore sample (Bond, 1961). This ratio is referred to the operating efficiency and is expressed in equation 2.1.

$$\text{operating efficiency} = \frac{\text{operating work index OWI}}{\text{Bond work index BWI}} \times 100\% \qquad [2.1]$$

The operating work index (OWI) is obtained from Bond's "third theory" of comminution, as described in by Bond (1952) and equation 2.2. By rearranging this formula the work index may be defined as in equation 2.3.

$$\frac{P}{T} = 10 * OWI\left(\frac{1}{\sqrt{P_{80}}} - \frac{1}{\sqrt{F_{80}}}\right) \qquad [2.2]$$

thus

$$OWI = \frac{P}{10T\left(\frac{1}{\sqrt{P_{80}}} - \frac{1}{\sqrt{F_{80}}}\right)} \qquad [2.3]$$

Where

P = power (kW)
T= throughput (t/h)
WI = work index (kWh/t)
P_{80} = 80% passing size for the product (µm)
F_{80} = 80% passing size for the feed (µm)

The closer the operating work index is to the Bond work index, the more efficient the milling process is, i.e. the closer the operating efficiency ratio will be to unity.

Musa and Morrison (2009) also reflected efficiency by dividing the operating work index by the laboratory Bond work index. The limitations of using the Bond method are a single value parameter for assumed parallel feed and product size distribution curves, and that it is independent of the path of comminution. This makes the method more applicable to ball mills rather than SAG or AG mills. Musa and Morrison's (2009) method to assess operating efficiency is based on the hypothesis that the energy required for size reduction is proportional to the new surface area formed, as described by Von Rittinger (1867). The limitations of this method were particularly evident at finer particle sizes as the calculated surface area per mass increases drastically with decreasing particle size. To address this limitation it was recommended that the total surface area in the ultrafine region be bounded with decreasing size – i.e. a limit is set. For their method Musa and Morrison (2009) indicate that the sub 75 µm fraction contributes at least 70% of the total surface area in a typical AG/SAG/Ball mill circuit. They then describe the specific energy per ton of -75 µm generated and compared this to the Bond grindability test for that material in the -75 µm fraction as a measure of grinding efficiency. They then went on to show that this relationship is linear and is generally close to unity. As will be seen later in the results of this thesis, this method is useful in analysing mill performance for the circuit investigated. The "specific energy per ton of -75 µm generated" term alone, as defined by equation 2.4, can be used as a tool to define efficiency – with higher specific energies indicating less efficient conditions. The specific energy at any screen size (other than 75 µm) can be calculated in accordance to equation 2.4, using the % passing data at that size.

$$\text{specific energy (kWh/t(-75}\mu\text{m))} = \frac{P}{T\left(\%\{-75\mu m\}_{generated}\right)} = \frac{P}{T\left(\%\{-75\mu m\}_{product} - \%\{-75\mu m\}_{feed}\right)} \quad [2.4]$$

Feurstenau and Abouzeid (2002) investigated comminution efficiencies based on size distributions by plotting reduction ratio as a function of specific energy. Reduction ratio may be defined as the size of the product relative to the size of the feed. This may be represented in terms of the size that a particular amount of material passes (e.g. P_{80} and F_{80}, as used in equation 2.3), or in terms of the % passing a certain size fraction (e.g. % -75 μm in the product and feed). For the purpose of this thesis, the term reduction ratio will refer to the latter example, as described in equation 2.5. Equation 2.5 can be used for any other screen size (not just 75 μm), granted that the specific % passing for that size is used. The gradient of the relationship between reduction ratio and specific energy was taken as an indication of the grindability of the ore: The greater the grindability, the more improved the reduction ratio will be at a particular specific energy. This technique can also be used to compare different milling conditions to identify optimum operating parameters. Feurstenau and Abouzeid (2002) also used simple techniques such as the analysis of particle size distribution curves of the obtained mill product to identify conditions where the greatest grindability was experienced.

$$\text{reduction ratio} = \frac{P_{80}}{F_{80}}$$

or

$$= \frac{\%\{-75\mu m\}_{product}}{\%\{-75\mu m\}_{feed}} \qquad [2.5]$$

Even though this method of using the reduction ratio is advantageous in that it considers the influence of the amount of particles already present in the feed, it has limitations similar to those described by Musa and Morrison (2009). The reduction ratio will be exponentially high if there are few particles in the reference size range of the feed. This is because it is the denominator in the relationship described in equation 2.5. To try to overcome this limitation one can consider reduction efficiency in a similar manner as operating efficiency described above. The reduction efficiency can be thought of as the ratio between the amount of particles in a size class that have actually been generated across the mill relative to the maximum amount that could have been generated. The maximum that could have been generated is considered to be 100% of the material passing that size class in the product less whatever fraction was present in the feed. In this manner the limitation of having too few particles in the reference size range in the feed is less pronounced than in the calculation of the reduction ratio. For the rest of this thesis, this reduction efficiency term will be

referred to as sieve efficiency and will be defined for the % -75 μm size range, as described by equation 2.6. Sieve efficiencies at other screen sizes can be calculated by adapting equation 2.6 to use the specific % passing values at that screen size.

$$\text{sieve efficiency} = \frac{\text{actual amount generated}}{\text{maximum possible generation}} = \left(\frac{\%\{-75\mu m\}_{product} - \%\{-75\mu m\}_{feed}}{100 - \%\{-75\mu m\}_{feed}} \right) x100\% \quad [2.6]$$

2.5 DESCRIPTION OF THE UG2 ORE TYPE AND ITS TREATMENT IN GRINDING CIRCUITS

The aim of this section is to understand the specific characteristics and challenges associated with the treatment of the UG2 ore type and the particular grinding requirements that are essential to successfully process this ore type. In order to fully understand this, one first needs to look at the PGM industry and the differences between the PGM ore types mined in South Africa. The particular complexities associated with the treatment of UG2 ores in grinding circuits is then investigated as the hypotheses in question are focused around the circuit orientation of the UG2 grinding circuit and the effect of grinding on the chromite fraction of the UG2 ore.

To start with, the platinum group metals (PGM's) are platinum (Pt), palladium (Pd), rhodium (Rh), ruthenium (Ru), iridium (Ir) and osmium (Os). According to the Newell (2008, parts 1 and 2) South Africa is the leading PGM producer in the world and supplied over 80% of the world's PGM needs in 2006. The massive resource of PGM's in South Africa arises from the Bushveld Igneous Complex (BIC), which is described by Newell (2008) as being a platinum-rich layered mafic intrusion. Two main economic layers formed from the slow cooling of the BIC, namely the Merensky and Upper Group 2 (UG2) reefs. A third PGM horizon formed in the northern limb of South Africa and was a much thicker and altered reef close to the surface. This ore body is referred to as Platreef.

The differences between these reef types are significant, as alluded to by Rule (2011). Rule (2011) further mentions that the difference in mineralogy between the reef types largely affects the recovery efficiencies of the ores through regular mineral processing operations. The Merensky reef was the first to be mined, back in 1926. The main reason for this was that it was a shallower reef,

generally had higher head grades with higher platinum ratios and was easier to process with better achievable recovery efficiencies. The UG2 reef has only been processed since the 1980's. According to Rule (2011) there has been a drastic shift in the milling profiles for Anglo American Platinum, the world's leading platinum producer. The company's mining plan used to be based wholly on the Merensky reef in the 1980's. However at the time that the paper was presented, the UG2 reef made up over 50% of the treated ore, followed by the Platreef ore. This movement from Merensky to UG2 is also mentioned by Valenta and Mapheto (2010).

This difference in recovery efficiency between the Merensky and UG2 ore types is of interest here. It would be in the best interest of any business to try to improve the recovery efficiency of its operations as this would mean more ounces produced for the same amount of treated material. UG2 and Platreef are more complex in terms of mineralogy. Valenta and Mapheto (2010) describe UG2 ore as platinum bearing chromitite ore. The main gangue species are chromite and silicates. Rule (2011) also describes the UG2 reef as having a bimodal form, meaning that the matrix is a mixture of silicate minerals and chromite spinel minerals in the chromitite reef. Cr_2O_3 is used as an indicator of the chromite content in UG2 ore. The occurrence of PGM's is predominantly in the silicate matrix in between the chromite spinels. UG2 contains only trace amounts of base metal sulphides (BMS) which are of significant importance as the PGM minerals are usually associated with them. The PGM minerals in UG2 are complex and are quite small. They rarely exceed 30 µm and the average grain size can be as fine as 6 µm, according to Valenta and Mapheto (2010). They also report that the chromite content can vary from 25% to 40%. The PGM grade can vary from 2.0 gpt to 5.5 gpt. The smaller sized PGM minerals and the fact that these minerals tend to be far less associated with the larger and more easily floatable sulphides (which would be more typical in Merensky ores) thereby decrease the ease with which the UG2 and Platreef PGM minerals may be recovered. This is also compounded by the UG2 and Platreef head grades being lower than that historically received from Merensky reefs. According to Rule (2011) the average head grade received reduced by around 42% from 1999 to 2010.

Mineralogical analysis reported by Rule (2011) determined that the majority of losses from UG2 operations were due to incomplete PGM liberation and to losses of very fine (<10 µm) but liberated PGM minerals. Napier-Munn *et al*. (1996) describe liberation as a measure of the association of a particle with other minerals or particles. A locked particle is one in which the mineral of interest is completely surrounded by another mineral and thus has poor liberation. A fully liberated particle is thus just the particle itself with no other mineral or species association. A partially liberated or

associated particle lies between fully locked and fully liberated conditions and depends on the amount of the particle being surrounded or attached by the other minerals. This emphasises the importance of liberating PGM minerals in a UG2 ore being treated, to improve plant extraction efficiencies. However the excessive generation of sub 10 µm particle sizes has to be limited as these tend to be more difficult to recover in the flotation separation process (even for liberated particles), as indicated by Rule (2011) in the mineralogical analysis of the tailings streams of UG2 operations. Thus the design of the grinding circuit for the processing of UG2 ore is of vital importance to ensure that the best particle liberation and size is presented to the flotation separation process to maximise PGM recovery.

The other challenge associated with the processing of UG2 ore is the high chromite content. Valenta and Mapheto (2010) as well as Minnaar, Smit and Terblanche (2005) describe how the high amounts of chromite in the feed affect the % of chromite in the final concentrate produced after the flotation process (a separation process based on sulphide flotation and hydrophobicity of mineral particles) and this causes major downstream operational issues at the smelting stage. This effect is significant enough such that smelters have had to put strict specifications of maximum chromite levels in concentrate received, and carefully manage the blending of UG2 concentrate with Merensky and/or Platreef concentrate to control the levels of chromite in the furnace feed. High levels of chromite in the concentrate smelted results in the build-up of highly refractory chrome spinel layers. This affects the separation efficiency and operation of the furnace. It also affects furnace availability and operating costs, as reported by Philips, Jone and Chennels (2008).

The design of a grinding and separation circuit to efficiently treat UG2 ore will then have to be able to successfully address the issues mentioned above. In this regard, the mill-float-mill-float (MF2) circuit had been adopted to ensure that the ore undergoes two stages of size reduction and subsequent flotation to try and maximise recovery efficiency, as described by Hinde and Kalala (2009). They also mention that chromitite ore is very friable and can be easily broken at low energies to liberate the chromite grains. This is consistent with what was reported by Bueno, Powell, Kojovic, Shi, Sweet, Philips, Durant and Plint (2011), who performed test work on UG2 ore in an autogenous (AG) mill on a pilot plant scale. They blended the UG2 ore with mined waste (mainly silicates) to try to quantify AG milling suitability for this application, and in so doing tried to model the different breakage rates of the chromite and silicate fractions in the ore. Rock breakage tests showed that the UG2 ore was fairly soft and the results for the waste indicated that it was much more competent than the UG2. For the individual component hardness comparison, they refer

to the silicate being hard and chromite being soft. It would seem that this is counter to what was inferred from Rule (2011), but these observations should be taken in the context of their application. When impact type breakage, which is characteristic of AG mill operation, is prominent the UG2 chromitite ore is friable in nature and breaks from the size of rocks to fine particle sizes quite readily. However, when dealing with more abrasion or attrition type breakage which is in the size fraction close to the grain size of the chromite particles, the chromite fraction is more difficult to reduce than its associated silicate neighbour. Thus when dealing with breakage in an AG mill scenario, as Bueno *et al* (2011) are referring to, the UG2 ore itself will exhibit good breakage rates but the waste material in the feed, which is predominantly silicate, will be more competent and difficult to break down. However, when addressing finer grinding where attrition and abrasion are more characteristic, such as the regrind milling conditions as described in Rule (2011), the chromite fraction of the UG2 ore is more resistant to breakage than the silicates because of the closeness to the particle size to the grain size of the chromite minerals.

Hinde and Kalala (2009) mention that an important lesson learnt from the review of the design of UG2 plants was the deportment of chromite and silicates in the secondary milling stage. The mainstream flow after primary milling and flotation would go through a hydrocylone for dewatering and size separation before entering the secondary mill, as per the MF2 circuit. After primary milling and flotation, the chromite was well liberated and had little PGM association. Most of the PGM's were associated with or locked in the silicates. The liberated chromite has a much higher density than the silicates and thus tends to preferentially report to hydrocyclone underflow, while the lighter silicates with the associated PGM's are expected to report to the overflow, as also mentioned by Rule (2011). Hinde and Kalala (2009) further mention that the desirable outcome would be to grind the silicates finer to liberate the locked PGM's to maximise recovery efficiencies, and to also minimise the energy spent in milling barren chromite. This led to the preference of running the regrind or secondary milling section in open circuit to prevent the over grinding of chromite. By limiting the over grinding of the chromite, the chances of recovering the chromite into the final concentrate from the flotation stage is lessened. This is because the major driver for chromite recovery in the flotation process is through entrainment, which is defined by Valenta and Mapheto (2010) as the "non-selective physical sub process where solids and water are transferred to the froth in the bubble lamella and bubble interstices". Finer sizes of chromite particles would be easier to entrain or be carried to the froth phase by water. Thus the over grinding of chromite would not only be an inefficient use of milling energy, but also propagate increased chromite in final concentrate by increasing the chance of recovery through entrainment in flotation. Furthermore the recovery of

chromite to the concentrate may be limited through the use of different technology in the flotation circuit, as described by Minnaar *et al* (2005). From the above the possibility of looking at expending less milling energy on the grinding of barren chromite would be advantageous in a UG2 regrind milling circuit, as described by the hypotheses of this study.

As a result of losses of PGM's in the tailings streams due to locked PGM particles in the silicate matrix as described by Rule (2011), further grinding of the silicates in particular was required to liberate these locked PGM's. This was not being achieved from the conventional ball mill due to fineness of the PGM grain size in UG2 ore and the limitations that the ball mill can grind to, as described by Partyka and Yan (2007). This then led to the development and roll out of fine grinding technology in the form of horizontally stirred milling at Anglo American Platinum. Xstrata Technologies developed the IsaMill to achieve much finer grinds through much higher energy intensities within the mill. The selection of the feed stream to the IsaMill circuit was a critical design consideration because as mentioned above, the locked PGM's in the large silicate particles need to be liberated but the large chromite particles are not to be ground finer to prevent chromite recovery through entrainment in the flotation section. The overflow of the first stage cyclone before the secondary mill was thus considered a good feed stream for the IsaMill circuit on a UG2 operation due to the presence of large silicates and the expected absence of coarse chromite particles. This formed the basis of the circuit change experienced at Waterval UG2 concentrator and will be discussed further in the methodology chapter. It is critical to note here that it becomes quite evident that the entire circuit effectiveness is dependant on the efficiency of the split at this hydrocyclone of silicates and chromites. Also, through the introduction of this circuit change, the secondary mill would not be performing according to the initial design specifications and thus there would be room for improvement in terms of its operation and efficiency, as described by the hypotheses of this study.

2.6 SUMMARY OF CHAPTER

The topics reviewed in this chapter are mill load behaviour, mill load measurement, techniques for analysing mill efficiency and the description of the UG2 ore type. The behaviour of the mill load was considered in terms of:

- charge shape with shoulder and toe position
- mill speed
- ball filling
- ball size
- slurry % solids
- slurry hold-up
- liner wear and design.

Various methods of measuring the mill load and understanding the motion of the load were described. These range from the classical stoppage and routine measurement inside the mill to advanced on-line conductive and inductive sensors within the mill.

The techniques used to analyse mill performance that were described include:

- grind across the mill
- operating efficiency
- specific reduction energy
- reduction ratio
- sieve efficiency

The different types of PGM bearing ore were described. Particular details regarding the UG2 ore type is discussed. The differences in the ore types highlights the need for them to be processed in different manners, thus the circuit configuration for a typical UG2 operation is explained. Of significance to this study is the difference between the silicate and chromite fractions in this ore type.

3 METHODOLOGY

3.1 PREFACE

This chapter introduces the method applied in performing the test work for this study. It begins with a description of the process at the plant where the test work was carried out. The circuit that was surveyed is then compared to the circuit before the introduction of the IsaMill, and the differences highlighted so as to understand the background to the first hypothesis presented in this study. Thereafter the process equipment involved in the part of the circuit that this study was focused around is discussed, as well as the control systems employed during the surveys conducted. The on-line ball and pulp load sensor used in this study, the Sensomag, is described. The experimental parameters and survey protocol are discussed so that an understanding is obtained for what was done in this investigation and how it was carried out on an industrial scale. Finally, the method of obtaining the mill discharge sample is considered and the verification of this sample as being representative is presented.

3.2 PROCESS DESCRIPTION

3.2.1 Current process

The test work for this study was carried out at Waterval UG2 Concentrator, which is an operation of Rustenburg Platinum Mines Ltd (RPM). The mine is owned by Anglo American Platinum Limited, which is a subsidiary of the Anglo American PLC. The operation is based in Rustenburg, which lies in the North-West Province of South Africa. The Concentrator was designed to treat 400 ktpm of platinum bearing ore from the UG2 reef. This is a chromitite reef with PGM content. The Concentrator receives ore from various shafts, owned by RPM, in the Rustenburg region.

The process is a mill-float-mill-float (MF2) setup, which simply means that there are two stages of milling preceding two respective stages of flotation, with the final product being in the form of a Platinum Group Element (PGE) rich concentrate. The surveys in this study were focused around the ball mill in the secondary milling stage of the process. Unrecovered material, or tailings, from the first stage of flotation forms the feed to the secondary milling circuit. The secondary milling circuit is split into two separate parallel streams with the use of a set of hydro cyclones. The cyclone overflow, containing the less coarse and less dense silicate rich fraction, is sent to the IsaMill circuit to undergo Mainstream Inert Grinding (MIG). The cyclone underflow, containing the coarser and denser chromite rich fraction, is sent to the secondary ball mill. The ball mill is in open circuit, meaning that the mill product is not classified in any way and there is no material circulated back to

the mill. This is typical of a secondary milling circuit on a UG2 application and it is to prevent the build-up and over grinding of the unwanted coarser and denser chromite rich fraction of the ore. The secondary mill discharge is combined with the IsaMill circuit final product stream in the secondary mill discharge sump, and is then pumped to the secondary rougher flotation cells for the final stage of flotation separation, as illustrated in figure 3.1. There is a mill dilution water line feeding directly into the feed hopper of the secondary mill which can be used to adjust the in-mill density as required.

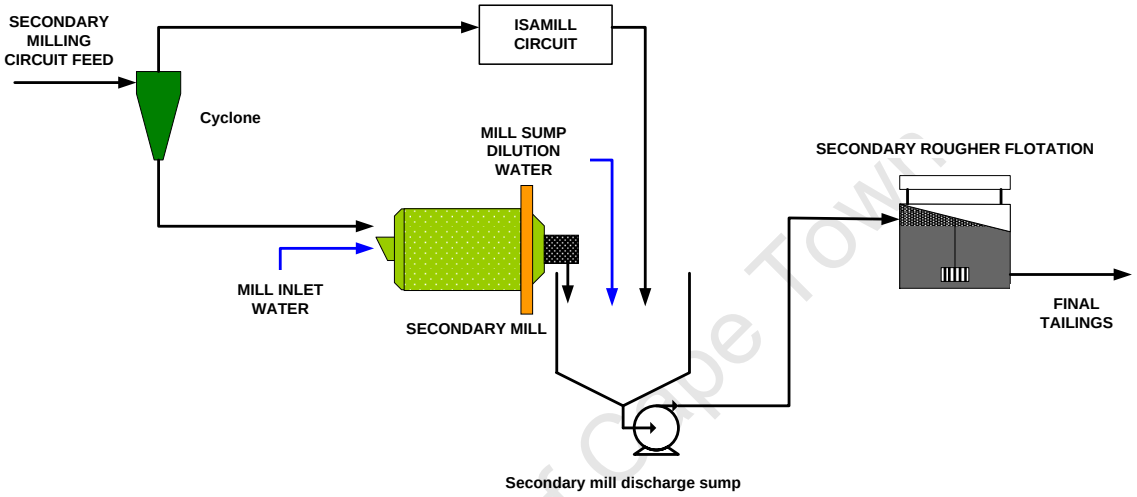

Figure 3.1 Schematic of the Waterval UG2 Concentrator secondary milling circuit post IsaMill inclusion

3.2.2 Circuit before IsaMill introduction

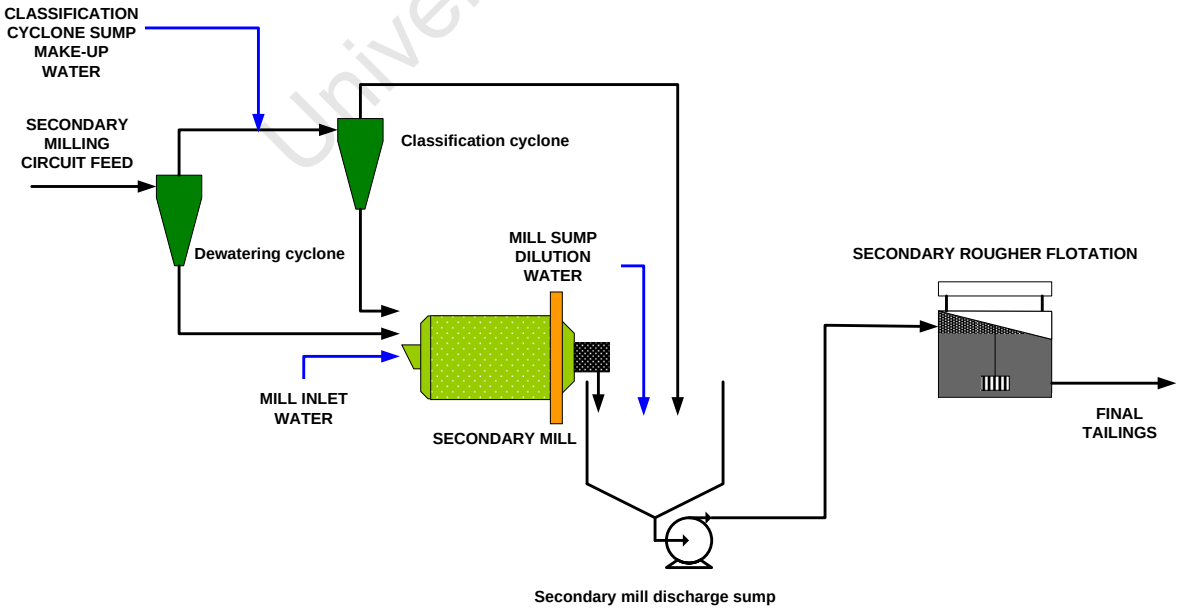

Figure 3.2 Schematic of the Waterval UG2 Concentrator secondary milling circuit before the inclusion of the IsaMill

The original circuit design did not include an IsaMill circuit. The IsaMill circuit at Waterval UG2 Concentrator was commissioned in 2007. Prior to this there would be two stages of cyclone separation before the secondary mill. The overflow of the first stage cyclone (dewatering cyclone) would form the feed to the second stage cyclone (classification cyclone) and both sets of cyclone underflows would make up the feed to the secondary mill. The overflow of the second stage cyclone bypassed the secondary mill and reported directly to the mill discharge sump, as indicated in figure 3.2. It is also important to note that when the IsaMill circuit is bypassed (for routine maintenance or IsaMill offline etc.), the old circuit prior to IsaMill installation is run for that duration.

The biggest effect of this circuit change for the secondary mill is the amount of material being fed to the mill. This means that since the IsaMill circuit was commissioned, the amount of material feeding the secondary mill has been lower than before the IsaMill introduction. Thus there is an opportunity to optimise the performance of the secondary mill circuit following this circuit change.

3.2.3 Process equipment

Ball mill

The tests for this study were performed around an industrial ball mill. The mill was in a secondary or regrind milling application with an overflow discharge configuration. The mill was manufactured by Fuller Vecor and is 7.32 m in diameter by 9.45 m long (EGL). The installed power is 10.4 MW and it is a fixed speed mill (operating at around 75% critical speed). The mill has rubber internal liners. The technical specifications of the mill are summarised in table 3.1. At the time of the surveys, typical mill operation was at around 30% steel ball filling by volume, with 40 mm diameter steel balls used to top up the ball charge. Actual mill load was measured from load cells installed below the trunnion bearings of the mill. Figure 3.3 shows a picture of the secondary mill at Waterval UG2 Concentrator.

Table 3.1. Technical specifications of the secondary ball mill at Waterval UG2 Concentrator

Size	7.32 m diameter x 9.45 m (EGL)
Make	Fuller Vecor
Application	Secondary / regrind mill
Installed Power	10.4 MW (2 x 5.2 MW motors)
Discharge Configuration	Overflow
Liner type	44 rows of rubber lifter bars with rubber shell plates in between
Mill Speed	75% critical (fixed speed)
Ball Size	40 mm (top-up size)

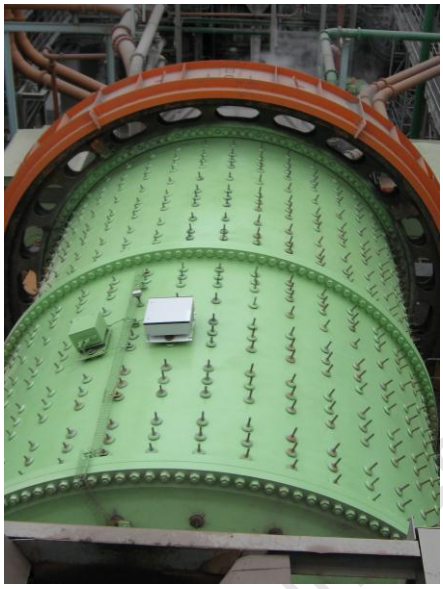

Figure 3.3 Picture of the secondary ball mill at Waterval UG2 Concentrator

Figure 3.4 Picture of the secondary milling circuit cyclone nest at Waterval UG2 Concentrator

Cyclones

The first stage cyclone specifications are given in table 3.2. These are in a cluster of five and at the time of the surveys all five cyclones were run in typical operation. The cyclones were vertical in orientation, as shown in figure 3.4. The cyclone operating conditions were controlled through an advanced process control system, and will be described in more detail in the next section. Changing cyclone configuration or operating numbers was not an option in this study due to site operational requirements and downstream effects.

Table 3.2. Technical specifications of the secondary milling circuit cyclones at Waterval UG2 Concentrator

Make	Multotec - HC
Orientation	Vertical
Number in nest	5 (all 5 open in normal operation)
Operating pressure	75 kPa
Diameter	500 mm`
Inlet diameter	196 mm
Cylinder length	430 mm
Vortex finder diameter	224 mm
Spigot diameter	82 mm
Cone angle	20 mm

3.2.4 Control equipment

The Sensomag®

The Sensomag unit was developed by Magotteaux as a mill optimisation and management tool. The objective of the unit is to get an online measure of the ball load and pulp filling within a running mill. This information, together with some other parameters for mill optimisation, is calculated from the shoulder and toe angles for the balls and pulp, as measured by the sensors of the Sensomag unit. The other parameters will be discussed later in this section.

The sensors of the unit measuring ball and pulp proximity are found within a beam that is placed in a specialised liner inside an operational mill. Figure 3.5 shows the specialised liner housing the beam containing the sensors inside the secondary mill at Waterval UG2 Concentrator and figure 3.6 shows a schematic of the sensor within an operational ball mill. The beam is made from a special wear resistant polyurethane material. There are two types of sensors in the beam – one that measures the ball proximity and one that measures the proximity of the slurry or pulp. The digital proximity sensor measuring the presence of ferromagnetic balls is an inductive proximity sensor. As described in Keshav *et al* (2011), the inductive sensor generates a magnetic field and any metallic object entering the sensor's magnetic field causes a variation in this field. The amplitude of this variation is detected by electronics in the sensor itself. The range of the inductive sensor is determined by the size of the magnetic coil within the sensor that generates the magnetic field, and

varies from as close as a few millimetres to some centimetres away. The presence of slurry or pulp is measured by a conductive sensor. A metallic, double-electrode conductive sensor conducts a current when in the presence of slurry and gives an indication of the pulp position within the mill.

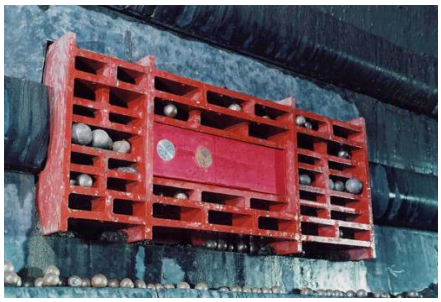

Figure 3.5 Specialised liner housing the beam with sensors of the Sensomag unit at Waterval UG2 Concentrator

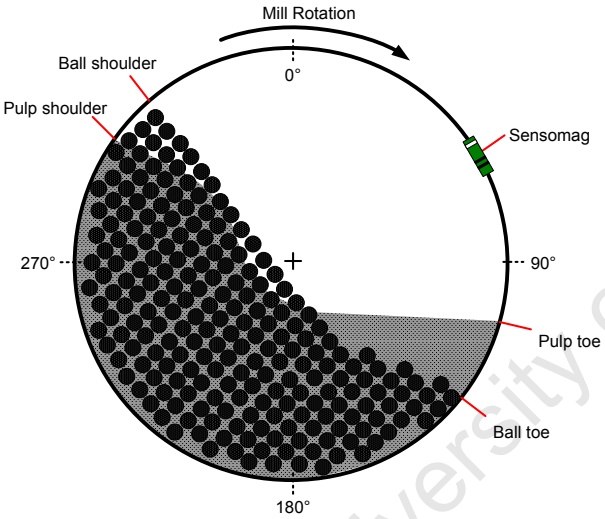

Figure 3.6 Schematic of angles obtained from the Sensomag

Figure 3.7 The components of the Sensomag installation on the shell of the mill

As mentioned above, the sensors sit within a liner inside the mill. Thus it picks up signals with every revolution of the mill for one particular segment along the length of the mill. The raw signals from every revolution are sent through a wireless transmitter on the outside of the mill shell to a central processing unit nearby the mill. The battery pack and network box are also placed on the outside of the mill shell, as shown in figure 3.7. Also measured with each revolution is a fixed reference angle via a proximity switch on the mill shell, such that the shoulder and toe angles of the ball and pulp filling may be consistently determined relative to this reference point. The highest point to which the charge is lifted by the motion of the mill is referred to as the shoulder and the point where the charge meets the mill shell across from the shoulder is referred to as the toe. The

shoulder and toe angles can be explained by figure 3.6, and are simply the angles at the top and the bottom of the charge, respectively, relative to the vertical position (0°) of the rotating mill.

Magoload® System

Another unit developed by Magotteaux is the Magoload. This unit is used to control the ball addition rate to a ball mill and is in operation at the secondary mill of the Waterval UG2 Concentrator. It consists of a bulk ball loading bin, into which the operator loads the steel balls to be added to the mill. The balls are then added into a smaller bin on load cells via a feeder. Once a certain mass is achieved in the smaller bin, the balls are added to the mill via the mill feed chute. The information from the load cells is fed to a central programmable logic controller (PLC) for the Magoload, which determines the frequency of ball addition from the required ball addition rate. Figure 3.8 shows some detail of balls being fed from the bulk ball loading bin into the smaller bin via a feeder.

Figure 3.8 Detail of the smaller ball loading bin on the Magoload unit

A further level of control can be achieved by incorporating the Sensomag and Magoload units into a combined ball addition and filling degree control system. The measurements as obtained from the Sensomag (the ball shoulder and toe angles in particular), together with operational data (e.g. mill power) can be used in a model to predict the volumetric ball filling degree of the mill. This calculated filling degree needs to be verified against manual measurements of the ball filling during opportunities such as mill stops, planned maintenance shut downs etc. to calibrate the model used to predict the filling degree. Verification of the model in terms of measured against predicted filling degree is shown in Appendix B. The calculated filling degree is compared to the required filling

degree set point and the ball addition, via the Magoload, is then controlled in accordance to this. Should the calculated filling degree be lower than the set point, the Magoload will add steel balls, according to the required addition rate, until the set point is achieved. Similarly, the Magoload will hold back on ball addition should the calculated filling degree be greater than the desired set point. In this way, experiments under controlled conditions at various required ball filling degrees could be undertaken for this investigation due to the effective ball addition control around the ball mill resulting from the integrated Sensomag/Magoload systems. This integrated system is schematically represented in figure 3.9.

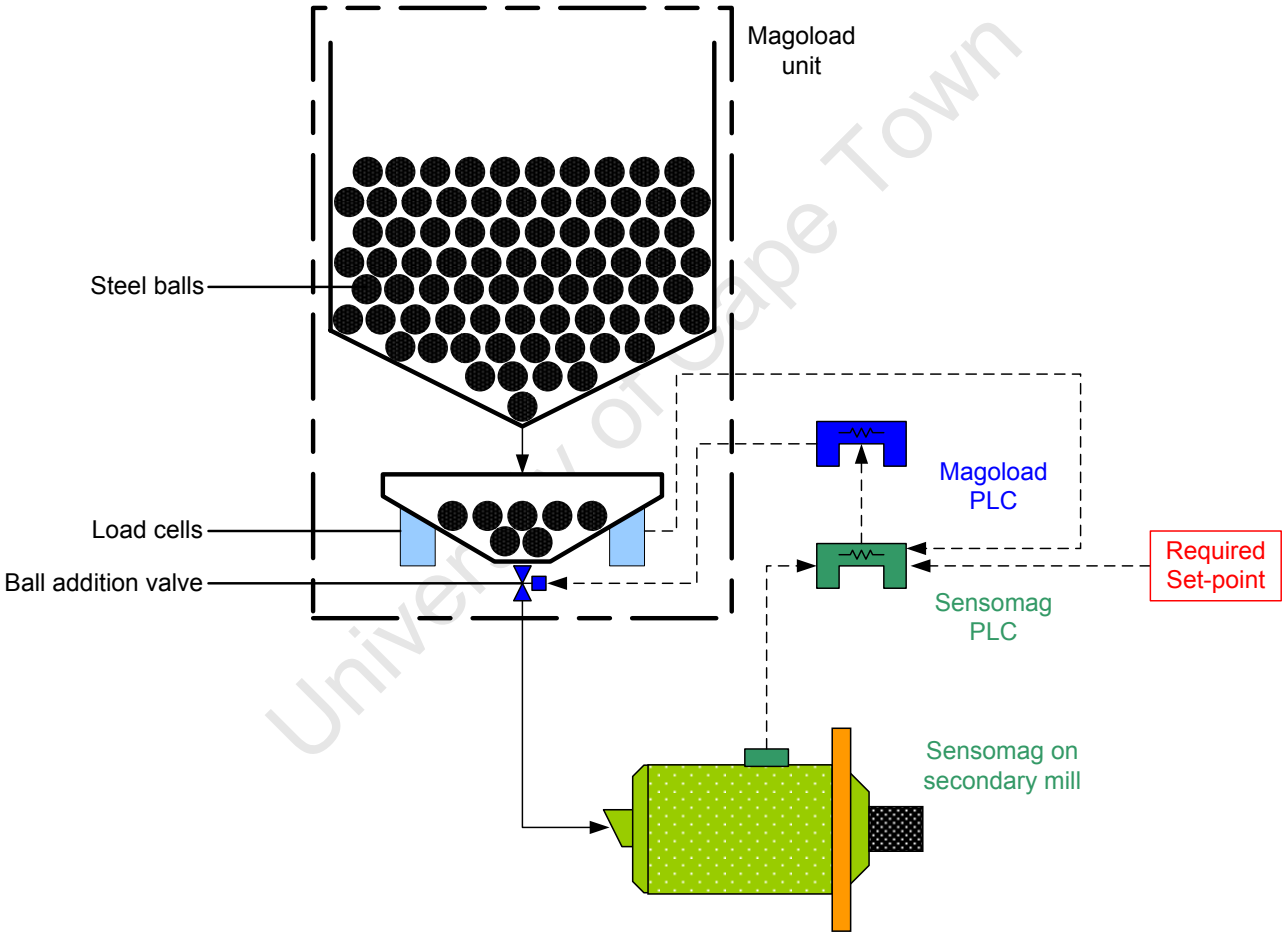

Figure 3.9 Schematic of the ball addition and filling degree control system at Waterval UG2 Concentrator

Advanced Process Control

The advanced process controller (APC) is a multi – variable controller developed within Anglo American Platinum. In this application it was used on the surge tank that fed the first stage cyclones of the secondary milling circuit. The aim of the controller was to stabilize the density and flow rate

(and hence cyclone operational pressure) to the cyclones by utilising the sump's surge capacity. Following the introduction of the controller, notably stable operation around the cyclones was observed. The number of cyclones operating in the nest however could not be a controller variable. A cyclone cluster of only 5 cyclones on this application did not leave sufficient resolution for the opening and closing of cyclones to achieve target pressure set points. The change from a single cyclone opening or closing would simply be too great to have finer control opportunities.

3.3 EXPERIMENTAL PARAMETERS

This section aims to explain the various parameters investigated through manipulation and measurement in order to study the hypotheses presented. In order to investigate the first hypothesis presented in this study, the manipulated mill operating conditions were varied to try and find the best operating conditions. These parameters were limited to in-mill pulp density (% solids by mass was used as a measure) and volumetric ball filling. These were adjusted through manipulating the amount of mill inlet water flow and by varying the steel ball addition rate to reach different ball fillings, as described in sections 3.2.1 and 3.2.4, respectively. The reason for only considering these two parameters was that they were the most common and available to be varied in terms of mill operation on site. The mill was a fixed speed installation so mill speed could not be varied. The ball size available was limited to site current practise; on an industrial plant any drastic changes would have to first be properly investigated and motivated. This is also the case for liner design. Due to the long lifetime of installed liner sets and the operational risk of changing liner design, this parameter was not investigated, except to the extent of worn versus new liners before and after a reline.

The standard mill operation at the plant was around 30% volumetric ball filling and between 68 - 72% in-mill solids (by mass). For the purpose of this study the targeted ball fillings were 25%, 30% and 33%. The in-mill % solids were targeted at 65%, 68%, 72% and 75% by mass. The range for the ball filling was limited by fears of compromised grind and hence product recovery efficiency at the low ball filling, and the available mill installed power at the high ball filling. For the in-mill % solids the range was limited again by the fear of compromised grind as well as maximum available flow for the inlet water at targeted low % solids. The high % solids limit was reached by running without any inlet water addition at all (around 75% solids).

There was however also a relining of the mill lifter bars that was planned within the survey period.

This allowed for another dimension to be explored within the experimental parameters, and the surveys before and after the relining could be compared to understand the effects of mill liner wear and profile on the mill charge behaviour and milling performance.

The measured responses from the surveys at the various conditions described above were particle size distribution, mass flow rate through the system, % solids at either end of the mill and species concentration through assay analysis for PGM and chromite. The characteristic operational mill monitoring parameters such as mill absorbed power, mill load (through load cells) and stream flow rates, as well as information from the Sensomag regarding shoulder and toe positions for the ball and slurry fractions, were obtained from the supervisory control and data acquisition (SCADA) system. This information was measured in order to investigate the other hypotheses presented in this study.

3.4 SURVEYS

This section describes the methodology used in the actual surveys performed in this study. By operating at each of the three ball filling and four % solids conditions, twelve survey conditions would be possible across the operating range. Table 3.3 describes the various targeted operating conditions for the different surveys. There was an additional two surveys performed pre-relining of the mill (survey 1 and 2) as well as one last survey for verification at typical plant operating conditions (survey 15) after the planned surveys at various conditions. This brings to total fifteen various surveys performed, each with a unique targeted operating condition in terms of ball filling, % solids and liner wear.

The desired in-mill % solids was attempted to be reached by varying the mill inlet water flow rate, as described in section 3.2.1. The water was set to a particular flow rate based on the mill feed tonnage in order to try and reach a desired in-mill % solids. There was no form on online control of in-mill % solids; hence the control was based on estimated calculations and operator control of the water flow rate. The actual in-mill % solids could only be verified from the sampling of the mill discharge.

The targeted mill ball filling conditions were obtained through the Sensomag and Magoload control system for ball addition, as described in section 3.2.4. The ball filling at each condition was verified by physical measurement within the mill at the monthly maintenance shut down.

Table 3.3 The range of target experimental parameters for this study

Survey No.	Date	Target ball filling	Desired inlet H2O flow (m3/hr)	Target in-mill % solids	RTD
Survey 1	27-Aug-09	30%	0	75%	Yes
Survey 2	27-Aug-09	30%	75	65%	No
Survey 3	17-Sep-09	30%	0	75%	Yes
Survey 4	17-Sep-09	30%	25	72%	Yes
Survey 5	18-Sep-09	30%	45	68%	No
Survey 6	18-Sep-09	30%	75	65%	No
Survey 7	14-Oct-09	25%	0	75%	Yes
Survey 8	14-Oct-09	25%	25	72%	No
Survey 9	15-Oct-09	25%	45	68%	No
Survey 10	15-Oct-09	25%	75	65%	Yes
Survey 11	04-Nov-09	33%	45	68%	No
Survey 12	04-Nov-09	33%	75	65%	Yes
Survey 13	05-Nov-09	33%	25	72%	Yes
Survey 14	05-Nov-09	33%	0	75%	No
Survey 15	27-Nov-09	30%	45	68%	No

For each survey, samples were taken for particle sizing as well as % solids analysis in order to investigate the performance of the mill at the various operating conditions. Residence time distribution (RTD) tests were also performed on seven of the surveys, as shown in table 3.3. Around 250 kg of fine table salt was added to the cyclone underflow stream and samples of the mill discharge collected at regular intervals. This was done with the objective of trying to understand the flow patterns and characteristics within the mill at different operating conditions, but is not a particular focus in this thesis. Pulp chemistry samples were also taken of the mill feed and discharge. These were analysed for pH, conductivity (mV) and temperature. This information could be useful in terms of understanding the effect of different mill operating conditions on the pulp chemistry – which could be significant for the flotation process downstream. Once again, this information will not be used as a particular focus point in this thesis.

The two streams sampled were the cyclone underflow (mill feed) and the secondary mill discharge. Manual cuts using a pelican type sample cutter were taken of the cyclone underflow to obtain the sample for particle sizing and % solids analysis. The flow rate of the cyclone underflow was a critical measurement to take as it proved to be the only measurable flow of slurry through the system. This measurement was performed with large plastic bags, a mass scale and a video camera for timing. The entire flow from a particular cyclone was captured in a plastic bag, and the sampling process was recorded with a video camera. The mass of the filled bag was measured with the scale. The time taken for that mass to be collected was obtained from the video frames as captured by the camera. The flow rate from each cyclone was captured in this manner and summed to get the total mass flow into the secondary mill for each survey. In trying to improve the accuracy of this method,

many iterations of sampling and recording were done per survey to reduce the standard error involved. The inlet water flow rate was retrieved from the plant SCADA system as there is a flow meter on the line. The mill discharge was sampled through a sampler installed below the trommel screen and in the mill discharge sump itself, and will be discussed in more detail in section 3.5. Figure 3.10 illustrates the positions where various samples were taken during the surveys. After each survey, the rest of the online mill circuit information (e.g. mill power, Sensomag shoulder and toe positions etc.) was gathered from the SCADA.

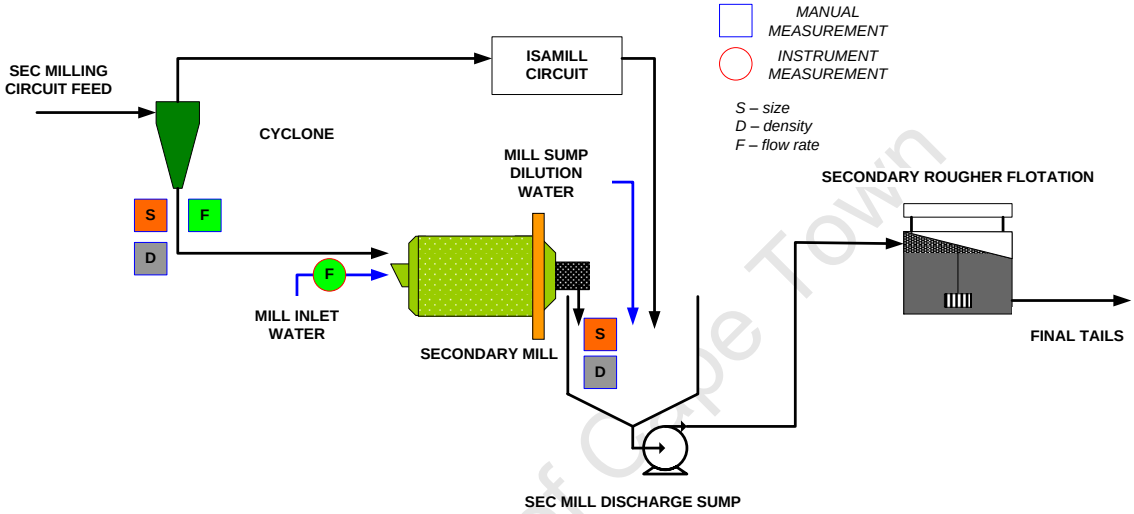

Figure 3.10 Sampling points around the circuit for the various surveys performed

3.5 MILL DISCHARGE SAMPLER DESIGN AND VERIFICATION

A critical part of being able to perform this study was to obtain an accurate sample of the mill discharge. This section explains how this crucial sample was obtained and investigates the confidence in how representative this sample was. The design of the discharge sump with the IsaMill product coming into it meant that obtaining a representative sample of the mill discharge presented a challenge. Space was very limited and conditions very harsh and aggressive for any conventional sampling to take place. As a result, a sampler was designed on site and installed within the sump itself. Figure 3.11 shows an illustration of the mill discharge sampler used for the surveys. The installation consisted of a simple collection trough directly below the discharge trommel that passed the mill discharge sample into a sloped pipe, which allowed the sample to gravitate out to the accessible sampling point on the side of the sump.

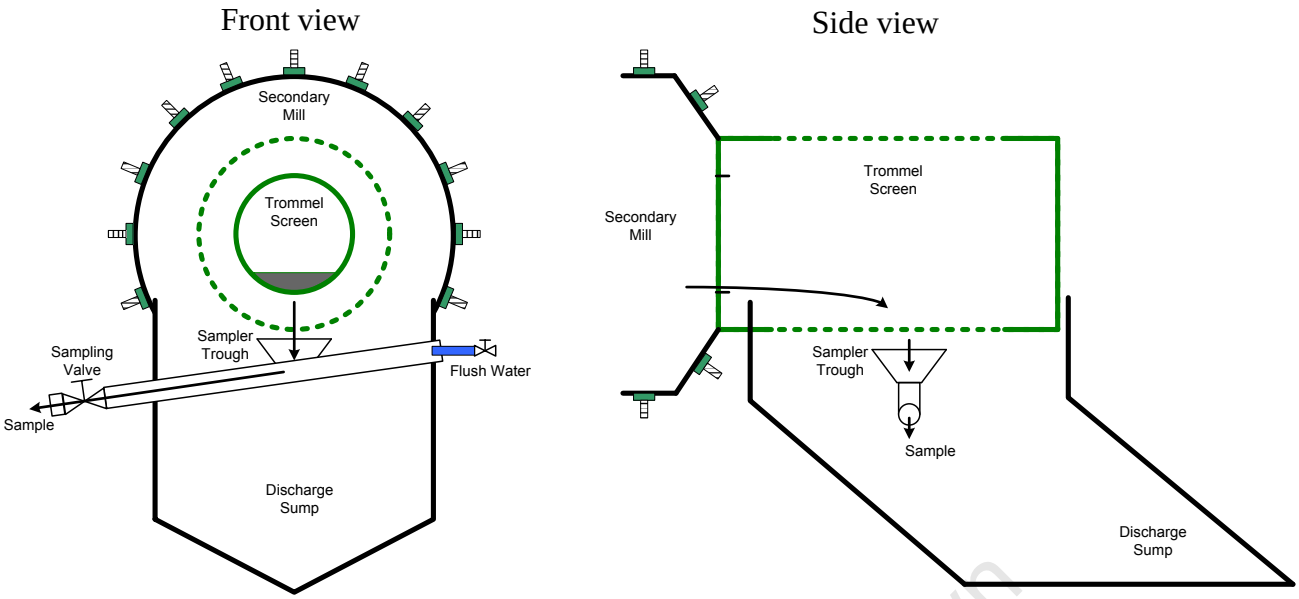

Figure 3.11 Illustration of the secondary mill discharge sampler

Due to the distance of the sampler trough from the beginning of the trommel screen, there were some concerns as to whether the sample collected would be representative and unbiased. A verification survey thus had to be performed to check the accuracy of the sample collected. This was done during a period of IsaMill maintenance where the circuit configuration was as described in section 3.2.2 (IsaMill circuit was bypassed). The second stage cyclone underflow now also formed part of the mill feed, and the overflow was sent directly to the discharge sump, as per the original circuit design. Thus a survey around the discharge sump itself could be performed as the second stage cyclone overflow as well as the secondary rougher feed (sump product) could be sampled and mass balanced. This result could then be compared to the sample obtained from the discharge sampler. Samples were analysed for particle size distribution, % solids and grade (PGM's and Cr_2O_3). The flows were obtained from instrumentation around the circuit and used together with the analysis results in the mass balance. JKSimMet® was used to mass balance the flows, % solids and particle sizes. The results from this balance are shown in figure 3.12. The experimental or measured data compares very closely to the balanced data, as shown by the particle size distribution curves. The assays were then used to further tighten the mass balance, and the resulting parity chart comparing the measured and balanced data is shown in figure 3.13. The points lie very close to the linear line, meaning that the measured and balanced values are very similar. Thus it can be considered that the sample collected from the discharge sampler does not have any form of bias, and can be assumed accurate and representative.

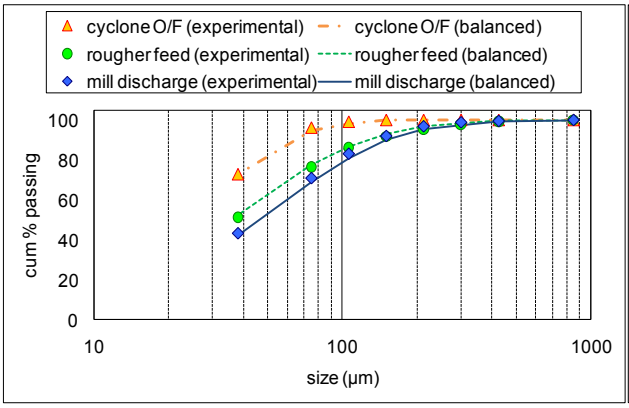

Figure 3.12 Particle size distribution curves for the experimental and balanced data from the sampler verification survey

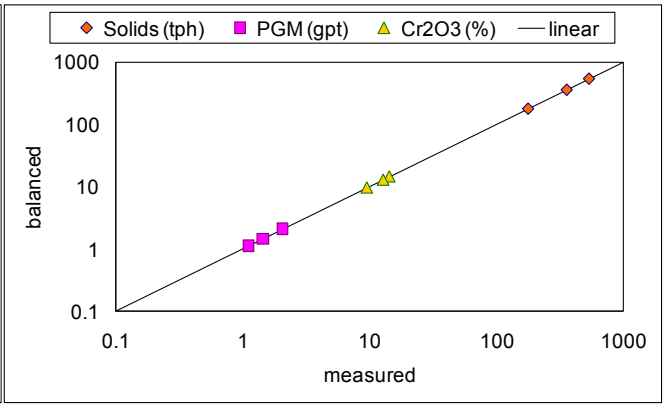

Figure 3.13 Parity chart showing the measured against the balanced values for the mass balance around the discharge sump

The verification survey proved the accuracy of the sampler. However, one further test was performed to measure the consistency of the sampler. A number of samples were taken in succession over a period of time and each sample density measured. Table 3.4 shows that the samples collected for two separate runs were consistent over the period of time, with the relative standard deviation for the two tests being as little as 0.43% and 1.11%. Thus it can be said with confidence that the samples obtained from the discharge sampler are consistent, accurate and representative of the actual mill discharge stream.

Table 3.4 Sample density results of two different runs for the check on sampler consistency

Measurement	Run 1 (kg/L)	Run 2 (kg/L)
1	2.26	2.22
2	2.26	2.24
3	2.26	2.18
4	2.28	2.24
5	2.26	2.24
6	2.26	2.26
7	2.26	2.24
8	2.28	2.26
9	2.28	2.26
10	2.26	2.26
Average	**2.27**	**2.24**
Standard deviation	**0.01**	**0.02**
Relative standard deviation	***0.43%***	***1.11%***

3.6 SUMMARY OF CHAPTER

This chapter has described the circuit at the plant where this test work was performed. The difference in the secondary milling circuit after the IsaMill introduction was discussed and promotes the notion of an opportunity to optimise the secondary mill operation due to changed circuit conditions. The secondary mill and cyclones around which the surveys were conducted were described. The Sensomag unit on the secondary mill gives on-line ball and pulp load measurements, as well as ball and pulp shoulder and toe positions. This was used together with the Magoload to control mill ball filling.

The fifteen surveys performed in this test work were done at three targeted ball fillings and four targeted in-mill % solids conditions. The range of ball filling and % solids that the surveys were restricted to was explained. Surveys were also done to compare the effect of worn and new lifter bars on mill performance around a relining. To address the hypotheses of this study, the results of the surveys around the secondary mill that were to be analysed included particle size, measured % solids, species concentration (assay), as well as circuit operational and control information such as mill power, shoulder and toe positions etc.

Finally, the obtaining of the mill discharge sample was identified as being crucial to isolate the performance of the secondary mill, and the difficulties in actually getting this sample were explained. The method of obtaining a sample from under the trommel screen within the discharge sump was explained and the samples obtained were verified by sampling and a mass balance around the discharge sump.

4 DATA AND RESULTS

4.1 PREFACE

The results and data acquired from the various surveys performed in this study are presented in this chapter. The general results for all surveys performed are presented in the first section. Thereafter the analysis focuses on different survey conditions (ball filling, slurry % solids and mill liner wear). The key aspect of this first section is to show the difference in milling performance across the different survey conditions so that optimal operating conditions can be identified. The discussion focuses on the particle size reduction and energy efficiencies obtained from the various surveys and conditions, based on the test matrix described in section 3.4.

The performance of the mill in terms of size reduction of the chromite and PGM fractions of the ore is considered in the next section. The results are presented in a similar format as in the first section, with the exception that the results are per species rather than for the general material passing through the mill.

The data acquired from the online ball and pulp load sensor are reported in the third section of this chapter. This is followed by a brief section on the model fitting of the experimental results obtained from this study. Finally the summary of the results is presented which forms the basis for the discussion chapter that follows. A summary of the survey results can be found in Appendix C.

4.2 GENERAL MILL PERFORMANCE FOR DIFFERENT SURVEYS

In this section results for basic mill performance are presented. The in depth results and analysis at varying operating conditions is considered in the next section. Figure 4.1 shows the particle size distributions (PSD) for the mill feed and discharge streams at the various surveys performed. Although feed particle size distributions are quite similar, variation can be seen in the discharge. The trend showing the percentage passing 75 μm in the feed and discharge samples taken across the mill from each survey is shown in figure 4.2. The operation uses this measure of grind to assess the milling circuit performance relative to a target grind. One of the reasons for using this particular measure is that it is an easily obtainable result (by simply wet screening in a lab) from a sample taken, and is a good benchmarking value for this sort of circuit, as discussed by Musa and Morrison (2009). The target grind passing 75 μm for the mill discharge sample was back calculated from the target tailings final grind, the IsaMill circuit grind and a simple mass balance around the mill discharge sump.

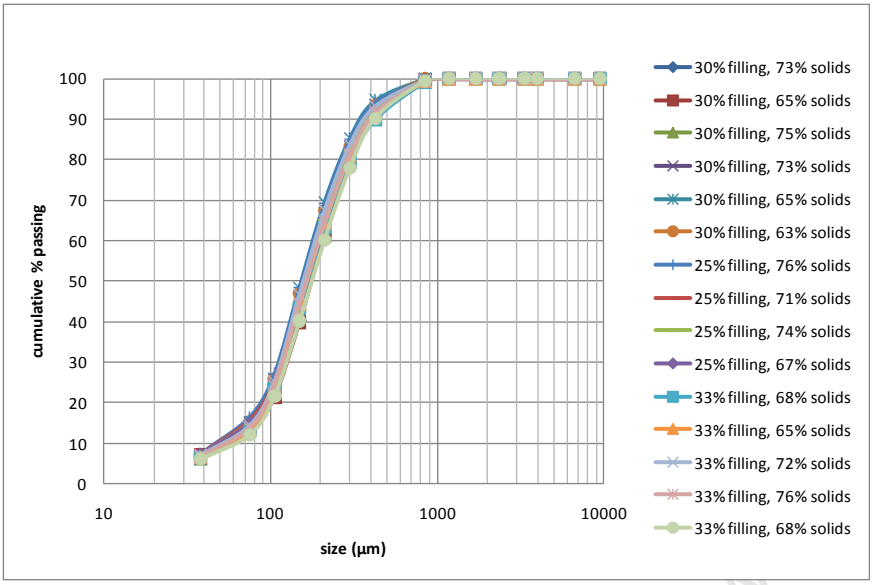

Figure 4.1(a) Mill feed sample PSD's for different survey conditions

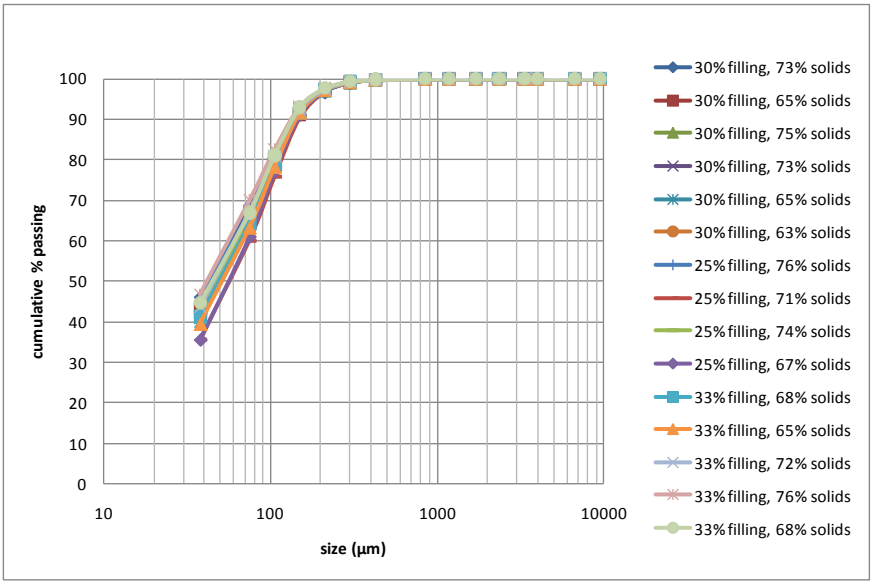

Figure 4.1(b) Mill discharge sample PSD's for different survey conditions

Figure 4.3 shows the specific energy required per survey condition. The specific energies obtained for the 106 and 75 µm sizes are very similar. The specific energy for the 38 µm size is however significantly greater than that of the other two size classes. Even though little variation in the feed was observed using the particle size distributions, the reduction ratio and sieve efficiencies are used to try and obtain more resolution, as described in section 2.4, and are presented for the various surveys.

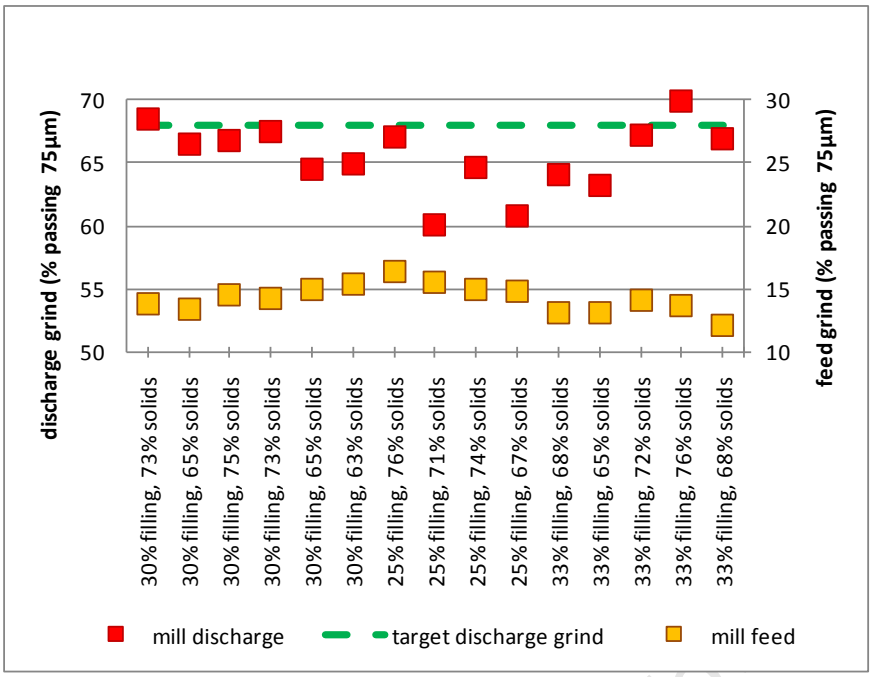

Figure 4.2 Grind % passing 75 µm for the survey mill feed and discharge samples

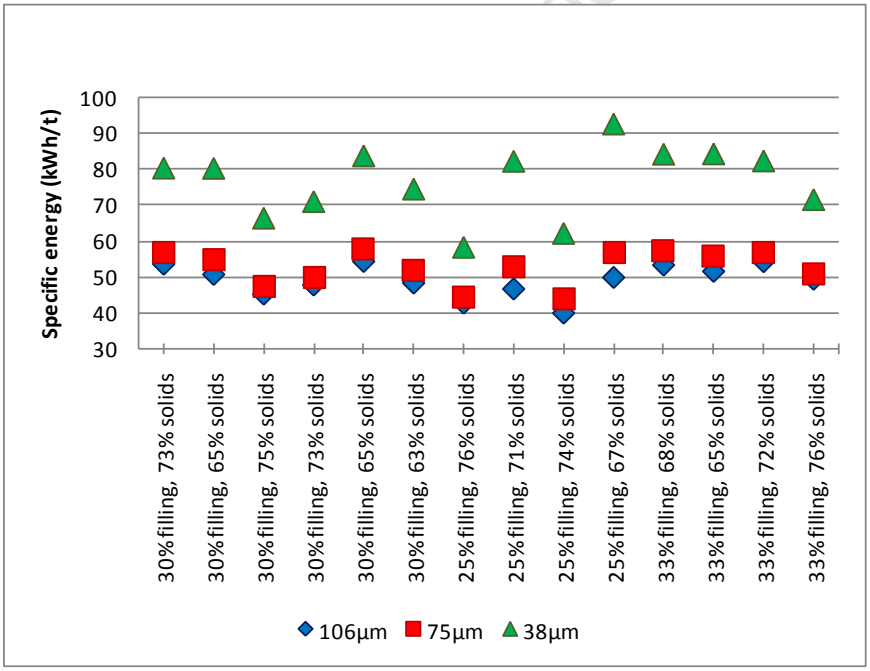

Figure 4.3 Specific energies at different size classes for the various surveys

Figures 4.4 and 4.5 show the reduction ratios and sieve efficiencies, respectively, for the surveys performed. The results are again presented for the sub 106, sub 75 and sub 38 µm size classes. For the purpose of this study the material below 106 µm will be assumed to have an improved chance of being liberated to minimise major PGM losses through locked particles and would no longer be considered as coarse particles, as described by Becker, Mainza, Powell, Bradshaw and Knopjes

(2008). The sub 75 µm fraction is the standard size class used in benchmarking the grind performance of the circuit, as mentioned already. The sub 38 µm will be considered as fine particles in this study – the target class wherein significantly improved PGM liberation is expected while the Cr_2O_3 particles are also expected to be liberated and sufficiently fine to increase the possibility of unwanted recovery through entrainment in the flotation process. In general the greatest reduction ratios are achieved in the sub 38 µm class and the lowest for the sub 106 µm fraction. There also seems to be a larger variation in reduction ratios within the smaller size classes than the coarser size fractions. The greatest sieve efficiency is obtained for the sub 106 µm fraction and the lowest for the sub 38 µm fraction. The variation in sieve efficiencies within the size classes is less pronounced than the variation in reduction ratios. Figure 4.6 shows the specific energy input per size fraction for the surveys. The sub 38 µm fraction has in general the highest specific reduction energy, while the specific energies for the 106 and 75 µm fractions are quite similar.

Figures 4.6 and 4.7 indicate how the net material generated and sieve efficiences, respectively, are influenced by the specific energy per size class for the surveys performed. Both graphs are expected to show a linear relationship originated at zero. The coarser size fraction exhibits a greater gradient than the finer size fraction. It should be noted that the linear trendline has to pass through zero at zero specific energy for this fit.

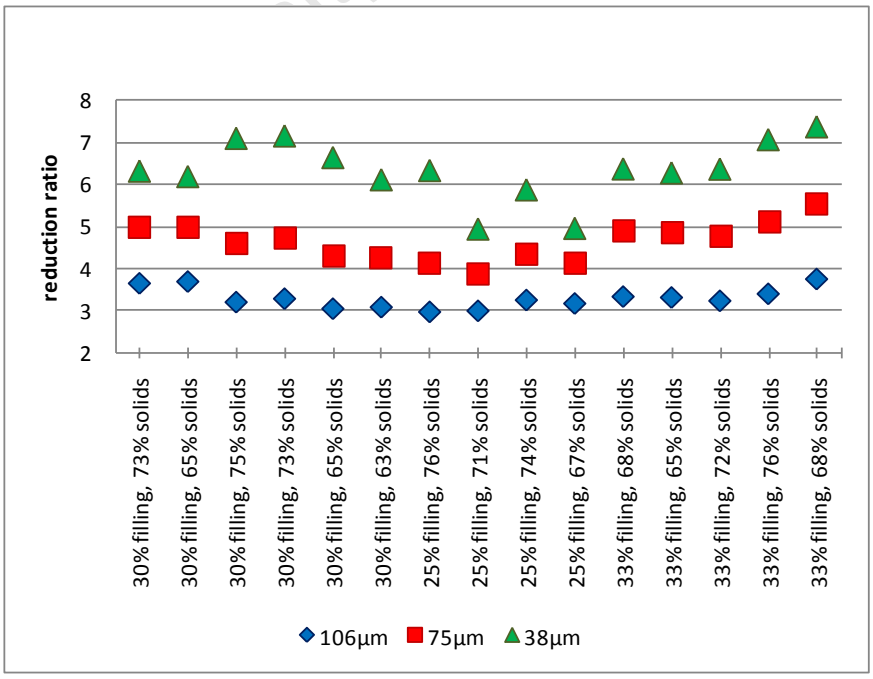

Figure 4.4 Reduction ratios at three size classes for the various surveys performed

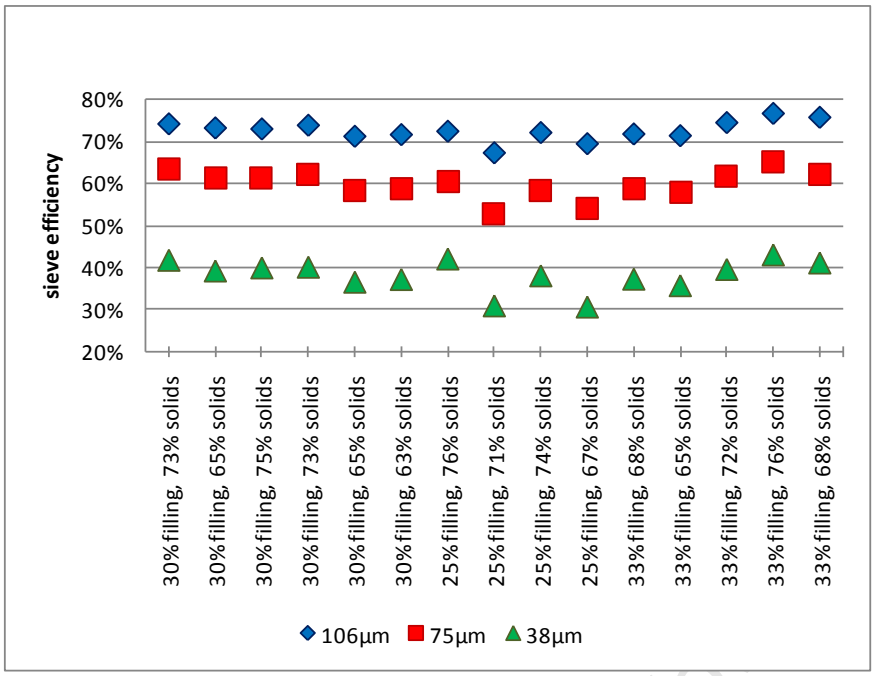

Figure 4.5 Sieve efficiencies at three size classes for the various surveys performed

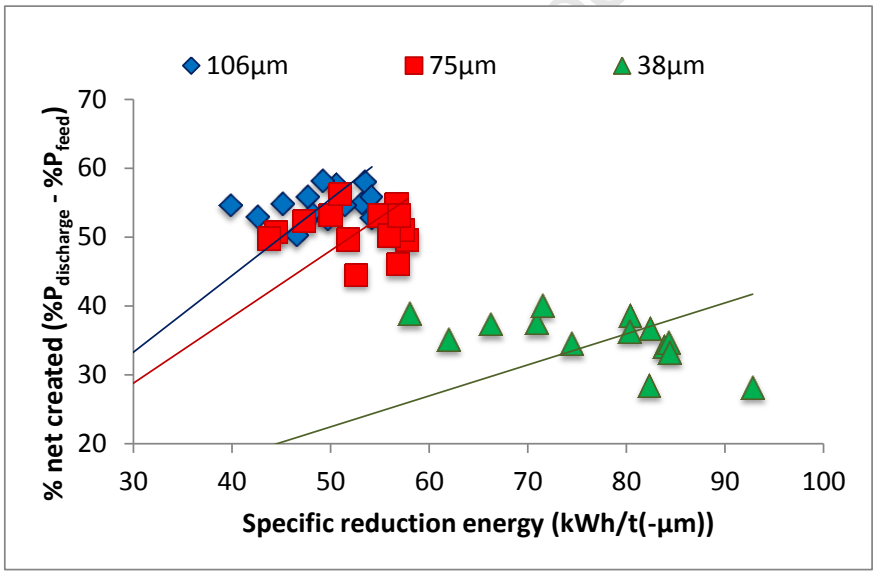

Figure 4.6 Net material created as a function of specific energy for the three size classes

In this section general results obtained from the surveys were considered in terms of mill performance. The next section will look more into detail with regards to the effect of the different operating conditions on mill performance.

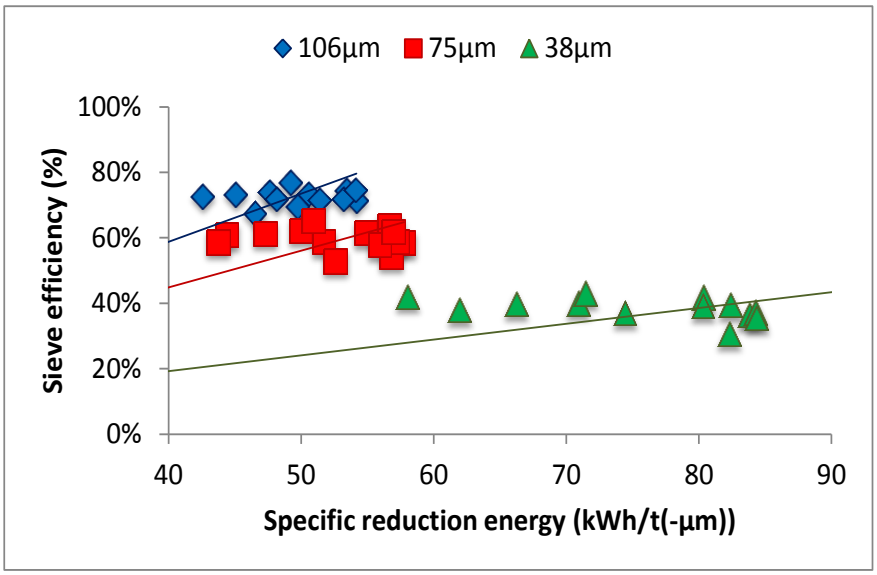

Figure 4.7 Sieve efficiency as a function of specific energy for the three size classes

4.3 CONDITION SPECIFIC MILLING PERFORMANCE

In the previous section the general mill performance results for the fifteen surveys was presented. The focus in this section is to understand the effect of specific milling conditions on performance. These varying conditions are primarily the ball filling and % solids; the secondary condition is the effect of old and new mill liners. Also, instead of presenting results for all three size classes, only the sub 75 µm fraction will be presented for reasons discussed in section 2.4.

The mill product grind for the various conditions of ball filling and % solids surveyed are separately compared to the target grind in figures 4.8 and 4.9, respectively. The grind performance seems to start peaking around 30% ball filling. The grind performance continues to increase as the % solids gets greater. Figure 4.10 shows both ball filling and % solids conditions on the same graph. The low ball fillings and the low % solids conditions appear to be furthest away from the target grind. The 67 – 73% (medium) and 63 – 67% (low) solids conditions seem to indicate a maximum in grind at around 30% ball filling. Figure 4.11 shows the specific energies at 75 µm for the different ball fillings and % solids. For 73% - 76% solids (high) conditions, lower ball fillings appear to have lower specific energies. The specific energy increases with increasing ball filling for this high % solids condition. For the low and medium % solids conditions however, specific energy seems to far more constant with increasing ball filling. The higher % solids also seem to reduce the specific energy required. The reduction ratios and sieve efficiencies are greater at higher ball fillings and higher % solids, as shown in figures 4.12 and 4.13, respectively. Reduction ratios appear to increase with increasing ball filling and are greater for the higher % solids. There seems to be a maximum in

sieve efficiency at around 30% ball filling, especially for the medium and low % solids conditions and this trend has similarities to what was observed in figure 4.10.

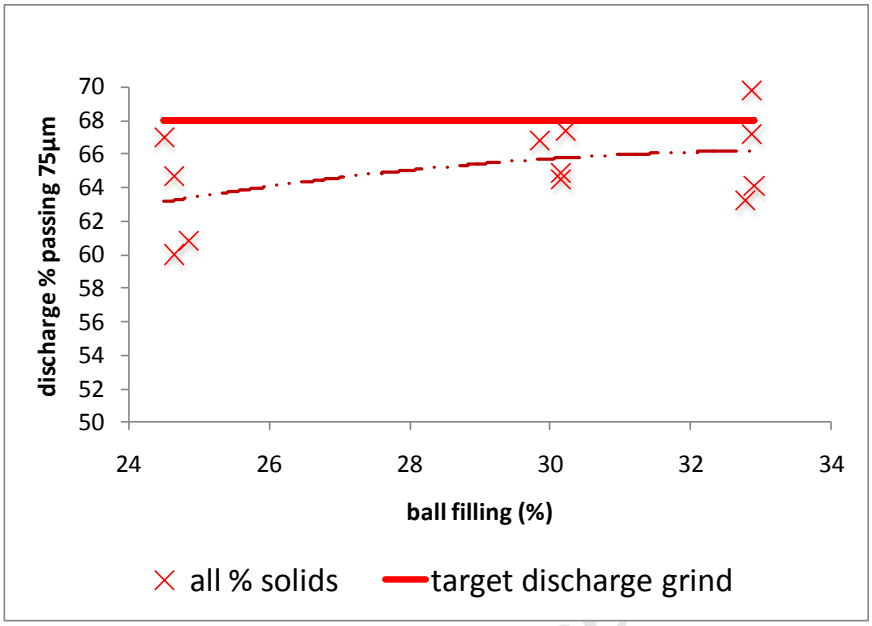

Figure 4.8 Grind % passing 75 µm at different ball fillings

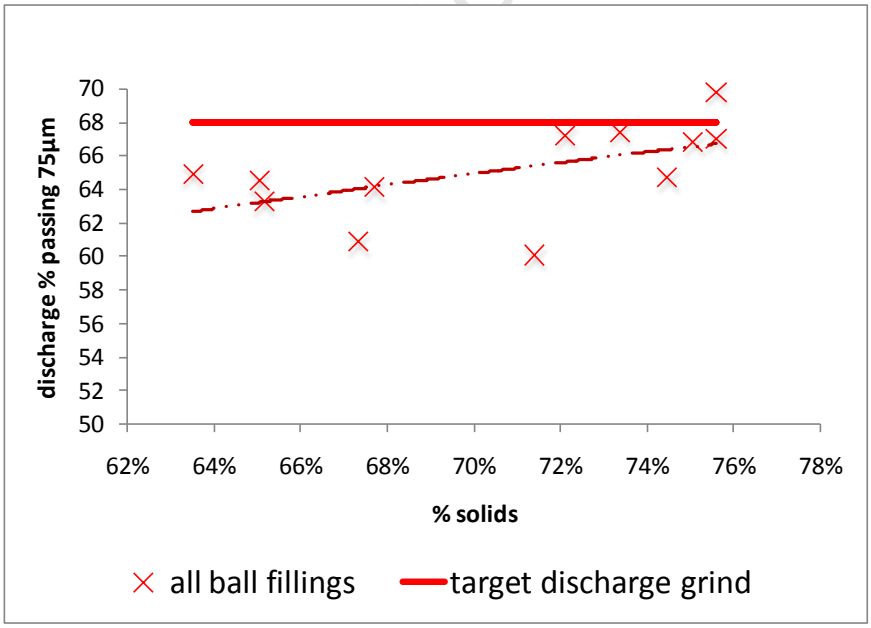

Figure 4.9 Grind % passing 75 µm at different % solids

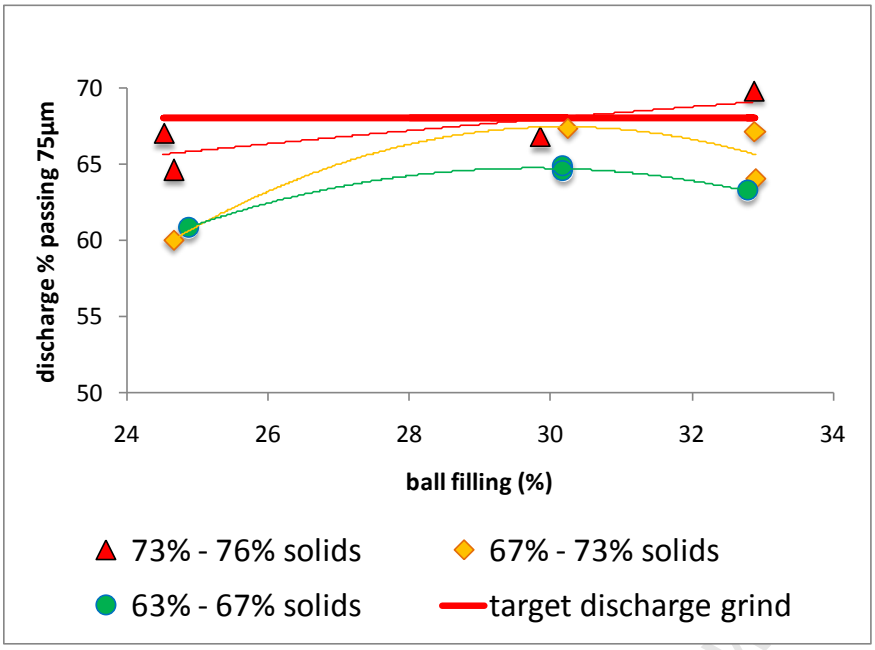

Figure 4.10 Grind % passing 75 µm at different ball fillings and % solids

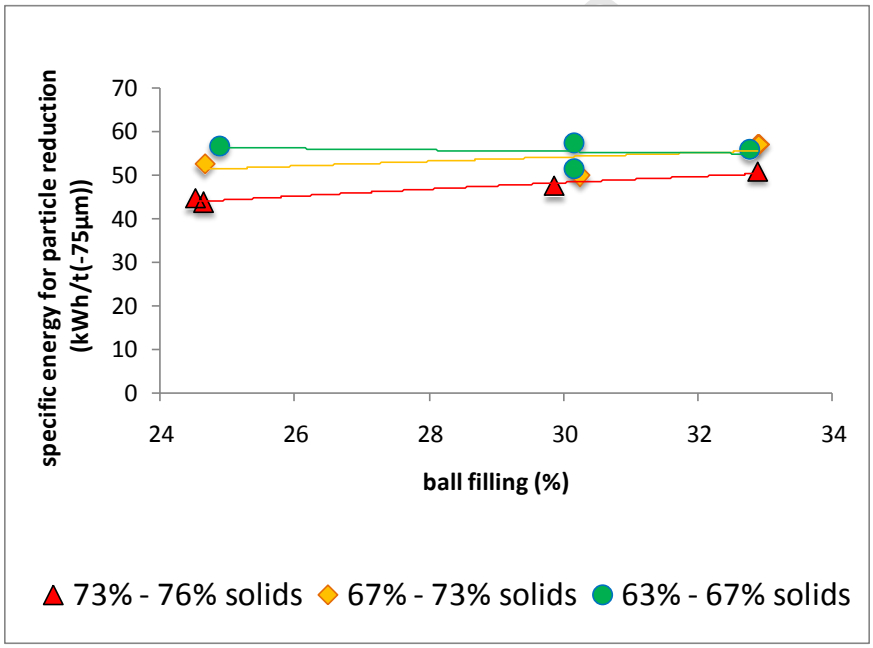

Figure 4.11 Specific energies at 75 µm for different ball fillings and % solids

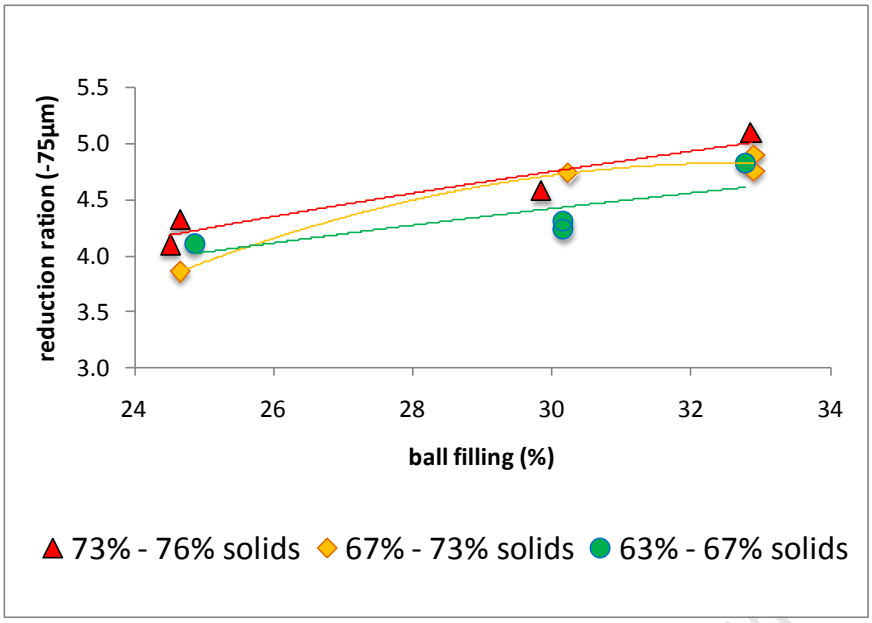

Figure 4.12 Reduction ratios at 75 µm for different ball fillings and % solids

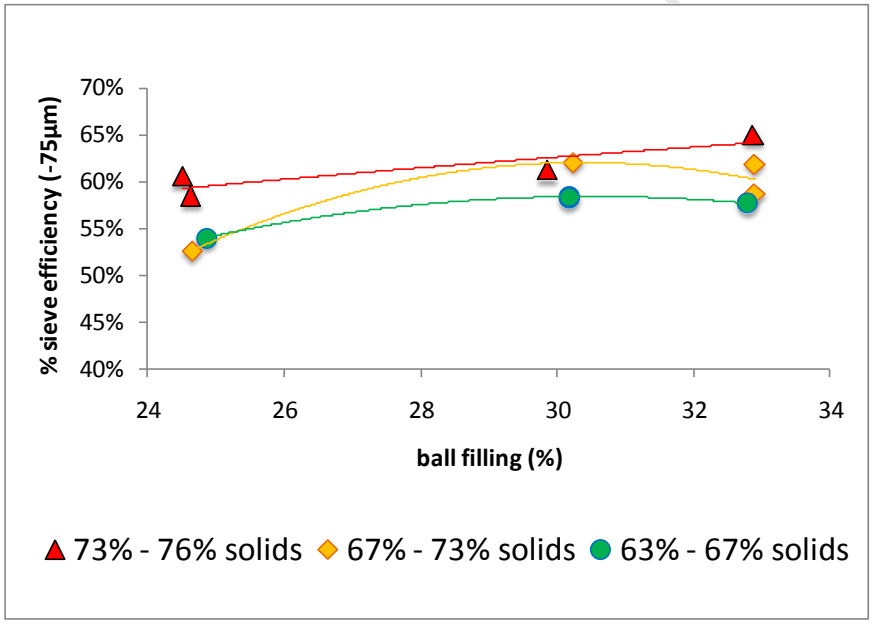

Figure 4.13 Sieve efficiencies at 75 µm for different ball fillings and % solids

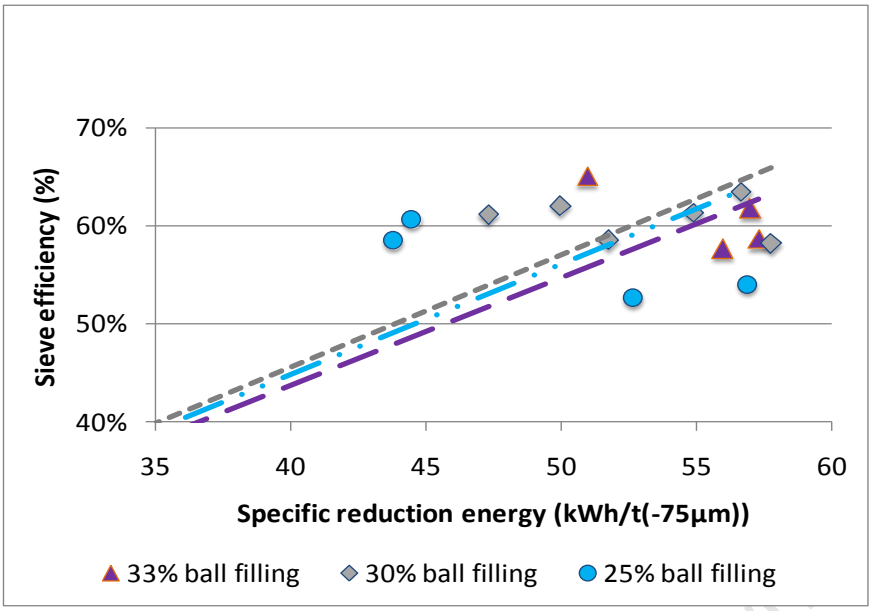

Figure 4.14 Sieve efficiency as a function of specific energy for different ball fillings

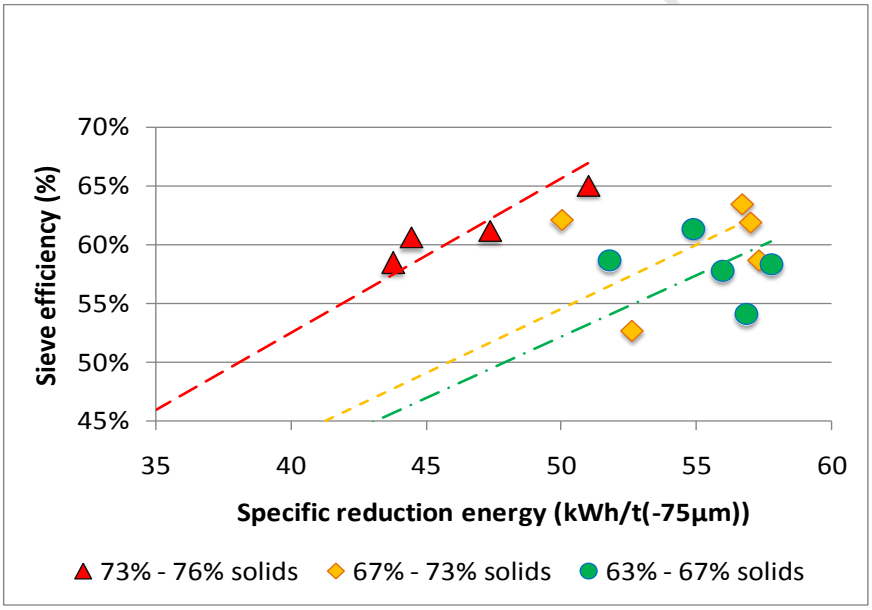

Figure 4.15 Sieve efficiency as a function of specific energy for different % solids

Figures 4.14 and 4.15 show the plots of sieve efficiencies for various specific energies for the ball filling and % solids conditions tested, respectively. For a particular specific energy input, sieve efficiencies seem to drastically increase with increasing % solids. The results indicate that as % solids increases, the relationship between sieve efficiency and specific energy moves up and to the left. The effect of specific energy on sieve efficiency with varying ball filling seems to be less clear than that for % solids. The fitted trend lines for the varying ball filling conditions lie almost on top of each other. Once again the line starts from zero at zero specific energy.

Surveys were also performed across a reline on the secondary mill. This afforded the author of this thesis an opportunity to compare the performance of worn and new liners. Figures 4.16, 4.17 and 4.18 show the effect of old and new mill liners on grind, reduction ratio and sieve efficiency, respectively. The ball filling condition was constant at 30% and % solids were varied for the four surveys. The results show that better mill performance was obtained from old liners and that performance still improved with increasing mill % solids.

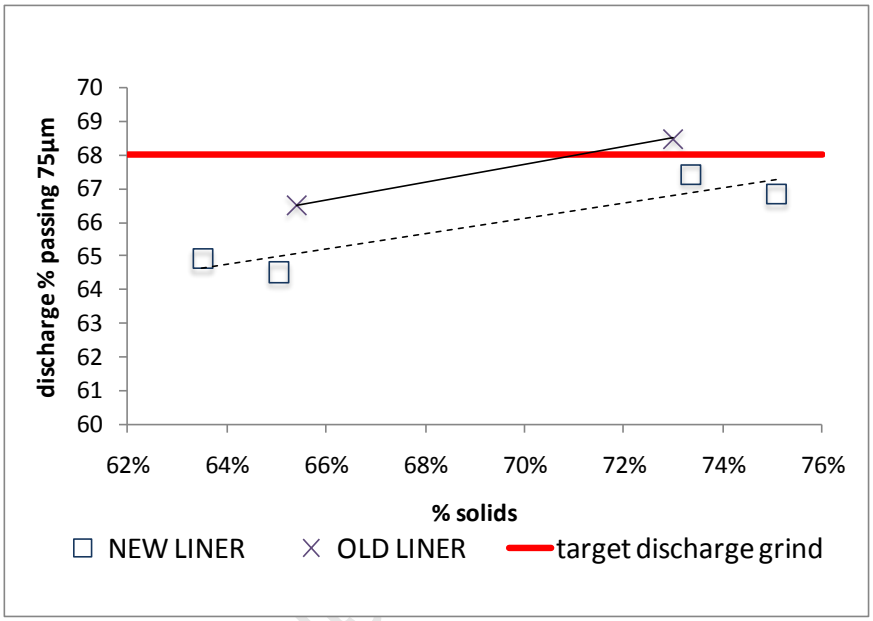

Figure 4.16 Grind % passing 75 µm for old and new liner conditions

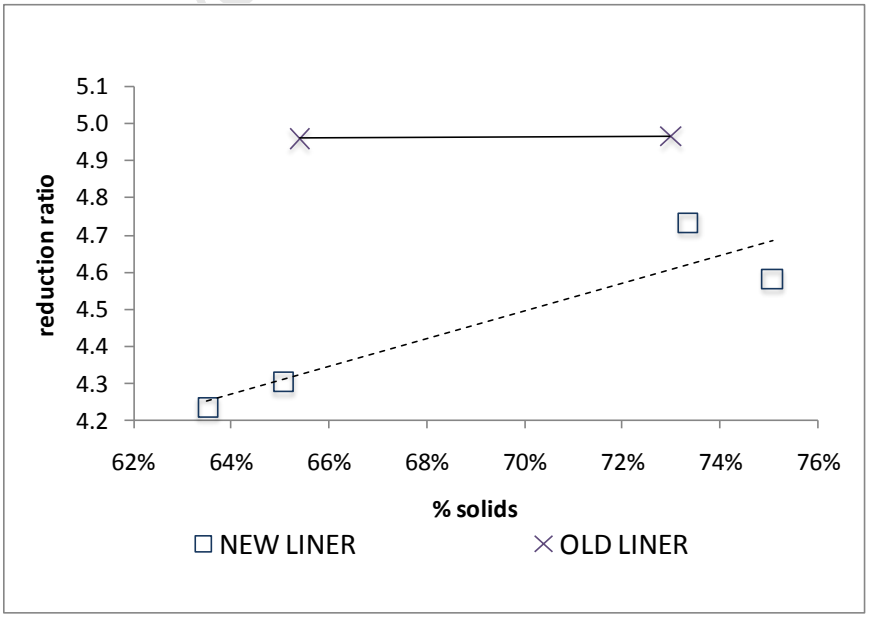

Figure 4.17 Reduction ratios for old and new liner conditions

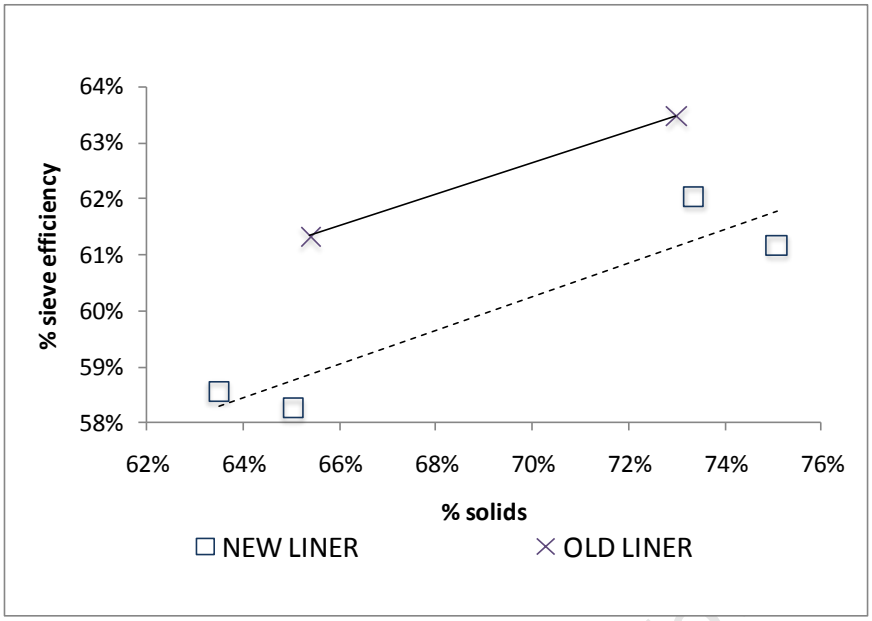

Figure 4.18 Sieve efficiencies for old and new liner conditions

4.4 SPECIES SPECIFIC MILLING PERFORMANCE FOR PGM AND Cr_2O_3

The results for the surveys conducted at various milling conditions, and the specific influence of ball filling and % solids on the size reduction and sieve efficiency, were presented in the previous sections. This section is concerned with the effect of the different operating conditions on the grinding and deportment of the PGM and Cr_2O_3 species.

To begin with, the actual distribution of the species per size class in both the mill feed and discharge streams would be of interest. Figure 4.19 shows a series of graphs depicting the distribution of particles as well as PGM and Cr_2O_3 according to size classes, for the mill feed and product streams. These graphs are presented below each other on a single page for ease of comparison across the different species. A common observation across the particle and the species distributions is that the plus 106 µm is depleted after the milling stage and that there is a significant increase in the sub 38 µm class. As mentioned in section 2.5, the change in the plus 106 µm fraction is of particular interest for the distribution of the PGM species and figure 4.20 shows the significant reduction in the plus 106 µm fraction across all surveys. Figure 4.21 shows the considerable increase in the Cr_2O_3 distribution within the sub 38 µm fraction across all surveys.

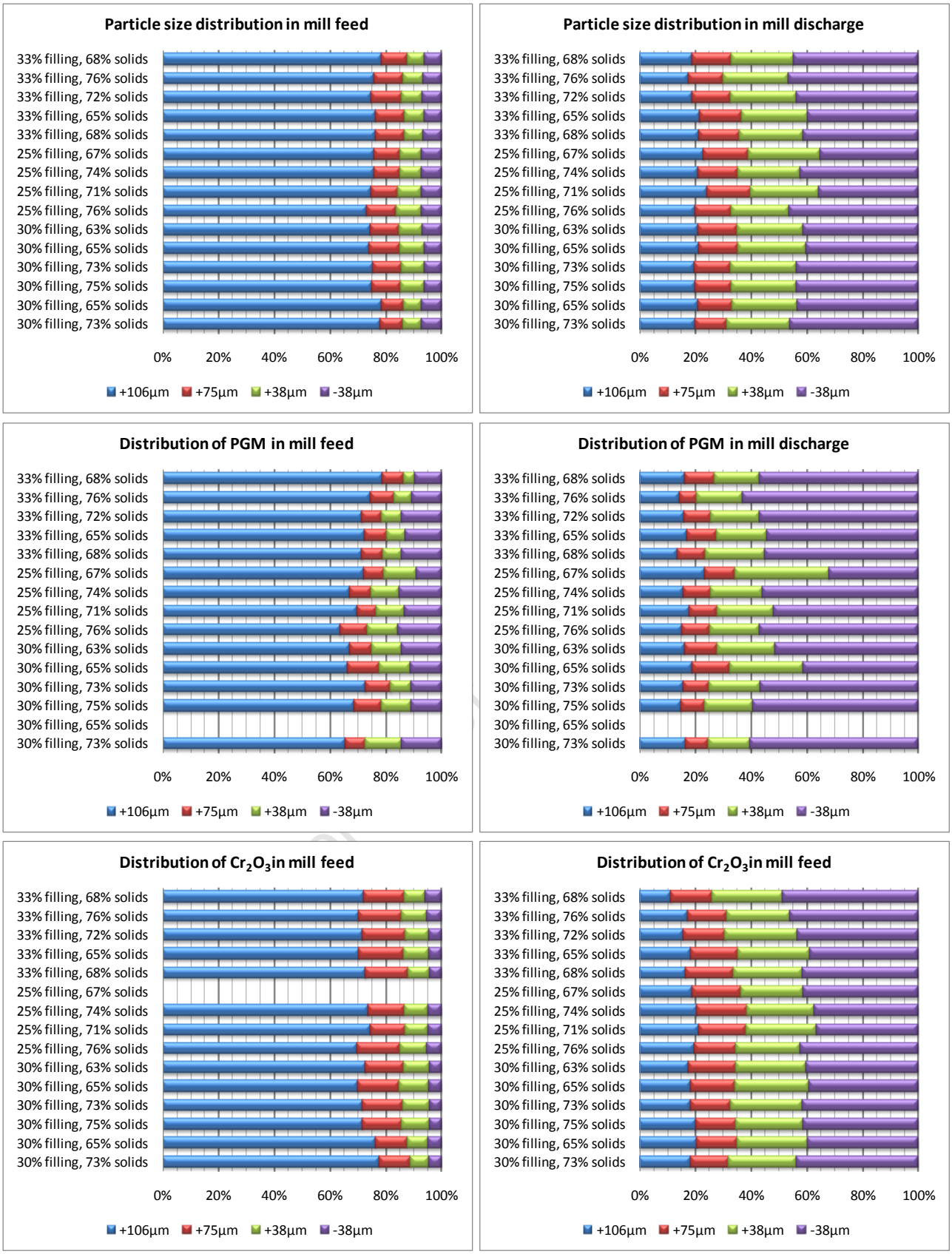

Figure 4.19 Survey particle, PGM and Cr_2O_3 distributions in the feed and discharge streams

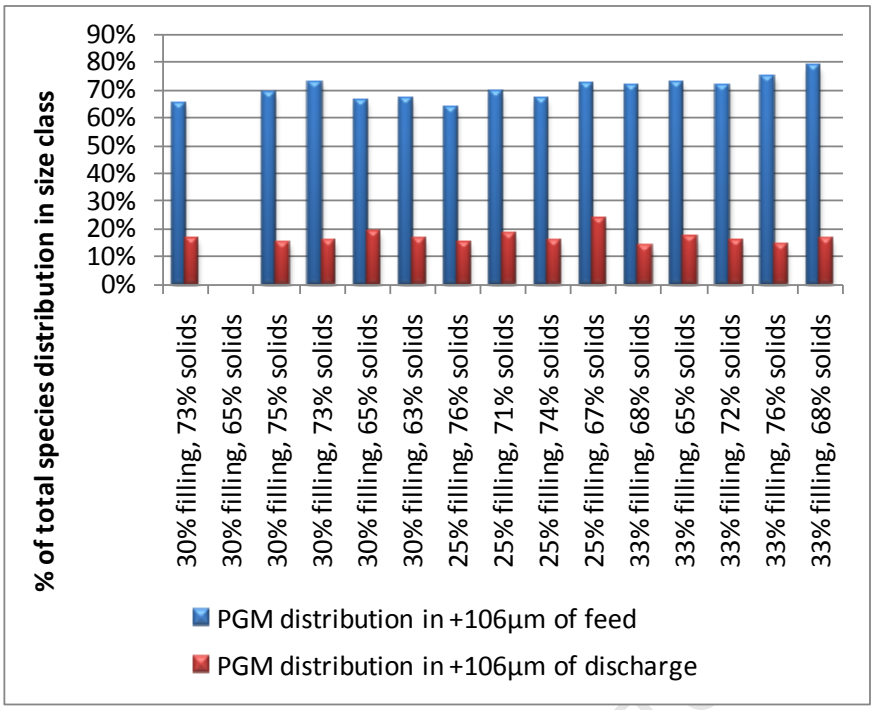

Figure 4.20 Change in PGM distribution in the +106 µm size class

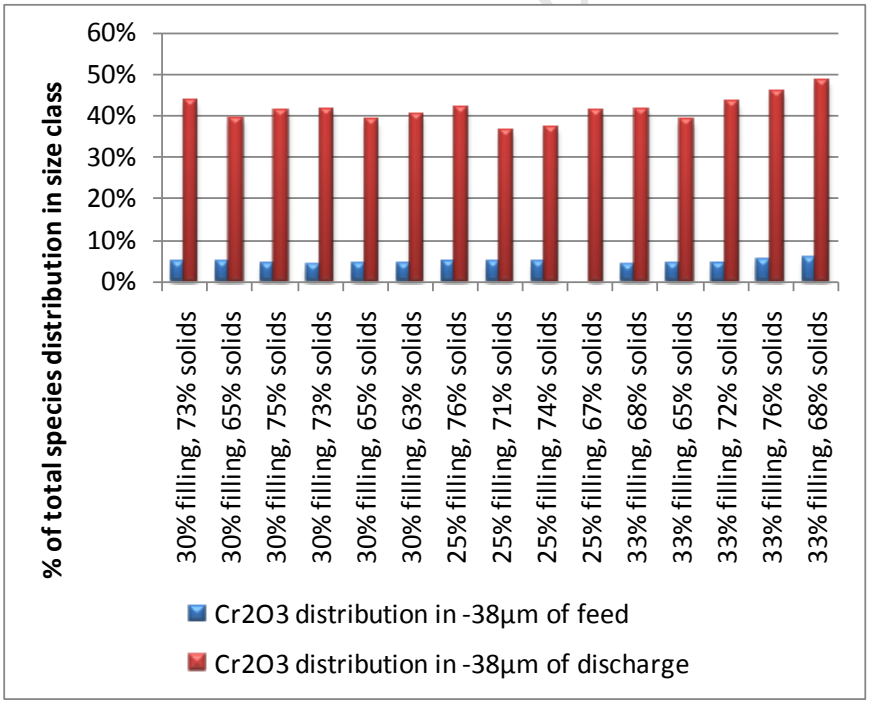

Figure 4.21 Change in Cr_2O_3 distribution in the -38 µm size class

Unlike the general particle size reduction analysis in the previous section, one cannot perform the specific energy comparison for the different species. The reason for this is that the specific weighting or distribution of the fraction of total energy consumed by each particular species is unknown. This requires much more specific analysis with regards to the individual species work

index and breakage energy requirements at a fundamental level, which is outside the scope of this study.

To gain a better understanding of the change in the distribution of the species per size class, the reduction ratio and sieve efficiency parameters are used again. The reduction ratio for a species indicates the degree of change in the species distribution in a size class from the mill feed to the discharge. Similarly, the sieve efficiency for a species indicates the degree of change in species distribution in a size class relative to the maximum change in distribution that could have occurred. Figure 4.22 (a) to (f) shows the reduction ratios and the sieve efficiencies for the PGM and Cr_2O_3 species per size class for the various conditions surveyed. All three size classes have been represented in the results and only the standard sub 75 μm size. This is because of the importance of reducing PGM occurrence in the coarser fractions to improve downstream recovery efficiencies, as well as the need to minimise the deportment of Cr_2O_3 in the fine class to limit entrainment into the final product (refer section 2.5). When looking at the reduction ratios only, there seems to be a big difference between PGM and Cr_2O_3 species, especially in the finer size class. The sieve efficiencies however show that PGM distribution change is more significant than that of Cr_2O_3, especially at higher % solids. The obtained reduction ratios and sieve efficiencies increase with higher % solids for PGM's. However, these parameters do not seem to change as much for Cr_2O_3 with varying % solids. The results also seem to indicate that the species sieve efficiencies for the PGM and Cr_2O_3 fractions are very similar at lower % solids. The effect of ball filling is however not clear in this figure.

In order to get a more detailed understanding of the effect of the varying ball filling and % solids on the species distribution across the mill, sieve efficiencies similar to those in figure 4.22 are plotted in figure 4.23 (a) to (f). Trend lines for % solids conditions per species are included. While figure 4.22 showed the general difference between PGM and Cr_2O_3 behaviour, figure 4.23 shows the sieve efficiencies for PGM and Cr_2O_3 separately and the effect of varying % solids and ball filling by size class can be evaluated for the individual species. It can be seen that for PGM's the sieve efficiency increases more significantly with higher % solids than for Cr_2O_3. There is much less variation or sensitivity to changing % solids conditions on Cr_2O_3 sieve efficiency. The increase in sieve efficiency with greater ball filling is also more pronounced for PGM than for Cr_2O_3, especially at the low % solids condition.

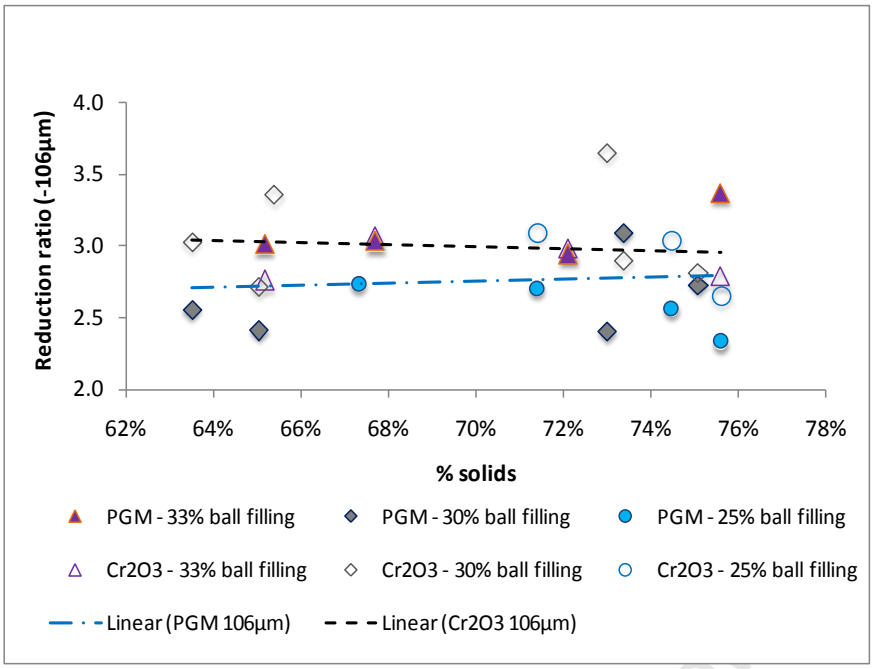

Figure 4.22(a) Reduction ratios at 106 µm for PGM and Cr_2O_3 distribution

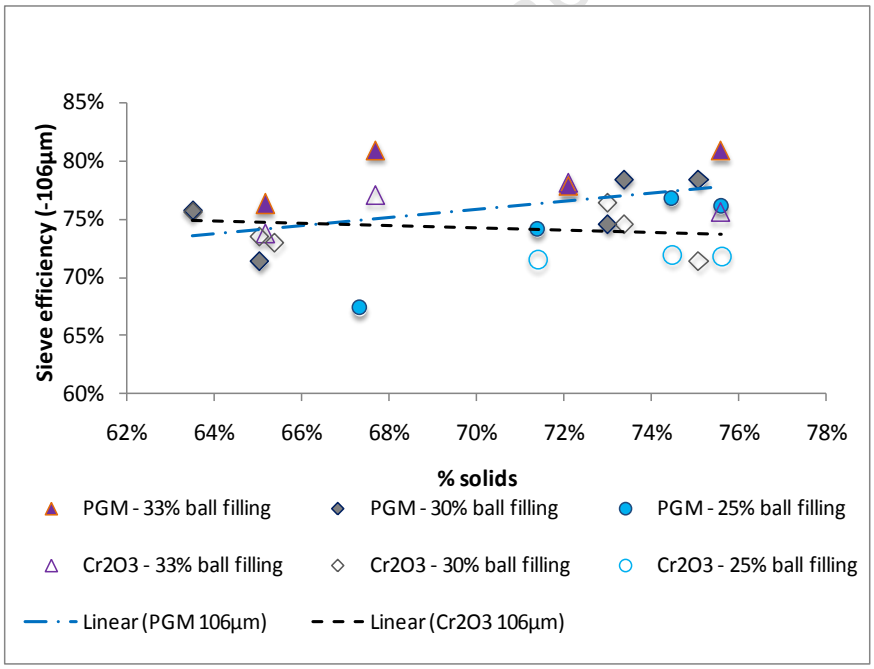

Figure 4.22(b) Sieve efficiencies at 106 µm for PGM and Cr_2O_3 distribution

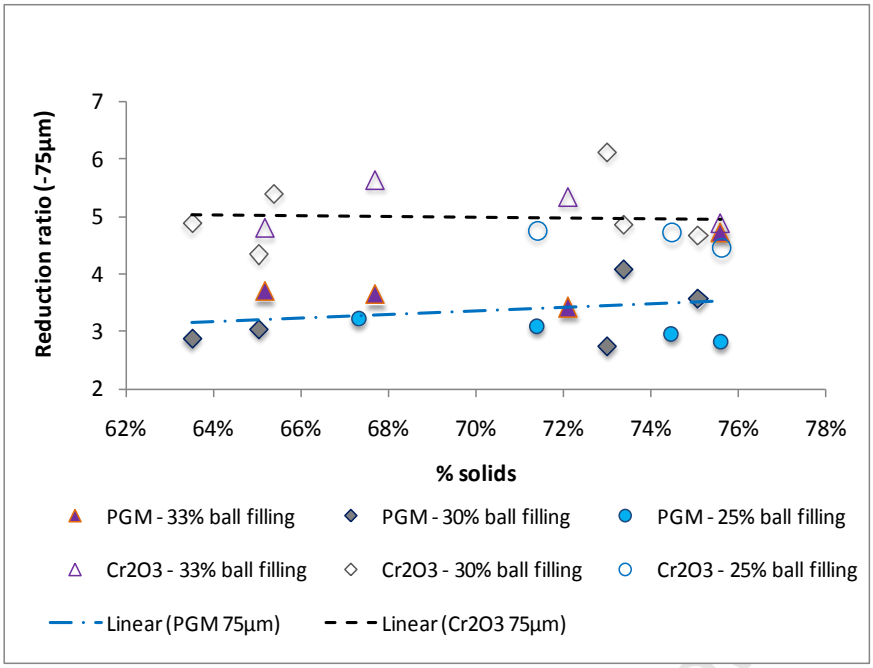

Figure 4.22(c) Reduction ratios at 75 µm for PGM and Cr_2O_3 distribution

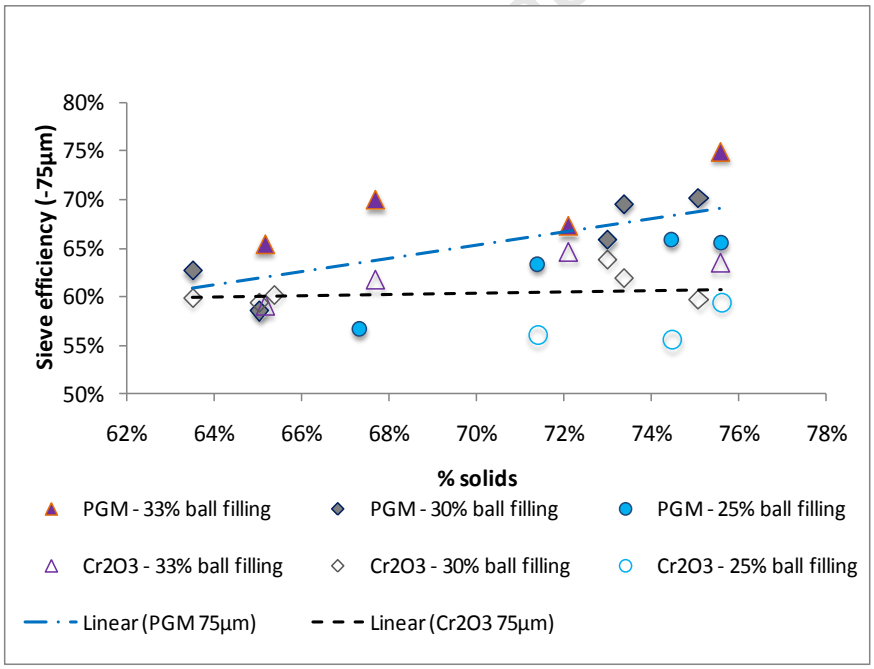

Figure 4.22(d) Sieve efficiencies at 75 µm for PGM and Cr_2O_3 distribution

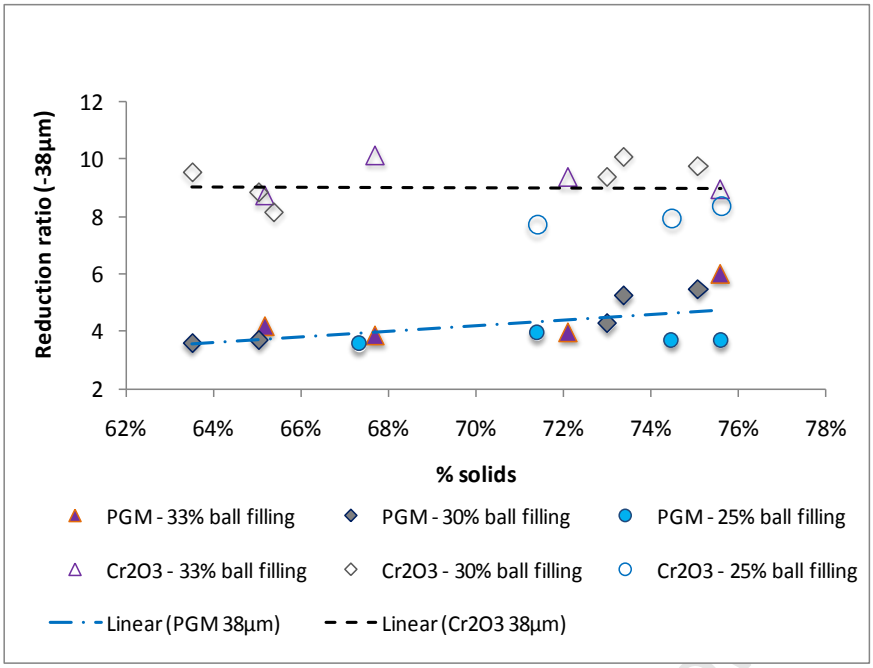

Figure 4.22(e) Reduction ratios at 38 µm for PGM and Cr_2O_3 distribution

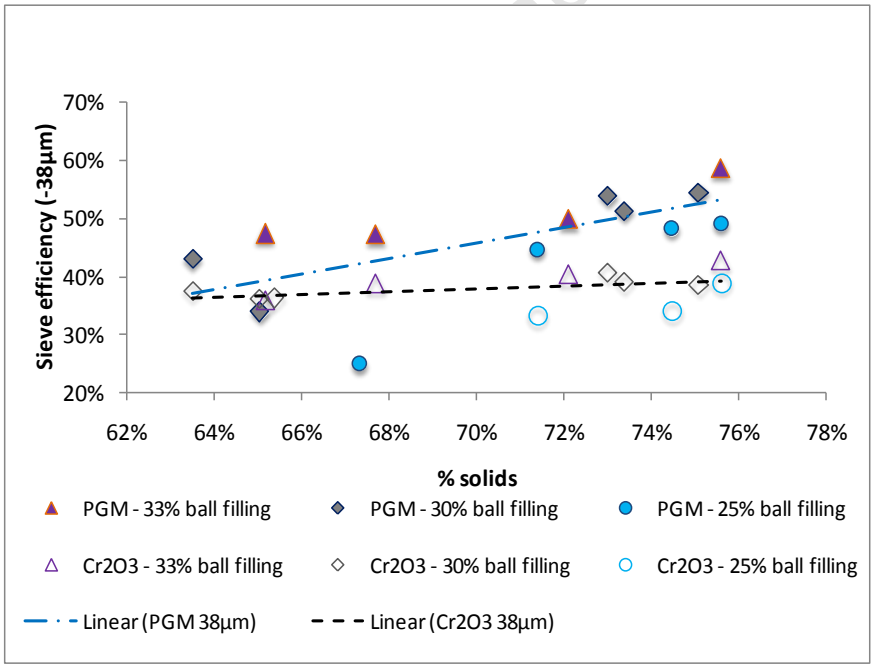

Figure 4.22(f) Sieve efficiencies at 38 µm for PGM and Cr_2O_3 distribution

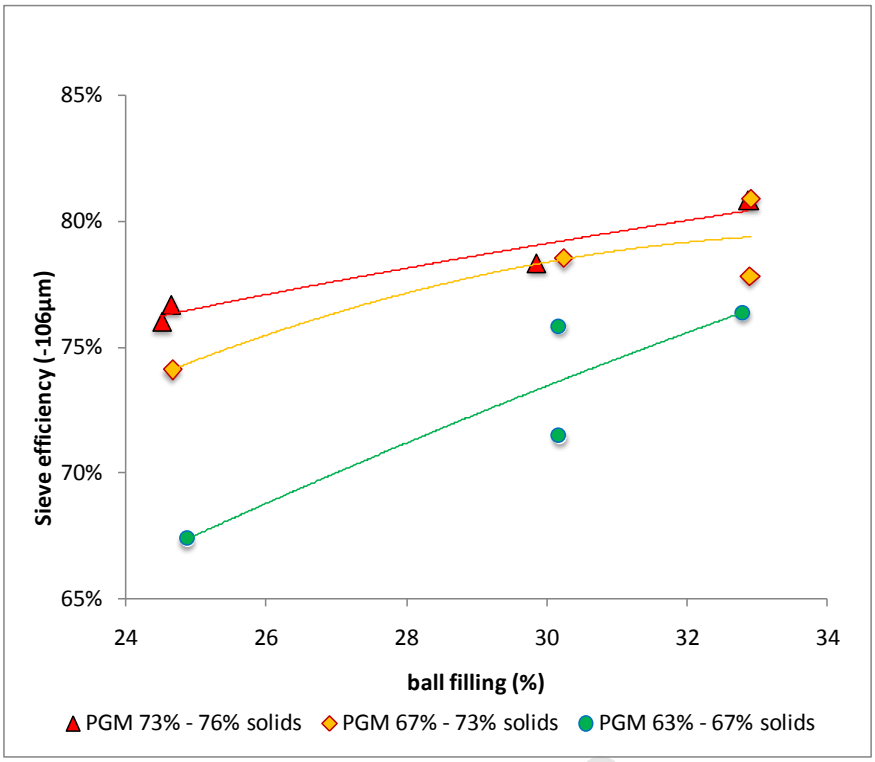

Figure 4.23(a) Sieve efficiencies at 106 µm for PGM distribution at the various ball filling and % solids conditions

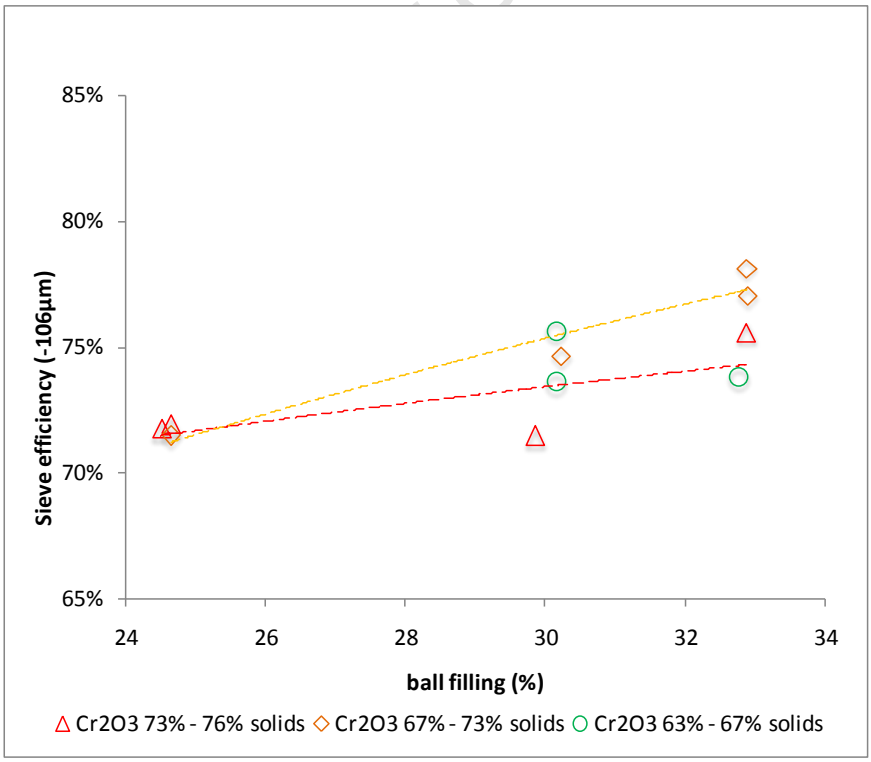

Figure 4.23(b) Sieve efficiencies at 106 µm for Cr_2O_3 distribution at the various ball filling and % solids conditions

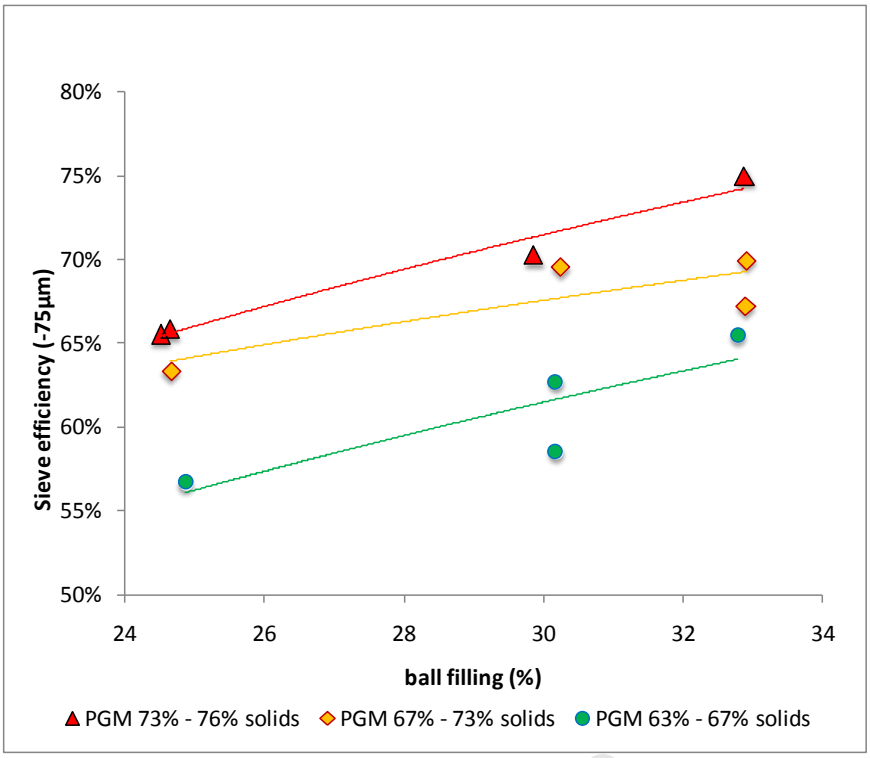

Figure 4.23(c) Sieve efficiencies at 75 µm for PGM distribution at the various ball filling and % solids conditions

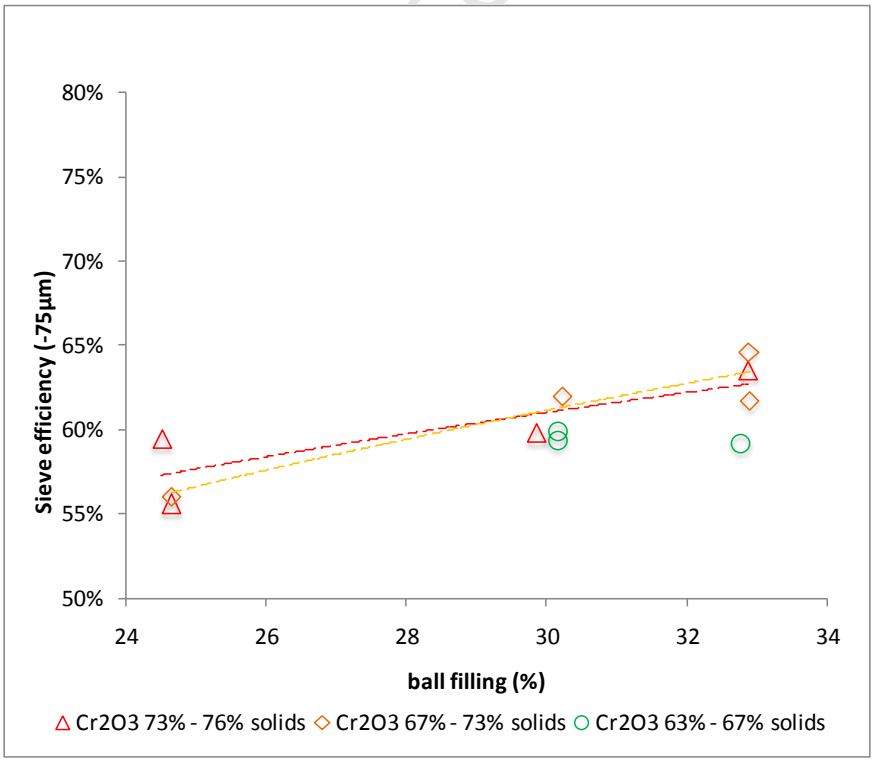

Figure 4.23(d) Sieve efficiencies at 75 µm for Cr_2O_3 distribution at the various ball filling and % solids conditions

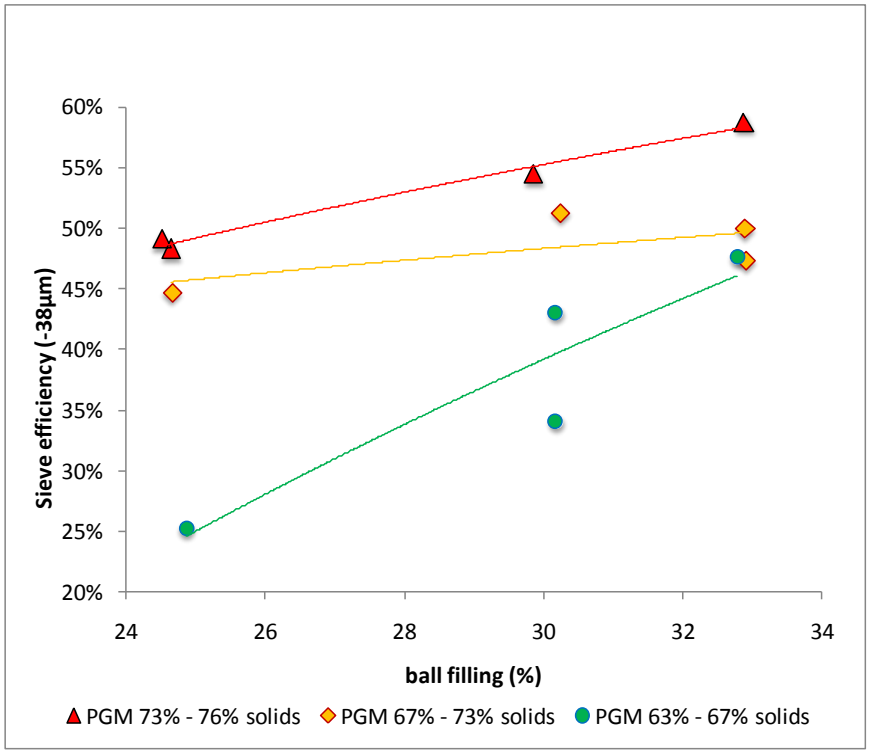

Figure 4.23(e) Sieve efficiencies at 38 µm for PGM distribution at the various ball filling and % solids conditions

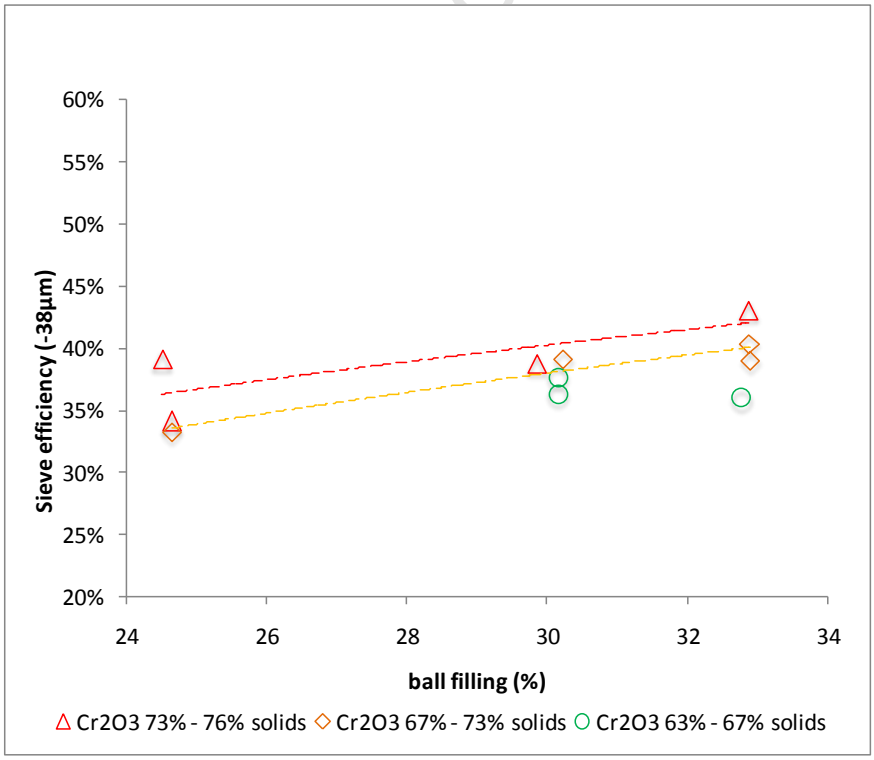

Figure 4.23(f) Sieve efficiencies at 38 µm for Cr_2O_3 distribution at the various ball filling and % solids conditions

4.5 DATA ACQUIRED FROM THE ONLINE SENSOR

In this section the results obtained from the Sensomag unit under the various survey conditions are presented. The main results of interest from the unit are the shoulder and toe angles for the pulp and ball positions. These give an indication of the slurry and ball charge behaviour at different operating conditions. The operating conditions considered here are still ball filling and % solids, as well as liner life (old vs. new liner). A set of comparative surveys were performed before and after a scheduled mill shell lifter bar reline to understand how the liner profile, which is influenced by liner life, affects the mill charge behaviour.

4.5.1 Change in ball filling and % solids conditions

Figure 4.24 (a) to (d) shows how the shoulder and toe angles varied for the different % solids and ball filling conditions. As mentioned in section 3.2.4, the angles reported are with reference to the vertical position on top of the mill being 0° and that at the bottom being 180°, with the radial position increasing in the direction of mill rotation. The following observations can be made:

- The pulp shoulder angle increases with increasing ball filling and decreases with increasing % solids.
- The pulp toe angle seems to be relatively unaffected by changing ball filling conditions but increases slightly with increasing % solids.
- The ball shoulder angle increases significantly with increasing ball filling but appears to be unaffected by % solids.
- The ball toe angle decreases significantly with increasing ball fillings and also decreases as the % solids increase.
- For almost all conditions the pulp shoulder angle was greater than the ball shoulder angle.
- The pulp toe angles were significantly less than the ball toe angles.

The results in section 4.2, 4.3 and 4.4 show how the changing % solids and ball filling conditions affected mill performance in terms of grind, reduction ratio, sieve efficiency etc. Figure 4.24 shows how the changing % solids and ball filling conditions affect the mill load dynamics in terms of pulp and ball component shoulder and toe angles. To understand the grinding performance of this mill in terms of mill load dynamics, figures 4.25 to 4.28 relate the effect of the various shoulder and toe angles obtained in the surveys to the grind achieved. Figure 4.25 (a) and (b) indicates that the grind increases with increasing pulp shoulder and toe angle. Figure 4.26 (a) and (b) shows that the grind increases with higher ball shoulder angles and decreases with increasing ball toe angles.

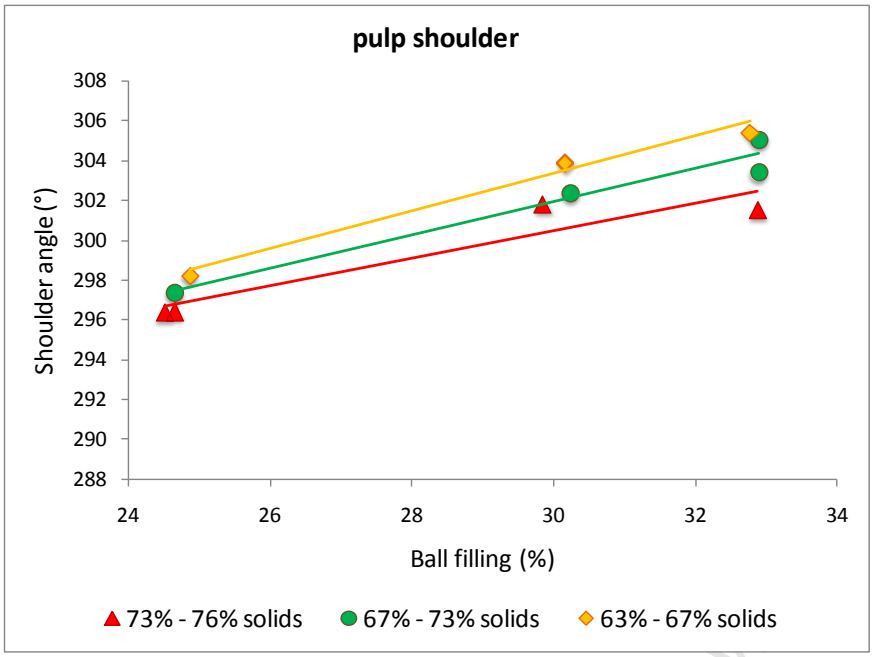

Figure 4.24(a) Pulp shoulder angles obtained at different survey conditions

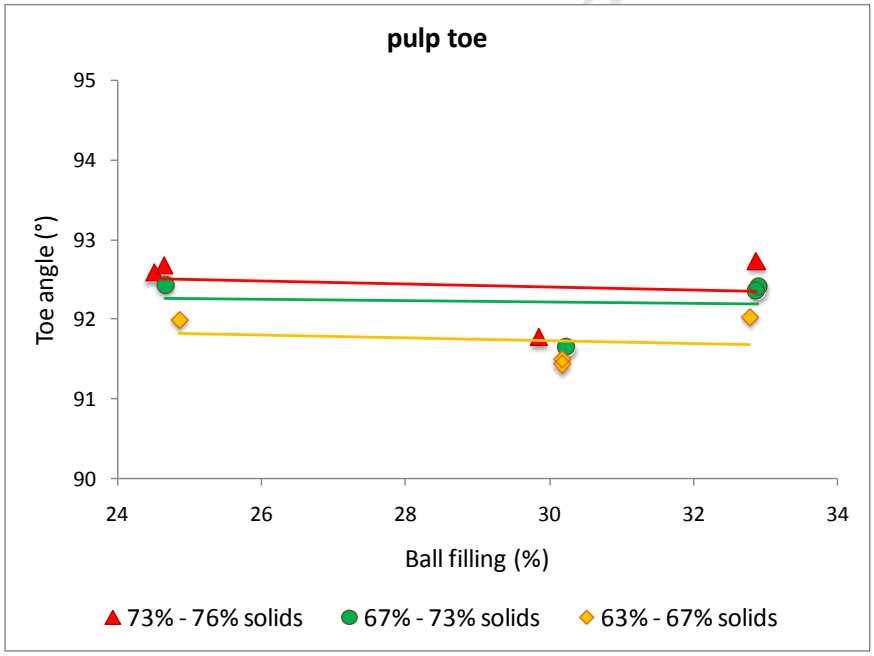

Figure 4.24(b) Pulp toe angles obtained at different survey conditions

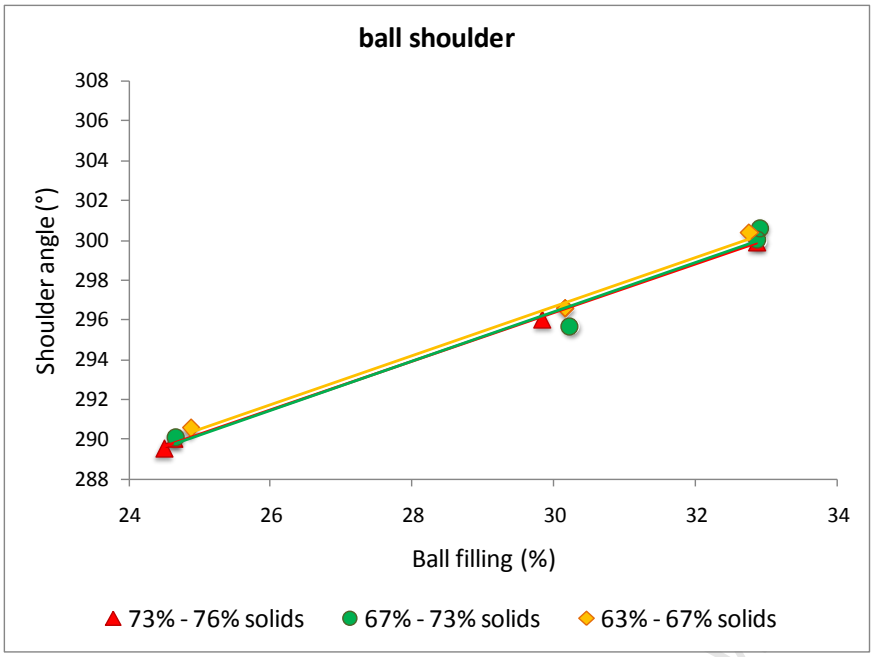

Figure 4.24(c) Ball shoulder angles obtained at different survey conditions

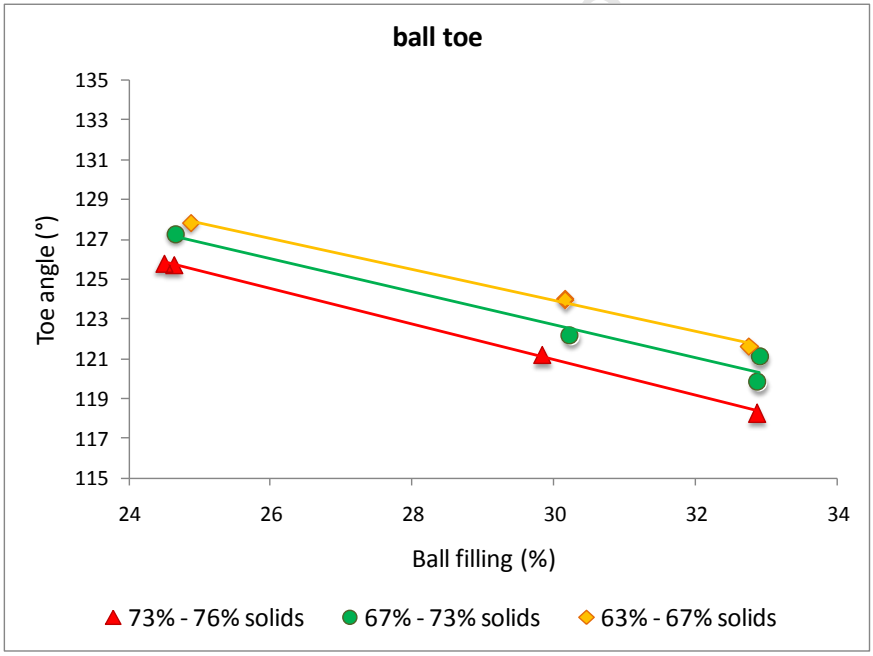

Figure 4.24(d) Ball toe angles obtained at different survey conditions

Figure 4.25(a) Grind results passing 75 µm at different pulp shoulder angles

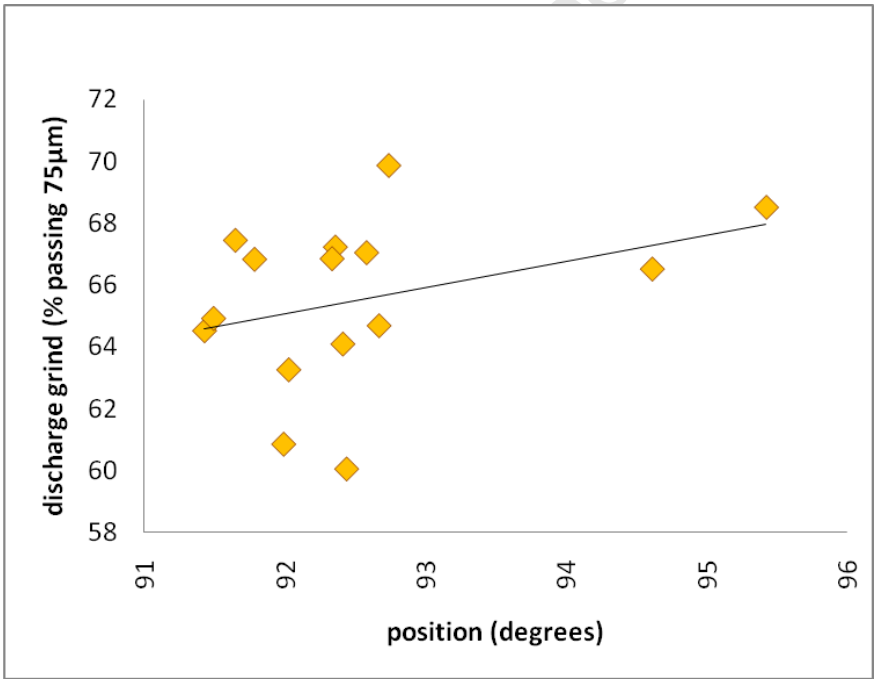

Figure 4.25(b) Grind results passing 75 µm at different pulp toe angles

Figure 4.26(a) Grind results passing 75 µm at different ball shoulder angles

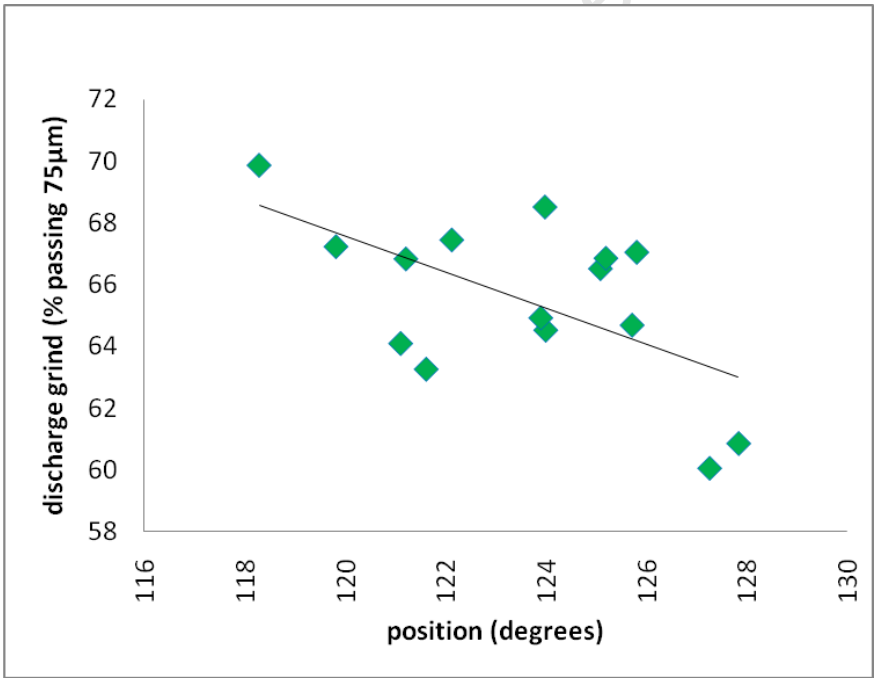

Figure 4.26(b) Grind results passing 75 µm at different ball toe angles

In order to understand the combined effect of changing ball and pulp shoulder/toe positions, the concept of free pulp shoulder and free pulp toe angles is introduced. By definition these would be the difference between the pulp shoulder and ball shoulder angle or the pulp toe and ball toe angles, respectively, as shown in equation 4.1.

$$\text{free pulp angle} = \text{pulp angle} - \text{ball angle} \quad [4.1]$$

These numbers would be an indication of the amount of pulp that is not interacting with the ball load and is schematically represented in figure 4.27. The influence of these parameters on grind is portrayed in figure 4.28 (a) and (b). The results indicate that the best grinding performance is obtained at the lowest free pulp angles. This implies that the smaller the amount of pulp not interacting with the balls in a dynamic load, the better the expected grinding performance of that mill.

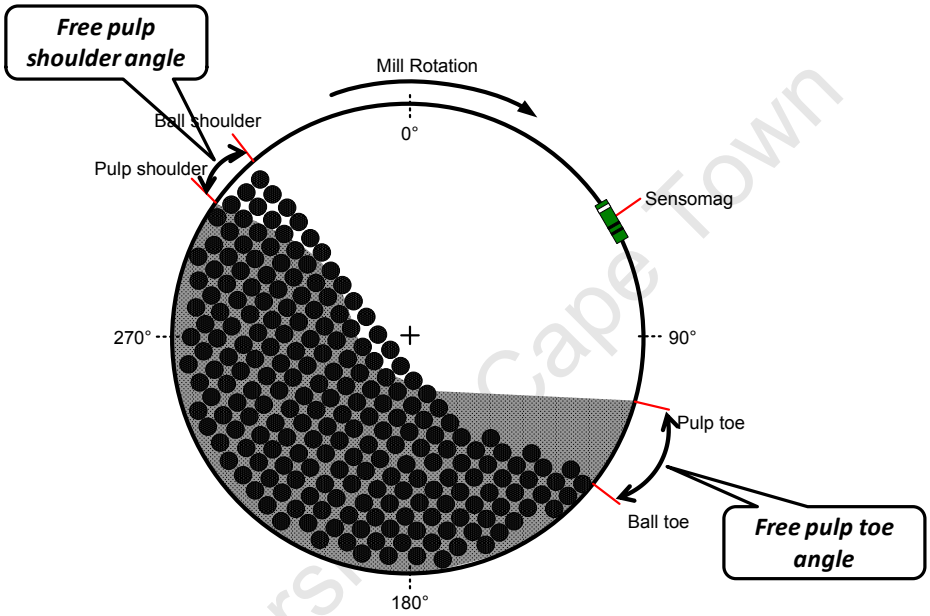

Figure 4.27 Schematic showing free pulp shoulder and free pulp toe angles

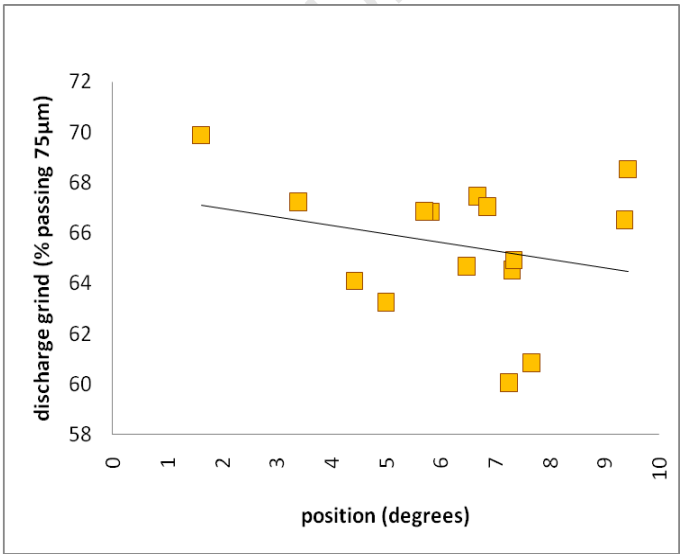

Figure 4.28(a) Grind results passing 75 µm at different free pulp shoulder angles

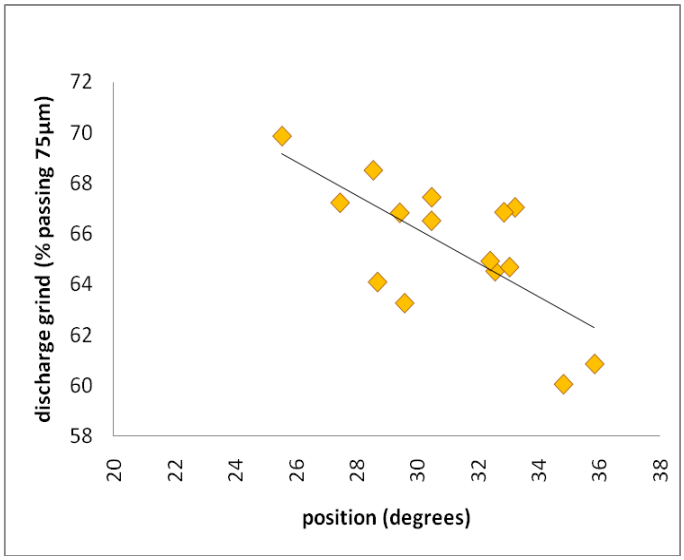

Figure 4.28(b) Grind results passing 75 µm at different free pulp toe angles

4.5.2 Change in liner profile

The effect of the liner face angle or design can be understood through the change in performance observed at the end of a liner life as compared to a new installation. Figure 4.29 (a) to (d) shows the pulp and ball shoulder and toe positions obtained from the Sensomag for surveys performed just before and after a mill reline. These results are shown with % solids on the x- axis due to all surveys being performed at 30% ball filling. The conditions before a reline would be of worn liners with less aggressive face angles, whereas after a reline there would be more aggressive liners with steeper face angles. The following observations on performance were made as the liner lifetime increases (more old/worn liners or shallower face angles):

- There is not much difference in pulp shoulder position as the liners wear.
- The pulp toe angle increases as the liners wear.
- The ball shoulder angle decreases as the liners wear.
- The ball toe angle increases as the liners wear.
- Similar reactions as to that mentioned in section 4.5.1 above with changing % solids were observed for the shoulder and toe positions.

The effect of liner lifetime on the grinding performance of the mill is already presented in figure 4.16 and shows better grinds were achieved with the old liners. Figure 4.30 (a) and (b) summarises the effect of liner wear on grinding performance achieved in terms of the total pulp and ball angle. This is defined as the difference between the shoulder and toe angle and gives an indication as to the degree of compactness of the pulp or ball load.

$$\text{total angle} = \text{shoulder angle} - \text{toe angle} \qquad [4.2]$$

The results indicate that the pulp and ball load total angles are smaller or more compacted for older liners and that improved grind is obtained at these conditions.

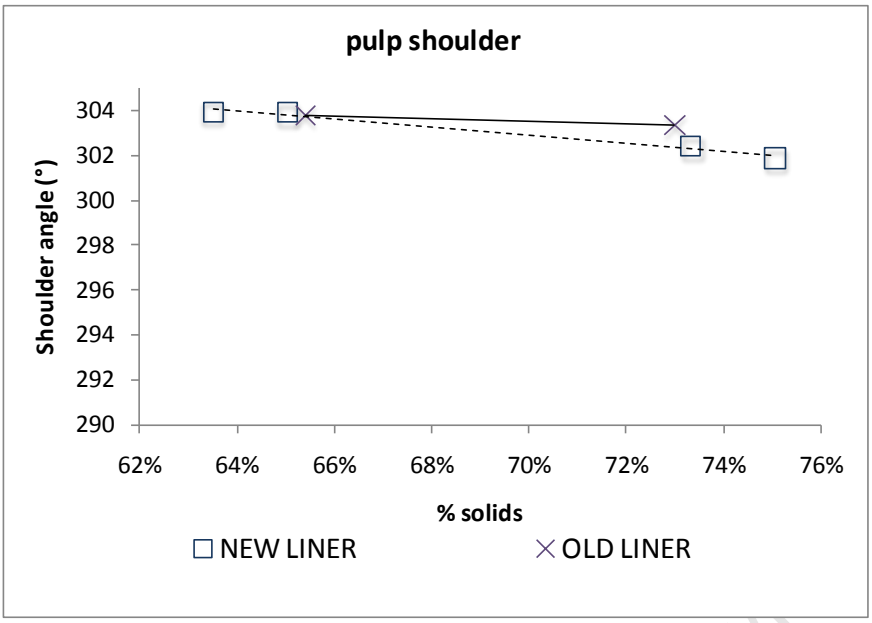

Figure 4.29(a) Pulp shoulder angles obtained from surveys with old and new liner conditions

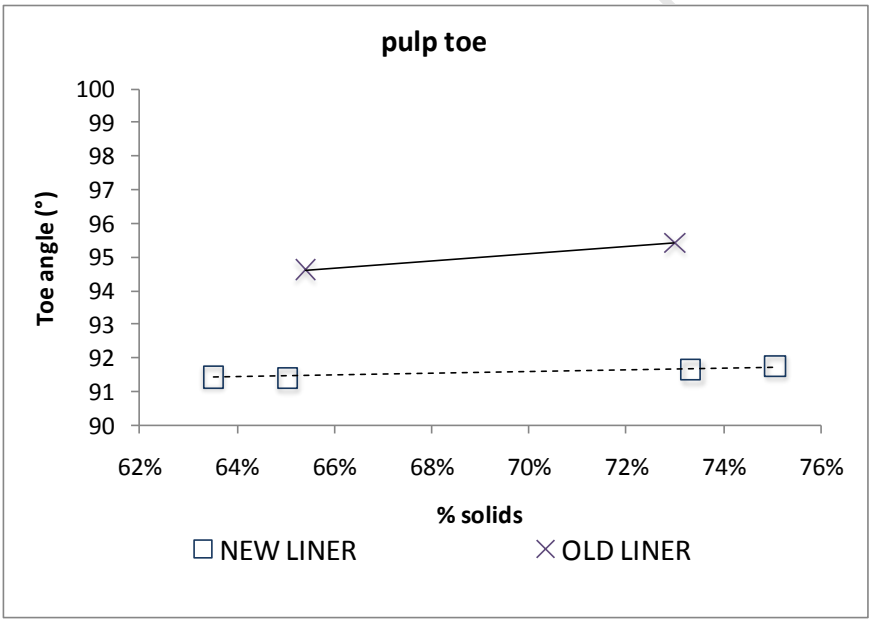

Figure 4.29(b) Pulp toe angles obtained from surveys with old and new liner conditions

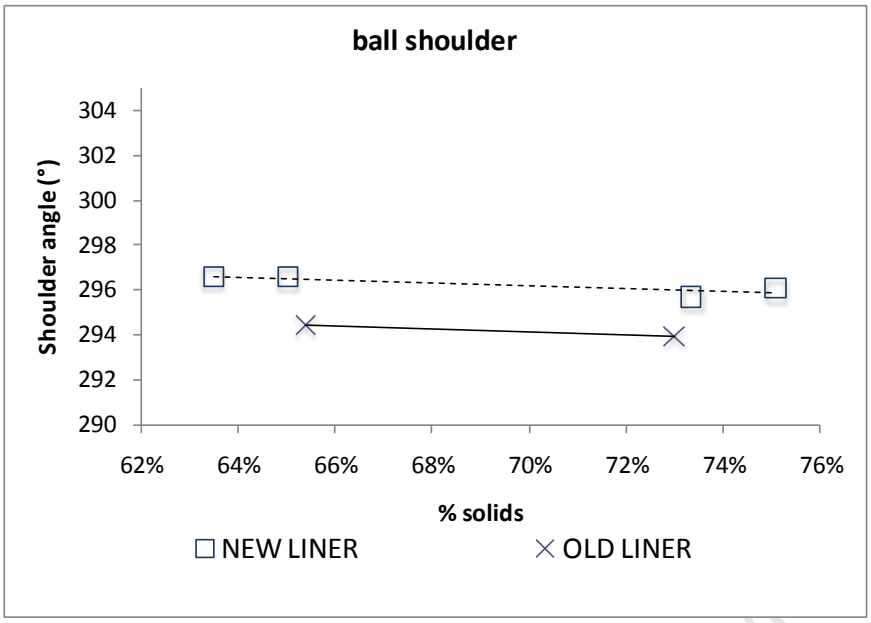

Figure 4.29(c) Ball shoulder angles obtained from surveys with old and new liner conditions

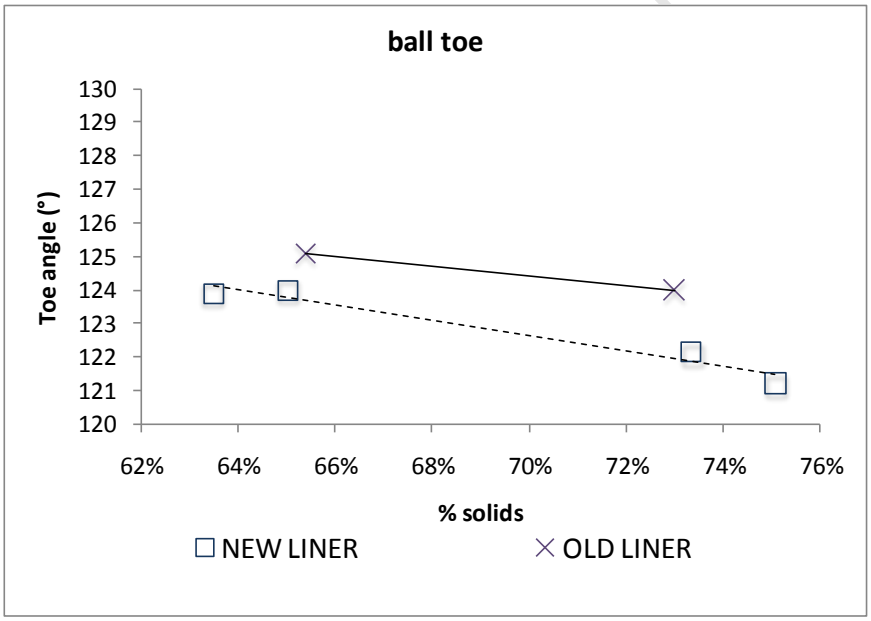

Figure 4.29(d) Ball toe angles obtained from surveys with old and new liner conditions

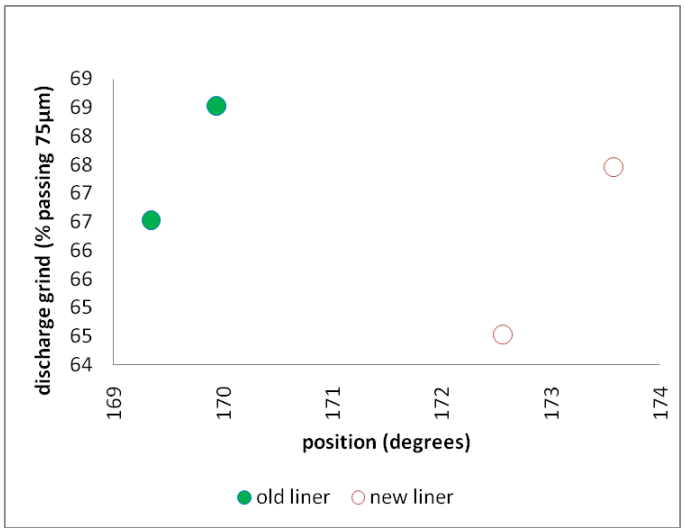

Figure 4.30(a) Grind results passing 75µm at different total ball load angle for old and new liners

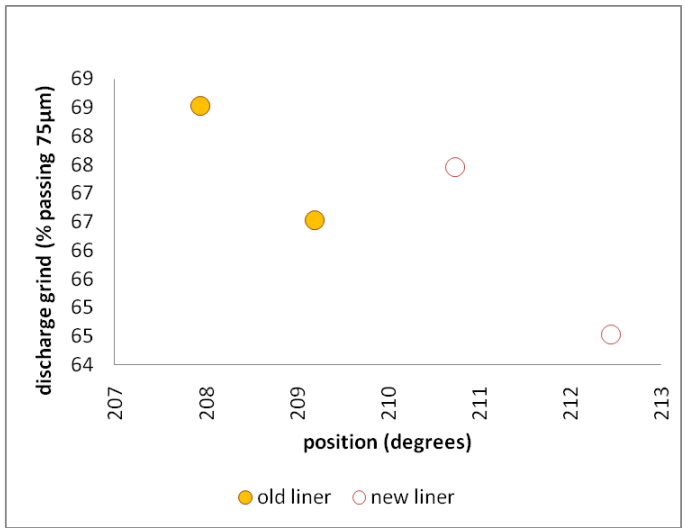

Figure 4.30(b) Grind results passing 75µm at different total pulp load angle for old and new liners

4.6 MODEL FITTING AND SIMULATIONS FROM EXPERIMENTAL DATA

In this section the experimental data is model fitted to verify the results obtained from the surveys performed. The data from the test work was fitted using the perfect mixing ball mill model in JKSimMet - a steady state simulating software package developed by Whiten at the JKCentre in Australia. The perfect mixing model in JKSimMet considers a ball mill as a perfectly mixed tank with contents described by a vector size distribution (JKSimMet Manual, Version 5.2, 2001). Fitting the ball mill model in JKSimMet involves inputting the ball mill dimensions and the size distribution data for the mill product and the streams providing the feed to the ball mill. For the test work performed in this study the first stage cyclone (dewatering cyclone) underflow stream was the feed to the ball mill. The mill discharge sample was collected during the survey and the size distribution obtained from this sample was used in the modelling work. The solids concentration and the mass flow rate from the flow rate measurements performed during the survey were used in modelling.

R/D* is the breakage rate function, as defined by Napier-Munn *et al* (1996), and is described as a model fitting parameter from which mill scaling and simulations at varying operating conditions may be carried out within certain limitations. Four R/D* spline knots were used during model fitting in this study on the Waterval UG2 Concentrator secondary mill. The volumetric % ball filling and model fit parameters for each test are summarized in table 4.1. The breakage rates expressed as R/D* appear to be consistent for all tests and follow the trend given in figure 4.31.

Table 4.1 Summary of the fitted (R/D) for each knot for all the surveys*

Test No.	Size, mm		0.106	0.15	0.212	0.355
	Ball filling	% Solids	R/D*			
1	30	73	0.753	1.728	2.602	3.449
2	30	65	0.845	1.953	2.948	4.015
3	30	75	0.806	1.784	2.757	3.592
4	30	73	0.858	1.881	2.818	3.78
5	30	65	0.923	2.033	2.897	3.911
6	30	63	1.007	2.095	3.013	4.043
7	25	76	0.816	1.587	2.684	3.623
8	25	71	0.141	1.642	2.524	3.524
9	25	74	0.618	1.689	2.79	3.787
10	25	67	0.0918	1.778	2.609	3.882
11	33	68	0.714	1.837	2.778	4.033
12	33	65	0.751	2.002	2.952	4.089
13	33	72	0.801	1.909	2.745	3.753
14	33	76	0.873	1.87	2.807	3.842

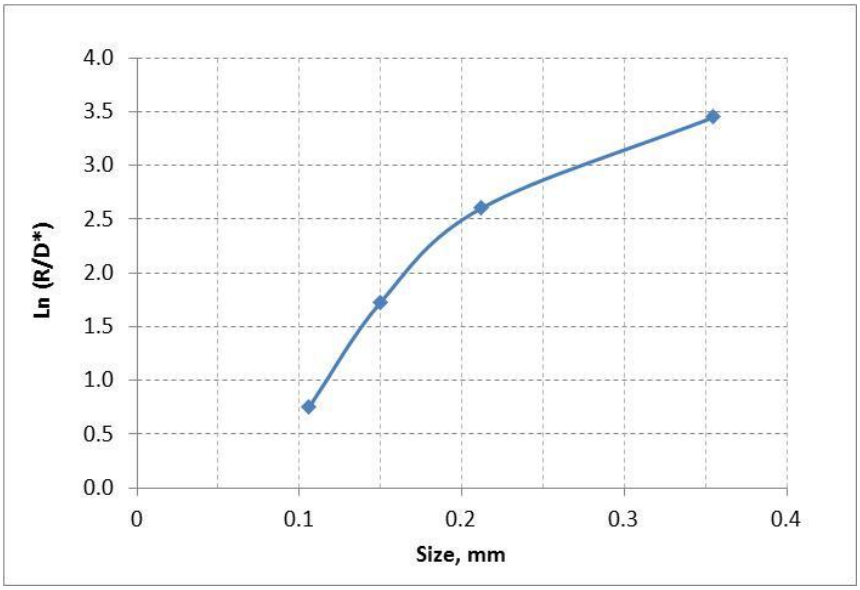

Figure 4.31 The fitted breakage rates for the Waterval UG2 Secondary Ball Mill

A summary of the comparison between fitted and experimental data for one of the tests is given in table 4.2 and the full dataset is presented in Appendix D. It can be seen that the fitted results match the experimental data closely. Since the fitted data matched the experimental data closely, simulations were performed to normalise the results to the same throughput. Table 4.3 shows an example of the simulation performed to normalise the throughput from 386 t/h to the highest throughput achieved in the tests, which was 464 t/h. The comparison between experimental and simulated data shows that increasing the throughput from 386 t/h to 464 t/h results in a coarsened secondary ball mill product.

Table 4.2 Comparison of the experimental and fitted data from one of the tests

Stream	Solids (t/h)		% Solids		% Sub 0.0750mm		P80	
	Exp	Fit	Exp	Fit	Exp	Fit	Exp	Fit
Ball mill feed	386	386	73	73	13.79	13.79	0.301	0.301
Ball mill product	386	386	73	73	68.52	68.11	0.106	0.105

Table 4.3 Results of simulations performed to normalise the throughput to match the test with highest tonnes per hour

Stream	Solids (t/h)		% Solids		% Sub 0.0750mm		P80	
	Exp	Sim	Exp	Sim	Exp	Sim	Exp	Sim
Ball mill feed	464	464	73	73	13.79	13.79	0.301	0.301
Ball mill product	386	464	73	73	68.52	65.05	0.106	0.113

The aim in the experimental work was to perform tests where the secondary mill feed and product streams had targeted solids concentration by weight. Although it was difficult to set up a control strategy that would give the exact levels of the required solids concentration, it was possible to obtain results that were either at the desired solids concentration or within 3% of that value. This is described in section 4.3 where % solids were banded in three classes – low (63–67%), medium (67-73%) and high (73-76%) for the purpose of presenting and comparing results. However, to ensure that comparisons were made at the desired solids concentrations, simulations were performed to normalise the data. Table 4.4 shows a comparison of the experimental and simulated data after normalising the throughput and the solids concentration. Table 4.3 shows that after normalising the throughput and the solids concentration the simulated product is slightly coarser than the experimental results obtained at a reduced feed rate and slightly lower solids concentration level. Table 4.4 shows that increasing the solids concentration from 73% to 75% in the simulation resulted in a slightly finer product indicating that for this ore operating at higher solids concentration had an advantage, as has been seen by the results in the previous sections. Due to the known limitations of the model and the limited scope over which the mill was surveyed, the % solids were only slightly changed in simulations. The model appeared to give reasonable results in all cases and the record of results from all simulations performed is given Appendix D.

Table 4.4 Results of the simulation performed to normalise the % solids

Stream	Solids (t/h)		% Solids		% Sub 0.0750mm		P80	
	Exp	Sim	Exp	Sim	Exp	Sim	Exp	Sim
Ball mill feed	464	464	75	75	13.79	13.79	0.301	0.301
Ball mill product	386	464	73	75	68.52	66.02	0.106	0.110

There was no attempt to normalise the feed size distribution because the plots in figures 4.1 and 4.2 shows that the size distribution was fairly consistent across all tests. However, a correction was made by plotting the net production of the sub 75 microns when assessing the influence of ball filling degree and feed solids concentration on the performance of the secondary ball mill. Figure 4.32 shows the variation of the net production of the sub 75 microns with ball filling degree for different feed solids concentration. It can be seen that when operating at either 65 or 70% solids the mill performance peaks at the ball filling in the region around 30% ball filling. However, at 75% solids, the net production of sub 75 microns appeared to increase with % solids and no evidence of the optimum was seen within the ball filling range tested. These findings from the simulation results are again similar to those observed in the previous sections from the experimental results, and will be discussed in more detail in the next chapter.

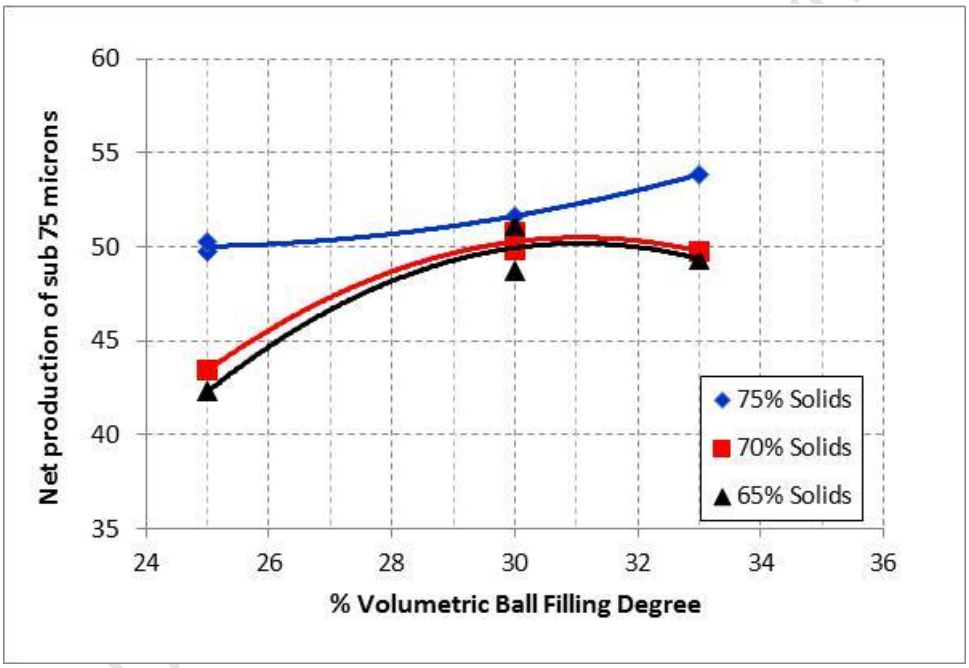

Figure 4.32 The influence of ball filling degree and mill feed solids concentration on the net production of sub 75 microns particles

4.7 SUMMARY OF CHAPTER

The results of interest from performing the test work were presented in this chapter and form the basis of the discussion given in the next chapter. The target grind for the mill was achieved at higher operating % solids and 30% ball fillings, which has some similarities with the findings from the articles reviewed in section 2.2. This could also be seen with the reduction ratios and sieve efficiencies for different size classes obtained for the various % solids and ball filling conditions. The specific reduction energy decreased at higher % solids, but no clear trend emerged with variations in ball filling degree.

There is a significant reduction in the distribution of particles in the +106 µm (coarse) fraction across the mill, and consequently a great increase in the distribution of particles in the -38 µm (fines) fraction. With regards to species milling performance between the PGM and Cr_2O_3 fractions, the specific reduction ratios for PGM's increased slightly with increasing % solids while those for Cr_2O_3 remained constant. However, the reduction ratios at a particular condition appeared to be generally greater than those for PGM's. The species specific sieve efficiencies, however, were similar for PGM's and Cr_2O_3 at lower % solids. The PGM sieve efficiency increased significantly with increasing % solids whereas the Cr_2O_3 sieve efficiencies remained fairly constant. This resulted in much higher sieve efficiencies at higher % solids for PGM's than Cr_2O_3. When looking at the species sieve efficiency results at the various test conditions in more detail, the data shows that PGM's reduction is affected by % solids and ball filling while Cr_2O_3 reduction is not affected by % solids at low ball fillings. Slightly improved sieve efficiencies are however observed for Cr_2O_3 at higher ball fillings.

The information obtained from the online Sensomag at the different survey conditions was presented. The charge behaviour was described in terms of variations in the shoulder and toe angles for both the pulp and ball charge at the different operating conditions tested. The pulp shoulder angle decreased as the % solids increased, and increased as the ball filling increased. However, the ball shoulder angle did not show any significant changes with increasing % solids but increased with increasing ball load. The pulp toe angle increased slightly with increasing % solids but seems to be relatively unaffected by changing ball filling conditions. The ball toe angle decreased as the % solids increase and also decreased significantly with increasing ball fillings. Improved grind was achieved at reduced free pulp shoulder and free pulp toe angles. This implies that the smaller the amount of pulp not interacting with the balls in a dynamic load, the better the expected grinding performance of the mill. The effect of liner wear on mill charge behaviour was also considered and showed that, as the liner wears, the pulp shoulder is not really affected. The pulp toe and ball toe angles increases, and the ball shoulder angle decreases. Improved grind results were obtained from the older liners from what appears to be a more compacted ball and pulp load at these conditions.

Finally, the model fitted and simulated results correspond well to the experimental results and the observations made on mill performance are similar from simulated and experimental data.

5 DISCUSSION AND OBSERVATIONS

5.1 PREFACE

In the previous chapter the results obtained from the test work performed on the industrial scale ball mill were presented. This chapter focuses on the discussion and interpretation of these results. The results obtained will also be compared to the literature reviewed in chapter 2.

In the first section the results for the general mill behaviour will be discussed in terms of basic mill performance. Thereafter a more detailed analysis of the results from the various mill operating conditions will be made. These mill operating conditions include ball filling, % solids and liner wear. Following this the results and analysis of the species specific breakage and milling performance for PGM's and Cr_2O_3 will be examined. A discussion of the results obtained from the Sensomag unit with regards to the charge behaviour is also presented. Finally, a summary of this section will be highlighted in the context of the set out hypotheses for this study.

5.2 GENERAL MILL BEHAVIOUR

In this section the results presented in section 4.2 are discussed. The general mill behaviour results show that surveys with high % solids and ball filling exceeded the grind target, whereas surveys with low % solids and ball fillings were well below the grind target. This range of results was significant as the feed to the mill had a fairly similar particle size distribution across the surveys. Since the feed was fairly similar, the differences observed can be attributed to the changes in the mill operating conditions. This then gives support to the first hypothesis in that operating conditions can be altered to obtain high size reduction for the mill in a given circuit configuration.

In order to understand the general milling performance behaviour better, a technique more elaborate than just looking at the final grind size was used. As discussed in section 2.4 the reduction ratio indicates the ratio of the amount of material in the discharge to the amount in the feed for a specific size class. The sieve efficiency was defined as the ratio of how much material was actually generated in the discharge stream relative to the maximum amount that could have been generated. The greatest reduction ratios were achieved for the finest size class. However, the lowest sieve efficiencies were also obtained for the finest size class. This ambiguous result highlights the difference in these two techniques and hence the danger in using only one of them. The classical reduction ratio figure, similar to the term used by Feurstenau and Abouzeid (2002), is driven high due to the small amount of fines in the feed. This small value is in the denominator of the

calculation and hence results in high reduction ratios for size classes with small amounts in the feed. This limitation is similar to that described by Musa and Morrison (2009). The sieve efficiency, however, as per definition in section 2.4, accommodates for the amount in the feed by considering the material generated in that size class relative to the amount of material that could have been generated should there have been complete reduction of all material in the feed for that size class (i.e. against best possible reduction in that size class, which is 100% passing that size class in concern less the amount that was already present in the feed).

The surveys with very low ball fillings and those with low % solids at high ball fillings were the furthest away from the target grind. They also had the lowest reduction ratios and sieve efficiencies. This will be discussed in more detail in the next section and once again alludes to the hypothesis that optimal operating conditions for a given circuit configuration can be found and that the performance varies with changing operating conditions as well changes in design variables.

The specific reduction energies were the greatest for the fine size class. This is again as a function of the small amount of material present in comparison to the larger size classes. The specific reduction energies for the 106 µm and 75 µm size classes are actually quite similar. This might indicate that the mill is efficient at reducing these coarser sizes. Also, the highest specific energies coincided with the highest ball fillings and the low % solids conditions, which is consistent with the surveys that had the lowest grind, reduction ratios and sieve efficiencies.

The plots of the specific energy against the amount generated or sieve efficiency, as depicted in figures 4.6 and 4.7, can be considered to be signature plots for the mill operation. The mill performance within this particular data set appears to be linear for a particular size class. This does not seem consistent with the observations made by Feurstenau and Abouzeid (2002), who showed that for a ball mill the reduction ratio has an exponential relationship to increasing specific energy based on results obtained from test work by Fuerstenau and Kapur (1994). However, the difference in their study was that it was done on quartz and in a dry batch ball mill. The work reported in this thesis was done on an industrial scale wet ball mill treating UG2 ore and the relationship appears to be linear for the experimental conditions considered. Another difference is that the specific energy defined in this study is the energy required per ton of the generated material in the particular size class (e.g. 75 µm), whereas the cited literature considered overall specific energy per ton treated. Using the specific energy per ton of material generated we get a better representation of the useful energy consumed and its effectiveness in creating size reduction from considering the amount of

material generated in that size class. This needs to be considered with caution, however, as it is not possible in the scope of this study to isolate the actual energy that goes into breakage and split it into the contribution from each size class.

These signature plots could be used to predict the expected mill performance for a particular energy input, or vice versa. The coarser size class has the highest gradient and values. This once again indicates the ease of size reduction in the coarser size class. The 106 µm and 75 µm classes are again quite similar, which could be a reflection of the efficiency of the mill at reducing the top sizes. The finer size class has a flatter size gradient and indicates less efficient breakage. This could be as a result of the particles getting closer to the grain size and is consistent with Partyka and Yan (2007). Signature plots pass through the origin as zero energy input implies no breakage or particle reduction. The trend for Feurstenau and Abouzeid (2002) shows a reduction ratio of 1 for zero specific energy. This is in essence the same result as a reduction ratio of 1 and indicates no particle breakage or reduction.

5.3 MILLING OPERATING CONDITIONS

The discussion pertaining to conditions specific to milling performance is presented in this section. The results for this section were only presented for the sub 75 µm size class but can be extended to other size classes. This allows one to focus on the effect of changing mill filling and % solids conditions on the mill performance.

As discussed in the previous section, the lowest ball fillings and % solids conditions were far below the target grind. This is consistent with the theory of Napier-Munn *et al* (1996), and in line with observations made by Liddell and Moys (1988) and Cleary (2001). This indicates that better milling performance is achieved with increased ball fillings and % solids. This is expected because improved ball - particle contact and interactions are more likely to occur with increasing ball filling and % solids – and this promotes particle breakage.

The reduction ratios and sieve efficiencies show a similar trend to the target grind with greater values at higher ball fillings and % solids. The reduction ratios and sieve efficiencies for the 30% and 33% ball filling conditions are however quite similar. There is no benefit in terms of milling performance when the mill is operated at ball fillings greater than 30%. The increased power draw and steel ball consumption might outweigh the benefit of improved grind, if any, at 33% ball filling.

The specific energy required decreases with increasing % solids. This again is in line with obserations presented by Napier-Munn *et al* (1996) and the general observations made by Tangsathitkulchai and Austin (1989), Lux and Claremont (2004), as well as Songfack and Rajamani (1999). Again this is expected to be due to improved ball – particle interaction. This will be discussed in more detail when looking at the effect on shoulder and toe angles in section 5.5. Unlike the ball filling condition which indicated a peak in performance around 30% filling, the milling performance with increasing % solids kept improving with an increase in % solids. These results are only partially consistent with those observed by Tangsathitkulchai and Austin (1989) as well as Lux and Clermont (2004). The work by these authors indicates milling performance tends to eventually get compromised as % solids are further increased. This is due to viscosity and transport related issues experienced at higher % solids which is detrimental to the milling performance. This suggests that within the limits of % solids conditions tested in this study, the point where slurry transport and charge motion within a mill are compromised, as described by Tangsathitkulchai and Austin (1989) and Napier-Munn *et al* (1996), was not reached. Hence there is scope in trying to increase mill % solids in this mill to get to the optimum performance.

For the signature plot presented in figure 4.14 there appears to be no trend in results obtained from tests performed at different ball fillings. However, reduced ball filling conditions lie at the lower energy end and increased ball filling conditions are at the higher energy end. The fit is however poor. The results reported by Cleary (2001), Napier-Munn *et al* (1996) as well as Liddel and Moys (1988) also show lower energy at lower ball fillings, with resultant poor grind. The energy and particle breakage increases with increasing ball filling. This is however less apparent at the higher end ball fillings. Even though there are more balls in the mill to draw further power at the higher ball filling, the actual energy used in the generation of particles through breakage (specific reduction energy at 75 μm) does not seem to change between 30% and 33% ball filling for this particular mill under the conditions tested.

When considering the influence of % solids by using the signature plot (figure 4.15), the data shows noticeable distinctions in mill performance for the distinct ranges tested. The line for higher % solids conditions lies well above the line for lower % solids conditions on the signature plot. This indicates that a particular sieve efficiency (or mill performance) can be achieved at lower energy input for higher % solids conditions than at lower % solids conditions. The operational philosophy of the mill can be reviewed to improve mill performance by targeting 30% ball filling and increasing the achievable % solids.

Survey results also show that the mill performs better with old liners compared to new liners as shown in figures 4.16, 4.17 and 4.18. The grind, reduction ratios and sieve efficiencies achieved were greater for conditions with old mill liners in comparison to new mill liners. This is also analogous to a shallower liner face angle. To understand this performance, once again the shoulder and toe angles will be discussed in section 5.5.

5.4 PGM AND Cr_2O_3 SPECIES BREAKAGE

The previous sections discussed the results for the general mill performance and specific milling conditions. In this section, how these varying operating conditions affect the milling performance specific to the PGM and Cr_2O_3 species is discussed. To start with the general particle distribution graphs support the previously stated observation that the mill is efficient at reducing the coarser fraction in the feed. The +106 µm fraction is reduced from around 75% in the feed to around 20% in the discharge. Subsequently there is a large increase in the sub 38 µm fraction.

When looking at the distribution of PGM across these size classes in the feed and discharge, the majority of the PGM's in the feed lie in the +106 µm fraction (around 70%). There was a significant increase in the distribution of PGM's in the sub 38 µm fraction for all the tests analysed – from 10% in feed to around 60% in the discharge. As described by Rule (2011), this would be good in terms of liberation of the PGM grains for better presentation to the flotation separation process, although supporting mineralogy to prove this was not available for this test work. Literature mentions that improved liberation is expected when grinding finer and as the particle size approaches the mineral grain size, as described in section 2.5. The grain size for PGM's in this ore body is expected to be around 6 µm as described in section 2.5.

The Cr_2O_3 distribution in the sub 38 µm fraction in the feed is as little as 5%. The majority of the Cr_2O_3 in the feed lies in the plus 106 µm size fraction (around 75%). This similarity in distribution in the coarser size class for the feed is quite striking for PGM and Cr_2O_3, even though their respective quantities are different in terms of orders of magnitude. Around 65% of the Cr_2O_3 in the discharge is found in size classes below 75 µm, which is expected to be bad for Cr_2O_3 suppression in the flotation process due to an increased chance of entrainment - as discussed by Minnaar *et al* (2005).

This similarity in distributions of PGM and Cr_2O_3 in the feed and discharge streams is of concern as it indicates non-preferential breakage of species across the mill for the UG2 ore. This implies that the feed presented to the mill circuit and the conditions tested within the investigation provide no motivation to perform further analysis to assess the presence of preferential breakage. This observation tends to disprove the second hypothesis which postulated a difference in breakage rates for the PGM and Cr_2O_3 species at different operating conditions. However, further work was done in this thesis to assess the effect on various size classes using the techniques discussed earlier.

The reduction ratios for the Cr_2O_3 species are in general greater than those for PGM's, especially in the fine size class. Again the fine fraction referred to in this study is sub 38 μm and the coarse fraction is the plus 106 μm size. In general, the fine size class also indicates a much higher reduction ratio than the coarser size class in both species. In comparison the coarser size class has the greatest sieve efficiency for both species, which is more in line with expected results from the literature reviewed in sections 2.2 and 2.5, and the accepted notion that larger particles are easier to break than fine particles (especially when getting closer to the grain size). The difference between these two mill performance parameters has already been described. Contrary to the observation from the general distribution graphs, the sieve efficiency for the PGM's seems to be greater than that for Cr_2O_3 in the fine size class, but quite similar in the coarser size classes. This then lead to conclusion that there might be some merit in the hypothesis of different breakage rates for the species at the coarse end and that the effect of the different milling conditions on the breakage of these species needed to be looked at in more detail.

The discussion in this section is based on the results shown in figures 4.22 and 4.23. The Cr_2O_3 reduction ratio and sieve efficiency were relatively constant for a given size class with varying mill operating conditions. However, there was variation with both ball filling and % solids for the PGM species. This supports the hypothesis that there is a difference in breakage rates between the species. The sieve efficiencies for PGM and Cr_2O_3 are similar at low % solids. The PGM sieve efficiency increases with increasing % solids while that for Cr_2O_3 remains relatively constant. There is also an increase in sieve efficiency with increasing ball filling for both species, and again the PGM change is more significant than that for Cr_2O_3. Thus at low % solids conditions, the sieve efficiencies for PGM and Cr_2O_3 species are similar. However, as the % solids increases, the increase in the sieve efficiency for PGM's is greater than for Cr_2O_3 and the differences between ball fillings become more apparent at higher % solids. This indicates that operating the mill at higher % solids results in better overall milling performance, and has more selective breakage of PGM's in

comparison to Cr_2O_3. The detailed analysis of sieve efficiencies has to be used to distinguish between the response of the PGM and Cr_2O_3 species to different milling conditions. Evaluating the distribution of these species per size class across the mill without considering the sieve efficiencies cannot give information leading to this conclusion. This then supports the hypothesis that the breakage rates for these species are different at varying mill operating conditions and that, in this application, higher mill % solids leads to an increase in PGM breakage rates compared to those of the Cr_2O_3 species. This is expected to result in more efficient milling operation and a better product to present to the flotation process for PGM recovery. There will still be fine Cr_2O_3 production at increased mill % solids, which would be detrimental to the flotation process in terms of chromite recovery through entrainment. The actual amounts of the two species present in the stream vary by order of magnitudes – Cr_2O_3 is present in percentage concentrations and PGM's are in parts per million (ppm or gpt). Thus even with a slight increase in Cr_2O_3 milling performance, the resultant increase in the actual amount of Cr_2O_3 generated in the undesired size class will be significant. The species specific results do not seem to indicate a peak in performance around 30% ball filling, as observed with the general mill performance results.

5.5 CHARGE BEHAVIOUR

The results from the Sensomag unit were presented in section 4.5. In this section those results are used to evaluate the effect of different operating conditions on mill charge behaviour. This will also help in explaining why certain mill operating conditions result in favourable milling performance, as described in the section 5.3.

As the % solids increase, the pulp shoulder angle decreased and the pulp toe angle increased slightly. This means that the pulp volume effectively decreased. This is consistent with the observations of Tansathitkulchai and Austin (1989) who showed that the slurry pool size decreased with an increase in % solids, which resulted in an increase in particle packing between the balls, resulting in improved milling conditions. There is also a very slight decrease in ball shoulder angle with increased % solids, and a more significant decrease in ball toe angle with increasing % solids. This implies that the ball charge is pushed further up the mill at low % solids. At high mill % solids, the charge is pushed up less with the rotation of the mill. The observed improved milling conditions at higher mill % solids can then be understood as the pulp being positioned into the area covered by tumbling balls; hence better ball – particle interaction occurs, leading to improved opportunity for breakage. This is justified because the pulp shoulder angle is always greater than the ball shoulder

angle and the ball toe angle is always greater than the pulp toe angle. This means that the volume in the mill occupied by the pulp is greater than that occupied by the balls. The concept of free pulp angle is discussed in section 4.5 to describe the amount of pulp not interacting with the ball charge. The effect of this free pulp angle on grind demonstrates that the best grinding performance is obtained when the free pulp angle is at its lowest. It can be assumed that not much particle breakage occurs in the portions of pulp not interacting with the ball charge. Thus it can be concluded that increasing the mill % solids results in more ball – particle interaction by reducing the free pulp angle, which provides a better opportunity for particle breakage. For the range of operational conditions tested, the results are partly consistent with the observations of Lux and Claremont (2004) as well as Songfack and Rajamani (1999). The % solids condition beyond which ball load expansion occurs was not reached in this study. This indicates that there is room for improvement in terms of operating the mill at higher mill % solids before performance is compromised.

As the ball filling increases the pulp shoulder angle increases and the pulp toe angle remains relatively constant. This indicates that there is greater pulp carry over at higher ball fillings. It was also observed that there was not much difference between pulp shoulder angles at 30 % and 33% ball filling, but a significant difference at 25% filling. The greater ball filling increased the ball shoulder angle and decreased the ball toe angle, as described by Cleary (2001), Napier-Munn *et al* (1996) as well as Liddell and Moys (1988). This is simply a result of a greater volume of balls in the mill. Thus the increase in ball filling can be understood to result in more ball – particle interaction in this configuration under the conditions tested. This would explain the improved milling performance at higher ball filling degrees. The observation of less significant improvement in milling performance between 30 and 33% ball filling cannot be explained using the data available. The similarities in pulp shoulder position at these two conditions might suggest that there is no significant benefit to be gained in terms of ball – particle interaction after a certain ball filling for this particular mill. The authors mentioned above do not explicitly discuss these specific conditions.

The angles obtained from the Sensomag for old versus new mill liners are also of interest in understanding the change in mill load behaviour with liner design or wear. The ball shoulder angle was lower and the ball toe angle was higher with worn liners. This indicates that there was compression of the ball charge, which could result in increased ball – particle interaction within the affected region. This decrease in charge lift with worn liners is consistent with the observations of Cleary (2001). Through mill operational experience, worn liners in the mill tend to give better grind

performance than new liners. This is also verified by the results obtained from this study and can be explained from the Sensomag results in terms of the compression of the ball charge, which results in more balls positioned in the effective grinding area. The pulp shoulder angle was hardly affected by the change in liner wear, whereas the pulp toe angle was greater with the old liner than the new liner. This effect on the pulp toe angle could be driven by the change in ball toe angle. The response to varying % solids conditions did not change. Thus better milling performance can be obtained for a ball mill in this configuration with less aggressive lifter bars (or more worn lifter bars), but the practicality against liner lifetime needs to be considered. Less aggressive lifter bars or more worn liners mean shorter liner lifetime and more frequent liner change, something that is not usually favoured in production plants. More aggressive liners would also seem to favour throughput as more impact breakage would be expected through more aggressive charge lift, as would be typical in a primary milling application. A coarser grind will however result from the more aggressive lifter, whereas the requirement of the circuit in this study is finer grind. One way of optimising the mill performance through different stages of a liner set life is by varying the mill speed to influence the mill load behaviour to reflect the favourable conditions met above, as alluded to by Cleary (2001). However, a mill with a variable speed drive (VSD) is typically required to have this flexibility and comes at a significant capital expense. The mill on which the test work in this study was performed was a fixed speed mill. Optimum ball and pulp angles can be controlled by the Sensomag by varying mill operating conditions to reach favourable mill load behaviour identified in this study.

The Sensomag may hence be used to identify mill load conditions during operation and to control the mill to conditions where optimal grinding performance can be obtained.

5.6 SUMMARY OF CHAPTER

The objective of this chapter was to discuss the results obtained in this work and to understand their significance in relation to the hypotheses of this study.

From looking at the results of the general milling performance, the variation in the results supported the first hypothesis that an optimum operating condition for the mill existed and that the mill was not being continuously operated at that optimum condition. The condition specific results showed that within the scope of variables tested in this study, the mill performance improved with increasing % solids, but the trend suggests that it was possible to operate the mill at higher % solids

than the highest condition tested. The results also showed that the ball filling had an optimum at around 30% ball filling. This is similar in terms of standard operating ball filling, but the standard operating mill % solids was not at an optimum. Thus the first hypothesis of the optimum operating condition could not be fully met as the mill % solids were restricted to those achieved in this study (maximum of 75% by mass). There is scope for further improvement in milling performance through changes that can be made to the circuit to further increase the mill % solids.

From the study of the species specific results at different milling conditions, the general particle distribution graphs across the mill seem to indicate similarity between the PGM and Cr_2O_3 distributions. However, performing the analysis in terms of reduction ratios and sieve efficiencies showed differences between the response of the PGM and Cr_2O_3 species for different milling conditions tested. The most unique observation is that the sieve efficiency of Cr_2O_3 stays relatively constant in comparison to that of PGM's with increasing % solids. The reduction ratio and sieve efficiency of the PGM species increases drastically at higher % solids. This then supports the hypothesis that the milling efficiencies for these species are different at distinct operating conditions and that in this application, higher mill % solids might help to take advantage of the increased PGM milling efficiency over Cr_2O_3 breakage. It must be noted though that even though PGM breakage seems to be significantly improved with higher % solids, the breakage of Cr_2O_3 is not reduced. Thus there will still be fine Cr_2O_3 production at increased mill % solids, which would still be detrimental to the flotation process in terms of chromite recovery by entrainment.

The Sensomag unit presented results in terms of mill load behaviour for the various surveys. Results from the samples collected were analysed in conjunction with the Sensomag data in an attempted to explain the observed load behaviour. As the mill % solids increased, the pulp volume decreased and the lift of the ball charge decreased. It is expected that this would result in better ball – particle interaction, leading to improved milling performance. The increase in ball filling resulted in an increase in ball volume in the mill as well as an increase in the lift of pulp load. Once again better ball – particle interactions are expected with resultant improved milling performance, but an optimum ball filling at around 30% was however found. The concept of free pulp angle was used to show improved grind results with reduced free pulp as a result of improved ball – particle interaction described above. Worn mill liners with decreased face or lift angle resulted in a more compact ball charge with reduced effective volume for the same amount of balls. It is expected that this would result in more efficient ball – particle interaction, leading to improved milling performance. Thus the final hypothesis of this study, which states that the data obtained from the

Sensomag can be used to indicate peak milling performance conditions and that the mill may be controlled at these conditions using this unit, holds true in that the online sensor does indicate the load behaviour. The Sensomag can be used to control and operate the mill at the optimum conditions by monitoring key variables such as shoulder and toe angles, which have been shown to provide information on mill performance.

6 SUMMARY OF FINDINGS AND CONCLUSIONS

6.1 PREFACE

In this final chapter of the dissertation the main conclusions are presented together with findings not directly related to the hypotheses of this study, but important for this sort of work. Recommendations based on the findings are also presented and further studies or investigations are discussed. Finally, the limitations and constraints to the scope of this study are considered and some of the assumptions made in this study are clarified.

6.2 SUMMARY OF FINDINGS

A summary of the various findings mentioned in this dissertation is given in this section. These findings are categorised into three parts – the mill performance at varying operating conditions, the effect on PGM and Cr_2O_3 reduction and the effect of the varying operating conditions on load behaviour. The importance of these three sections into which the summary is split relates to the set hypotheses for this study. The variable operating conditions for this mill were ball filling degree and % solids and the analysis focussed on their effect on mill performance, especially after the change in the circuit configuration at this operation. The effect on PGM and Cr_2O_3 reduction would indicate the milling response of the silicate and chromite fractions of the UG2 ore treated. This is of interest in trying to achieve maximum PGM liberation with minimal Cr_2O_3 grinding. Finally, by looking at the mill load information obtained by the online sensor, the effect of the different operating conditions on general mill performance and the reduction of the species may be interpreted in terms of the mill charge dynamic behaviour. This format is also consistent with the format in which the results and discussion are presented for this study.

For mill performance at varying operating conditions:

- Mill performance varied with different operating conditions. It improved with % solids and was optimal near 30% ball filling.
- An in depth analysis in terms of milling performance should be obtained through methods such as sieve efficiency and specific energy analysis rather than just observing grind or reduction ratio.
- Reduction ratio values can be misleading, especially when there are small amounts of particles in the relevant size/species for a particular class in the mill feed. The method of using sieve efficiency accommodated small amounts in the feed by considering the amount generated relative to the maximum that could have been generated. Thus sieve efficiency is

less sensitive to slight variations in the feed influencing the results, and can be used for more in-depth performance analysis.

- The mill in this study appeared to be efficient at reducing coarse size (plus 106 and 75 µm).
- The signature plot of specific energy against sieve efficiency is a straight line for the conditions tested here. This relationship can be used to roughly predict mill performance.
- In general, better milling performance was achieved with higher ball filling and higher % solids.
- An optimum in performance of this circuit seems to be reached around 30% ball filling, with little improvement observed above this with increased power and possibly steel ball consumption.
- Milling performance kept improving with increasing % solids. Eventually milling performance will be compromised as viscosity and transport issues start taking a toll at very high slurry densities. This point was not reached in this study and therefore scope exists to explore where this point lies to further optimise mill performance. This room for improvement in terms of higher mill % solids might be a result of the circuit change and less material reporting to the ball mill.
- Different ball filling conditions lie along a linear line for the signature plot.
- Increasing % solids conditions moves the signature plot line up and to the left, indicating better milling performance or reduced energy consumption with higher % solids.
- From effective reduction of mill top size, there is a resultant significant increase in sub 38 µm size class across the mill.
- Improved milling performance is observed with old liners than new liners.

For the effect of different operating conditions on PGM and Cr_2O_3 reduction:

- PGM and Cr_2O_3 distributions in the feed are very similar and slightly different in the discharge. Thus looking at only the species distributions across the mill does not indicate any difference in breakage rates or selectivity for the species.
- Reduction ratios for species distributions across the mill show significant differences but are highly influenced by subtle variations in feed distributions.
- At low % solids, sieve efficiencies indicate that the milling performance for PGM and Cr_2O_3 species is similar and almost independent of ball filling variation.
- PGM reduction increases significantly with increasing % solids, whereas Cr_2O_3 size reduction increases only slightly. At high % solids the effect of varying ball filling degree is

also much more pronounced on overall PGM and Cr_2O_3 milling performance. PGM breakage changes more significantly with increasing ball filling conditions than for Cr_2O_3.

- Detailed analysis highlights the difference in milling performance and indicates some sort of selectivity or breakage rate variation. This deeper level of resolution is required to be able to differentiate species specific milling performance in this instance and should be backed up with liberation and mineralogy analysis.

For the effect of varying operating conditions on mill load behaviour:

- As % solids increase, the effective volume of the pulp decreases in the mill and the ball charge is pushed less far up the mill. This results in better ball – particle interaction and thus improved milling conditions. Better grinds were achieved when conditions with lower free pulp angles were obtained.
- As the ball filling increases, the volume of balls in the mill increases and the pulp is carried further up in the mill. Optimum ball filling was determined to be around 30%, and there was little increase in pulp shoulder angle after 30% ball filling conditions. This has to be further investigated to try and understand what significance, if any, this might imply. Potentially this could be used as a mill control measure in terms of finding the optimal ball filling.
- Improved milling performance from worn liners was observed. This can be explained by the observation that worn liners have less lift on the ball charge and thus a more compressed ball charge results in better ball – particle interactions towards the end of the liner life.
- This condition of improved milling performance can be manipulated over the life of the liner by influencing another operational condition that affects mill load behaviour, such as mill speed. The Sensomag can be used to control a mill with several operational variables at conditions which result in optimum milling performance, as observed in this study.

6.3 CONCLUSIONS

The conclusions to this study will be laid out in terms of the set hypotheses. These hypotheses were described in section 1.3 of this study.

Hypothesis 1

There exists an optimum ball filling and % solids which gives the highest reduction in particle size.

The highest size reduction was achieved at the ball filling of 30% by volume. However, within the

range of % solids tested the results showed that the size reduction continued to increase with % solids. Due to practical limitations the optimum % solids level was not reached. The results showed that the common practice of inlet water flow rate control to dilute the feed % solids does not result in optimum grinding conditions since the maximum achieved slurry density resulted in the best milling performance. The trend shows that going higher in terms of mill % solids could still give greater size reduction.

Hypothesis 2

A combination of operating variables exists where the breakage behaviour of the silicates is different to that of the chromite fraction.

The majority of the PGM's in the UG2 ore are in the silicates and thus the PGM distribution results would indicate the amount of breakage in the silicate fraction. Cr_2O_3 is used as an indicator of the chromite content in UG2 ore. The sieve efficiency analysis shows that the reduction of the silicates increased with an increase in mill % solids and ball filling degree. For chromite, the mill % solids did not appear to have any effect at low ball fillings, but a slight shift was observed at the higher ball fillings tested. The trend suggests that the reduction of both silicates and chromite increased with an increase in ball filling, albeit at different rates.

Hypothesis 3

The charge kinematic information of shoulder and toe position for both pulp and balls can be related to grind performance of the secondary ball mill.

The shoulder and ball angles varied with different mill operating conditions. This was related to the grind performance of the mill in terms of the amount of free pulp (pulp not in contact with the ball charge) available at that condition. Improved grind performance was observed at conditions that resulted in lower free pulp angles. There was also a reduction in the total ball angle with old lifters compared to new lifters, which resulted in improved grind performance obtained with the worn liner set.

6.4 RECOMMENDATIONS AND WAY FORWARD

It is recommended that the mill continued to be operated at 30% ball filling and maximum in-mill density currently available (minimal mill inlet water).

In the continuation of this study the following recommendations need to be considered:

- The maximum in-mill density before deterioration in mill performance needs to be attained to understand the scope for further improvement in milling performance. This could be done through looking at the cyclone performance upstream and making certain changes. This is not difficult to achieve but the plant may suffer loss of production during this trial period. Such a change will also alter other aspects in the overall circuit operation – e.g. mass split, chromite and silicate split etc.
- An analysis of the benefit of increased PGM liberation against chromite breakage for increased mill % solids needs to be done. This is due to the effect of the difference in the magnitudes of the concentrations in which the species are found in the ore, and is very significant. This could mean that a slight increase in the breakage of the chromite species could result in a massive increase in the amount of fine chromite particles presented to the flotation process, which could be detrimental to the overall process performance.
- Mineralogical analysis should be considered to confirm the differences in PGM and Cr_2O_3 distribution, and hence the silicate and chromite distribution, in the feed and product streams of the secondary mill. This analysis will also be critical around the upstream cyclone separating the feed for the secondary mill and IsaMill circuit.
- To limit the over grinding of the chromite fraction, it is imperative to achieve the correct chromite – silicate upstream. Any chromite presented to the fine grinding IsaMill circuit will be detrimental to chromite recovery. Any benefit gained in achieving this correct separation would far outweigh the detrimental effects of allowing chromite grinding in the secondary mill.
- Alternatively, changes in the process utilising alternate technology might be investigated which limits the recovery of chromite e.g. column cells, upstream chromite removal plants etc. This might mitigate the risk of over grinding the chromite fraction and allow for maximum benefit from silicate reduction.
- The Sensomag can be incorporated into a mill controller that looks at more than just mill ball filling. As shown in this study, conditions that result in optimum mill efficiency can be identified and hence if these conditions are known, then the mill may be controlled using outputs from the sensor.

6.5 LIMITATIONS AND CONSTRAINTS

Many assumptions were made for the purpose of this study. This section describes the limitations and constraints of the results presented in this study.

- The size categories chosen assume improved PGM liberation and recovery below the "coarse fraction" (plus 106 μm).
- Size categories chosen assume increased chromite recovery through entrainment after "fine fraction" (sub 38 μm). This assumption considers that that chromite grain is fully liberated at the chosen size class.
- It is also assumed through separate PGM and Cr_2O_3 analysis in this study that the PGM association with chromite is minimal and that they are separately occurring species in the UG2 ore body. This also follows the assumption that chromite is fully liberated in the finer size fractions and has no significant association with silicates. Hence PGM association is assumed to be mainly with the silicate matrix or more specifically with base metals and sulphides.
- The Cr_2O_3 is an indication of the chrome/chromite species distribution in the ore – even though they are separate compounds. Chromitite is an ore type. Wikipedia (n.d.) describes chromite as the mineral which is found in chromitite ore (usually an iron chromium oxide $FeCr_2O_4$). It is the form in which the element chromium is found in the chromitite ore. Cr_2O_3 is an inorganic compound measured on a lab scale to indicate the composition of chromium in chromitite ore.

REFERENCES

Almond, D.G., Valderrama, W., 2004. Performance enhancement tools for grinding mills. *International Platinum Conference "Platinum Adding Value" - the South African Institute of Mining and Metallurgy.* Pg 103 – 110.

Austin, L.G., Shoji, K., Luckie, P.T., 1976. The effect of ball size on mill performance. *Powder Technology.* Volume 14 (1), Pg 71–79.

Becker, M., Mainza, A.M., Powell, M.S., Bradshaw, D.J., Knopjes, B., 2008. Quantifying the influence of classification with the 3 product cyclone on liberation and recovery of PGM's in UG2 ore. *Minerals Engineering*. Volume 21, Pg 549 – 558.

Behera, B., Mishra, B.K., Murty, C.V.R., 2007. Experimental analysis of charge dynamics in tumbling mills by vibration signature technique. *Minerals Engineering*. Volume 20, Pg 84 -91.

Bond, F.C., 1952. The third theory of comminution. *Trans SME/AIME*. Volume 193, Pg 484 – 494.

Bond, F.C.,1961. Crushing and grinding calculations. Part I. *British Chemical Engineering*. Volume 6 (6), Pgs 378-385. Part II. *British Chemical Engineering*. Volume 6 (8), Pgs 543 – 548.

Bueno, M., Powell, M.S., Kojovic, T., Shi, F., Sweet, J., Philips, D., Durant, B., Plint, N., 2011. Multi-component autogenous pilot trials, *International Autogenous and Semiautogenous Grinding Technology. Vancouver: University of British Columbia, Department of Mining and Mineral Process Engineering.*

Campbell, J.J., Holmes, R.J., Spencer, S.J., Phillips, P.L., Barker, D.G., Davey, K.J., 2006. The development of an on-line surface vibration monitoring system for AG/SAG mills. *International Autogenous and Semiautogenous Grinding Technology. Vancouver: University of British Columbia, Department of Mining and Mineral Process Engineering.* Volume 3, Pg 326 – 327.

Charles, W.D., Gallagher, A.E.J., 1982. Comminution energy usage and material wear. *Design and Installation of Comminution Circuits*. S.M.E – A.I.M.E., New York. Pg 248 – 274.

Cleary, P.W., 2001. Charge behaviour and power consumption in ball mills: sensitivity to mill operating conditions, liner geometry and charge composition. *International Journal of Minerals Processing*. Volume 63, Pg 79 – 114.

Clermont, B., De Haas, B., Hancotte, O., 2008. Real time management tools for stabilizing your milling process. *Third International Platinum Conference "Platinum in Transformation". The Southern African Institute of Mining and Metallurgy*. Pg 13 - 20.

Concha, F., Magne, L., Austin, L.G., 1992. Optimization of the make-up ball charge in a grinding mill. *International Journal of Mineral Processing.* Volume 34 (3), Pg 231–241.

Erdem, A. S., Ergűn, Ş. L., 2009. The effect of ball size on breakage rate parameter in a pilot scale ball mill**.** *Minerals Engineering.* Volume 22, Pg 660 - 664.

Feurstenau, D.W., Abouzeid, A.-Z.M., 2002. The energy efficiency of ball milling in comminution. *International Journal of Mineral Processing*. Volume 67. Pg 161 – 185.

Feurstenau, D.W., Kapur, P.C., 1994. A new approach to assessing the grindability of solids and the energy efficiency of grinding mills. *Miner. Metall. Process.* Pg 210 - 216.

Hinde, A.l., Kalala, J.T., 2009. The application of a simplified approach to modelling tumbling mills, stirred media and HPGR's. *Minerals Engineering.* Volume 22, Pg 633 – 641.

Järvinen, J., Laurila, H., Karesvuori, J., Blanz, P., 2006. Experiences in charge volume measurement and the potential of modelling. *International Autogenous and Semiautogenous Grinding Technology. Vancouver: University of British Columbia, Department of Mining and Mineral Process Engineering.* Volume 3, Pg 253 – 265.

Katubilwa, M., Moys, M.H., 2009. Effect of ball size distribution on milling rate, *Minerals Engineering*. Volume 22, Pg 1283 – 1288.

Keshav, P., de Haas, B., Clermont, B., Mainza, A., Moys, M., 2011. Optimisation of the secondary ball mill using an on-line ball and pulp load sensor – The Sensomag. *Minerals Engineering.*

Volume 24, Pg 325 – 334.

Kolacz, J., 1997. Measurement system of the mill charge in grinding ball mill circuits. *Minerals Engineering*. Volume 10 (12), Pg 1329 – 1338.

La Nauze, R.D., Temos, J., 2002. Technologies for sustainable operation. *CMMI Congress 2002*. Queensland. Pg 27 – 34.

Liddell, K.S., Moys, M.H., 1988. The effects of mill speed and filling on the behaviour of the load in a rotary grinding mill. *The Journal of South African Institute of Mining and Metallurgy*. Volume 88 (2), Pg 49 – 57.

Lux, J., Clermont, B., 2004. The influence of mill speed and pulp density on the grinding efficiency for secondary stage grinding. *International Platinum Conference "Platinum Adding value" - The South African Institute of Mining and Metallurgy*. Pg 89 - 93.

Makokha, A.B., Moys, M.H., 2006. Towards optimising ball-milling capacity: Effect of lifter design. *Minerals Engineering.* Volume 19, Pg 1439 – 1445.

Makokha, A.B., Moys, M.H., Bwalya, M.M., 2011. Modelling the RTD of an industrial overflow ball mill as a function of load volume and slurry concentration. *Minerals Engineering*. Volume 24, Pg 335 – 340.

Martins, S., Zepeda, J., Picard, B., Radziszewski, P., Roy, D., 2006. Investigating on-the-shell acoustics. *International Autogenous and Semiautogenous Grinding Technology. Vancouver: University of British Columbia, Department of Mining and Mineral Process Engineering.* Volume 3, Pg 300 – 310.

Minnaar, D.M., Smit, D.S., Terblanche, A.N., 2005. Technological solution to improvement in PGM recovery, upgrade ration and Cr2O3 reduction of UG2 ore. *Centenary of Flotation Symposium*. Brisbane. Pg 225 – 233.

Morrell, S., 2008. A method for predicting the specific energy requirement of comminution circuits and assessing their energy utilisation efficiency. *Minerals Engineering*. Volume 21 (3). Pg 5 - 9.

Musa, F., Morrison, R., 2009. A more sustainable approach to assessing comminution efficiency. *Minerals Engineering*. Volume 22, Pg 593 – 601.

Napier-Munn, T.J., Morrell, S., Morrison, R.D., Kojovic, T., 1996. *Mineral comminution circuits – their operation and optimisation*. Julius Kruttschnitt Mineral Research Centre, Indooroopilly, Queensland, Australia.

Newell, A.J.H., 2008. The processing of platinum group metals (PGM) – part 1. *Pincock Perspectives. Pincock, Allen and Holt*. Colorado. Issue 89.

Newell, A.J.H., 2008. The processing of platinum group metals (PGM) – part 2. *Pincock Perspectives. Pincock, Allen and Holt*. Colorado. Issue 90.

Olsen, T.O., 1976. Automatic control of continuous autogenous grinding. *Proceedings of Conference on Automation in Mining, Minerals and Metal Processing*. Johannesburg

Partyka, T., Yan, D., 2007. Fine grinding in a horizontal ball mill. *Minerals Engineering*. Volume 20, Pg 320 – 326.

Philips, R.E., Jone, R.T., Chennells, P., 2008. Commercialisation of the Conroast process. *Third International Platinum Conference "Platinum in Transformation", The South African Institute of Mining and Metallurgy*.

Powell, M.S., Nurick, G.N., 1996. A study of charge motion in rotary mills. Part II – Experimental work. *Minerals Engineering.* Volume 9 (3), Pg 343 – 350.

Rogers, R.S.C., Austin, L.G., 1984. Residence time distributions in ball mills. *Particulate Science and Technology 2*, 191.

Rule, C., 2011. Stirred milling at Anglo American Platinum. *International Autogenous and Semiautogenous Grinding Technology. Vancouver: University of British Columbia, Department of Mining and Mineral Process Engineering.*

Shi, F., Morrison, R., Cervellin, A., Burns, F., Musa, F., 2009. Comparison of energy efficiency between ball mills and stirred mills in coarse grinding. *Minerals Engineering*. Volume 22. Pg 673 – 680.

Si, G., Cao, H., Zhang, Y., Jia, L., 2008. A new approach to load measurement for industrial scale ball mill. *Proceedings of IEEE international Conference on Mechatronics and Automation*. Pg 302 – 307.

Songfack, P., Rajamani, R., 1999. Hold-up studies in a pilot scale continuous ball mill: dynamic variations due to changes in operating variables. *International Journal of Minerals Processing*. Volume 57, Pg 105 – 123.

Su, Z., Wang, P., Yu, X., Lu, Z., 2008. Experimental investigation of vibration signal of an industrial tubular ball mill: Monitoring and diagnosing. *Minerals Engineering.* Volume 21, Pg 699 - 710.

Tangsathitkulchai, C., Austin, L.G., 1989. Slurry density effects on ball milling in a laboratory ball mill. *Powder Technology*. Volume 59, Pg 285 – 293.

Valenta, M.M., Mapheto, H., 2010. Application of fundamentals in optimising platinum concentrator performance. *The 4th International Platinum Conference, Platinum in transition "Boom or Bust", The South African Institute of Mining and Metallurgy*. Pg 13 – 20.

Von Rittinger, P.R., 1867. Lehrbuch der Aufbereitungskunde. *Ernst and Korn*, Berlin.

Wikipedia, n.d., Chromium (III) oxide, viewed April 2012, *http://en.wikipedia.org/wiki/Chromium(III)_oxide*.

Wikipedia, n.d., Chromite, viewed April 2012, *http://en.wikipedia.org/wiki/Chromite*.

Wikipedia, n.d., Chromite (compound), viewed April 2012, *http://en.wikipedia.org/wiki/Chromite_(compound)*.

Wikipedia, n.d., Chromitite , viewed April 2012, *http://en.wikipedia.org/wiki/Chromitite*.

Yekeler, M., Ozkan, A., Austin, L.G., 2001. Kinetics of fine wet grinding in a laboratory ball mill. *Powder Technology*. Volume 114, Pg 224 – 228.

Zeng, Y., Forssberg, E., 1993. Monitoring operating state by measuring vibration and acoustic signals in an industrial scale ball mill. *Proceedings of the Conference on Mineral Processing.* Sweden. Pg 135 – 146.

APPENDICES

List of Appendices

Appendix A – Relationship between % solids and pulp density

From the definition of % solids (by mass):

$$\%solids = \frac{mass_{solids}}{mass_{solids} + mass_{water}} \times 100\% \qquad [A1]$$

Napier-Munn *et al*. (1996) also gives the % solids by mass as a function of the pulp and solids SG:

$$\%solids = \frac{\rho_{solids}(1-\rho_{pulp})}{\rho_{pulp}(1-\rho_{solids})} \times 100\% \qquad [A2]$$

By incorporating A1 and A2:

$$\rho_{pulp} = \frac{\rho_{solids}}{\left(\rho_{solids} - \left(\rho_{solids} \times \frac{\%solids}{100}\right) + \frac{\%solids}{100}\right)} \qquad [A3]$$

Appendix B – Sensomag filling degree verification

A few of the measured and predicted filling degrees around the period of the surveys are shown in table B1. The measured filling degrees were obtained from physical measurements taken inside the mill of the ball charge during a planned maintenance shut down and calculated from generic mathematical and geometric principles. The Sensomag filling degree value is that which was predicted from the angles measured and the model just prior to the stoppage of the mill. The table shows good correlation between the two values, with the absolute difference between the two values lying within the +0.8% to -0.7% range. Thus in essence, the model predicted value seems to be within ±0.8% (absolute). Given the inherent inconsistencies involved with the physical measurement taken inside the mill of the ball charge, this is not an unreasonable correlation. This correlation has been trended in figure B1 and helps to illustrate the closeness of these values.

Table B1 The difference between measured and predicted ball filling degrees for the Sensomag

Measured	Sensomag	Absolute difference	Relative difference
31.2%	30.38%	0.8%	2.5%
26.9%	26.21%	0.7%	2.6%
32.4%	33.10%	-0.7%	-2.2%
29.5%	29.19%	0.3%	1.1%
29.2%	28.93%	0.2%	0.8%

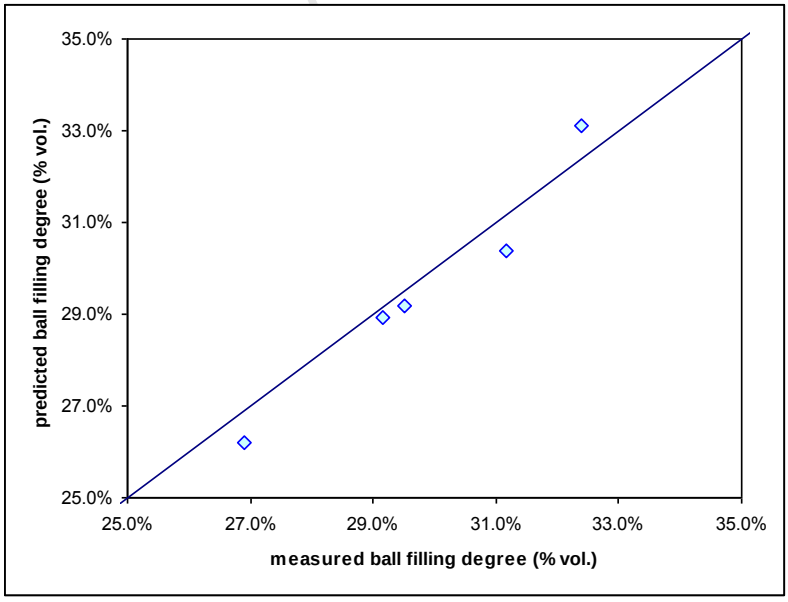

Figure B1 The measured ball filling degree against Sensomag predicted filling degrees

Appendix C – Survey results

The major survey results from this study are shown in table C1. Due to company confidentiality policies regarding intellectual property, the assay raw results for the PGM and Cr_2O_3 analysis have not been published.

Table C1 Summary of results obtained directly from the surveys performed

			Survey 1	Survey 2	Survey 3	Survey 4	Survey 5	Survey 6	Survey 7	Survey 8	Survey 9	Survey 10	Survey 11	Survey 12	Survey 13	Survey 14	Survey 15
	date		**27-Aug-09**	**27-Aug-09**	**17-Sep-09**	**17-Sep-09**	**18-Sep-09**	**18-Sep-09**	**14-Oct-09**	**14-Oct-09**	**15-Oct-09**	**15-Oct-09**	**04-Nov-09**	**04-Nov-09**	**05-Nov-09**	**05-Nov-09**	**27-Nov-09**
	condition	liner state	*old liner*	*old liner*	*new liner*	*new liner*	*new liner*	*new liner*									
	% solids	%	73%	65%	75%	73%	65%	63%	76%	71%	74%	67%	68%	65%	72%	76%	
	pulp SG	t/m^3	2.06	1.86	2.13	2.07	1.85	1.81	2.14	2.02	2.11	1.91	1.92	1.85	2.04	2.14	
	water	m^3/hr	0	63	0	25	47	76	0	26	44	76	47	76	23	0	
	cyclone UF flow	% solids	75%	75%	77%	76%	71%	78%	75%	76%	75%	75%	76%	76%	77%	77%	
	load	tons	945	901	976	952	936	912	832	808	839	794	978	968	1006	1015	
	power	MW	8.98	9.25	8.55	8.95	9.12	9.30	7.45	7.76	7.49	7.99	9.73	9.78	9.50	9.22	
	filling degree	%	29	29	30	30	30	30	25	25	25	25	33	33	33	33	28
	ball shoulder	°	293.9	294.4	296.0	295.7	296.6	296.6	289.5	290.1	290.0	290.6	300.6	300.4	300.0	299.9	293.8
	ball toe	°	124.0	125.1	121.2	122.1	124.0	123.9	125.8	127.3	125.7	127.8	121.1	121.6	119.8	118.3	125.2
	pulp shoulder	°	303.4	303.8	301.9	302.4	303.9	304.0	296.4	297.4	296.5	298.2	305.1	305.4	303.4	301.6	299.5
	pulp toe	°	95.4	94.6	91.8	91.6	91.4	91.5	92.6	92.4	92.7	92.0	92.4	92.0	92.4	92.7	92.3
grind																	
mill feed	**% passing 106µm**		21.86	21.37	24.97	24.49	25.94	25.70	26.92	25.49	24.32	24.33	23.86	23.91	25.08	24.25	21.56
	% passing 75µm		13.79	13.41	14.58	14.24	14.98	15.32	15.95	15.45	14.94	14.79	13.24	13.27	14.14	13.68	12.07
	% passing 38µm		7.27	7.01	6.14	6.11	6.06	6.76	7.21	7.27	7.22	7.13	6.34	6.15	6.85	6.62	6.05
mill discharge	**% passing 106µm**		79.93	79.04	79.83	80.36	78.78	79.01	79.48	75.68	77.25	78.13	78.85	78.29	80.99	82.43	81.08
	% passing 75µm		68.52	66.52	66.84	67.45	64.53	64.93	66.10	60.05	62.50	63.27	64.58	63.40	67.24	69.88	66.86
	% passing 38µm		45.86	43.32	43.48	43.62	40.21	41.25	44.61	35.66	40.22	39.43	41.50	40.02	43.57	46.69	44.54

Appendix D – Model fitted and simulation results

The experimental results are compared to the model fitted results and the simulated results in table D1 and D2 respectively.

Table D1 A comparison of model fit and experimental results for the surveys performed

Test No.	Stream	Solids (t/h) Exp	Solids (t/h) Fit	% Solids Exp	% Solids Fit	% Sub 75um Exp	% Sub 75um Fit	P80, mm Exp	P80, mm Fit
1	Mill feed	386	386	73	73	13.79	13.79	0.301	0.301
	Mill product	386	386	73	73	68.52	68.11	0.106	0.105
2	Mill feed	422	422	65	65	13.41	13.41	0.301	0.301
	Mill product	422	422	65	65	66.52	66.05	0.108	0.108
3	Mill feed	422	422	65	65	13.41	13.41	0.301	0.301
	Mill product	422	422	65	65	66.52	66.05	0.108	0.108
4	Mill feed	443	443	73	73	14.24	14.24	0.279	0.279
	Mill product	443	443	73	73	67.45	67.16	0.105	0.104
5	Mill feed	449	449	65	65	14.98	14.98	0.265	0.265
	Mill product	449	449	65	65	64.53	64.25	0.109	0.109
6	Mill feed	464	464	63	63	15.32	15.32	0.277	0.277
	Mill product	464	464	63	63	64.93	64.82	0.108	0.108
7	Mill feed	442	442	76	76	16.33	16.33	0.266	0.266
	Mill product	442	442	76	76	67.05	67.39	0.106	0.107
8	Mill feed	436	436	71	71	15.56	15.56	0.282	0.282
	Mill product	442	436	71	71	60.05	59.41	0.116	0.116
9	Mill feed	456	456	74	74	14.94	14.94	0.288	0.288
	Mill product	456	456	74	74	64.69	65.03	0.108	0.109
10	Mill feed	408	408	67	67	14.79	14.79	0.296	0.296
	Mill product	408	408	67	67	60.85	59.65	0.113	0.114
11	Mill feed	436	436	68	68	13.07	13.07	0.307	0.307
	Mill product	436	436	68	68	64.10	63.67	0.110	0.109
12	Mill feed	458	458	65	65	13.08	13.08	0.293	0.293
	Mill product	458	458	65	65	63.26	62.62	0.110	0.110
13	Mill feed	409	409	409	72	14.14	14.14	0.275	0.275
	Mill product	409	409	409	72	67.24	66.91	0.103	0.103
14	Mill feed	420	420	76	76	13.68	13.68	0.293	0.293
	Mill product	420	420	76	76	69.88	69.60	0.099	0.098

Table D2 A comparison of simulated and experimental results for the surveys performed

Test No.	Stream	Solids (t/h) Exp	Solids (t/h) Sim	% Solids Exp	% Solids Sim	% Sub 75um Exp	% Sub 75um Sim	P80, mm Exp	P80, mm Sim
1	Mill feed	464	464	75	75	13.79	13.79	0.301	0.301
	Mill product	386	464	73	75	68.52	66.02	0.106	0.110
2	Mill feed	464	464	65	65	13.41	13.41	0.301	0.301
	Mill product	422	464	65	65	66.52	64.54	0.108	0.111
3	Mill feed	464	464	75	75	14.58	14.58	0.277	0.277
	Mill product	451	464	75	75	66.84	66.21	0.106	0.107
4	Mill feed	464	464	75	75	14.24	14.24	0.279	0.279
	Mill product	443	464	73	75	67.45	67.35	0.105	0.104
5	Mill feed	464	464	65	65	14.98	14.98	0.265	0.265
	Mill product	449	464	65	65	64.53	63.71	0.109	0.110
6	Mill feed	464	464	65	65	14.98	14.98	0.265	0.265
	Mill product	449	464	65	65	64.53	63.71	0.109	0.110
7	Mill feed	464	464	75	75	16.33	16.33	0.266	0.266
	Mill product	442	464	76	75	67.05	66.07	0.106	0.110
8	Mill feed	464	464	70	70	15.56	15.56	0.282	0.282
	Mill product	442	464	71	70	60.05	58.98	0.116	0.117
9	Mill feed	464	464	75	75	14.94	14.94	0.288	0.288
	Mill product	456	464	74	75	64.69	65.22	0.108	0.108
10	Mill feed	464	464	65	65	14.79	14.79	0.296	0.296
	Mill product	408	464	67	65	60.85	57.07	0.113	0.119
11	Mill feed	464	464	70	70	14.79	14.79	0.296	0.296
	Mill product	408	464	67	70	60.85	59.07	0.113	0.115
12	Mill feed	464	464	65	65	13.08	13.08	0.293	0.293
	Mill product	458	464	65	65	63.26	62.42	0.110	0.110
13	Mill feed	464	464	70	70	14.14	14.14	0.275	0.275
	Mill product	409	464	72	70	67.24	63.90	0.103	0.109
14	Mill feed	464	464	75	75	13.68	13.68	0.293	0.293
	Mill product	420	464	76	75	69.88	67.52	0.099	0.103